

## **General Disclaimer**

### **One or more of the Following Statements may affect this Document**

- This document has been reproduced from the best copy furnished by the organizational source. It is being released in the interest of making available as much information as possible.
- This document may contain data, which exceeds the sheet parameters. It was furnished in this condition by the organizational source and is the best copy available.
- This document may contain tone-on-tone or color graphs, charts and/or pictures, which have been reproduced in black and white.
- This document is paginated as submitted by the original source.
- Portions of this document are not fully legible due to the historical nature of some of the material. However, it is the best reproduction available from the original submission.

DOE/NASA/0042-79/1  
NASA CR 159601  
BCS 40259-1

**AN EXPANDED  
SYSTEM SIMULATION MODEL  
FOR  
SOLAR ENERGY STORAGE  
(Technical Report)**

**Volume I**

A. W. Warren  
Energy Technology Applications Division  
Boeing Computer Services Company

(NASA-CR-159601) AN EXPANDED SYSTEM  
SIMULATION MODEL FOR SOLAR ENERGY STORAGE  
(TECHNICAL REPORT), VOLUME 1 - Final Report  
(Boeing Computer Services, Inc., Seattle,  
Wash.) 107 p HC A06/MF A01

N79-33881

Unclassified  
CSCL 09B G3/61 35947

August 1979

Prepared for  
NATIONAL AERONAUTICS AND SPACE ADMINISTRATION  
Lewis Research Center  
Under Contract DEN3-42

for  
**U.S. DEPARTMENT OF ENERGY**  
**Division of Energy Storage Systems**



DOE/NASA/0042-79/1  
NASA CR 159601  
BCS 40259-1

**AN EXPANDED  
SYSTEM SIMULATION MODEL  
FOR  
SOLAR ENERGY STORAGE  
(Technical Report)**

**Volume I**

A. W. Warren  
Energy Technology Applications Division  
Boeing Computer Services Company  
Seattle, Washington 98124

**August 1979**

Prepared for  
**NATIONAL AERONAUTICS AND SPACE ADMINISTRATION**  
Lewis Research Center  
Cleveland, Ohio 44135  
Under Contract DEN3-42

for  
**U.S. DEPARTMENT OF ENERGY**  
Division of Energy Storage Systems  
Washington, D.C. 20545  
Under Interagency Agreement EX-76-A-31-1026

1. Report No. NASA CR 159601	2. Government Accession No.	3. Recipient's Catalog No.	
4. Title and Subtitle <b>An Expanded System Simulation Model for Solar Energy Storage (Technical Report)</b>		5. Report Date August, 1979	
7. Author(s) A. W. Warren		6. Performing Organization Code	
9. Performing Organization Name and Address Energy Technology Applications Division of Boeing Computer Services Company Seattle, WA 98124		8. Performing Organization Report No.	
12. Sponsoring Agency Name and Address U.S. Department of Energy Division of Energy Storage Systems Washington, D. C. 20545		10. Work Unit No.	
15. Supplementary Notes Final report. Prepared under Interagency Agreement EX-76-A-31-1026. Project Manager, Larry H. Gordon, Power Generation and Storage Division, NASA Lewis Research Center, Cleveland, OH 44135		11. Contract or Grant No. DEN 3-42	
16. Abstract This effort completed the development of a comprehensive computer program for solar energy storage system simulation models. An acronym for this program is SIMWEST (Simulation Model for Wind Energy Storage) and was initially developed under a previous contract, NAS3-20385, August, 1977. The expanded SIMWEST program includes wind and/or photovoltaic systems utilizing any combination of five types of storage (pumped hydro, battery, thermal, flywheel and pneumatic). This expanded SIMWEST software package is available for the UNIVAC 1100 series and the CDC 6000 series computers. The level of detail of SIMWEST is consistent with a role of evaluating the economic feasibility as well as the general performance of wind and/or photovoltaic energy systems.		13. Type of Report and Period Covered Contractor Report	
		14. Sponsoring Agency Code DOE/NASA/0042-79/1	
The SIMWEST software package consists of two basic programs and a library of system, environmental, and load components. The first program is a precompiler which generates computer models (in Fortran) of complex wind and/or photovoltaic source/storage/application systems, from user specifications using the respective library components. The second program provides the techno-economic system analysis with the respective I/O, the integration of system dynamics, and the iteration for conveyance of variables.			
This report is one of four reports generated as a result of this effort. The reports are as follows:			
No.	Title		
Vol. 1	NASA CR 159601 DOE/NASA/0042-79/1		
Vol. 2	An Expanded System Simulation Model for Solar Energy Storage (Technical Report)		
Vol. 1	NASA CR 159602 DOE/NASA/0042-79/2		
Vol. 2	An Expanded System Simulation Model for Solar Energy Storage (UNIVAC Operation Manual Revisions)		
Vol. 1	NASA CR 159607 DOE/NASA/0042-79/3		
Vol. 2	SIMWEST: A Simulation Model for Wind and Photovoltaic Energy Storage Systems (CDC User's Manual)		
Vol. 2	NASA CR 159608 DOE/NASA/0042-79/4		
Vol. 2	SIMWEST: A Simulation Model for Wind and Photovoltaic Energy Storage Systems (CDC Program Descriptions)		
17. Key Words (Suggested by Author(s)) Energy Storage Computer Programs, System Simulation, Wind Energy Photovoltaic Energy		18. Distribution Statement Unclassified - Unlimited STAR Category 61 DOE Category UC-946	
19. Security Classif. (of this report) Unclassified	20. Security Classif. (of this page) Unclassified	21. No. of Pages	22. Price*

\* For sale by the National Technical Information Service, Springfield, Virginia 22161

## **FOREWORD**

This report presents results of work conducted by Boeing Computer Services Company under NASA Contract DEN3-42, "An Expanded System Simulation Model for Solar Energy Storage." The work was a continuation of the development effort for SIMWEST (Simulation Model for Wind Energy Storage). The current version of these codes also includes solar-photovoltaic energy systems modeling. This program was conducted under the sponsorship of the Division of Energy Storage Systems, DOE, under the direction of Dr. G. C. Chang, and was administered by the NASA-Lewis Research Center Thermal and Mechanical Storage Section with Mr. L. H. Gordon and Mr. R. H. Beach as Project Managers.

This report is in two volumes.

- I. Technical Report
- II. UNIVAC Operation Manual Revisions

The Boeing principal investigator for this program was Dr. A. W. Warren. Co-investigators were Dr. Y. K. Chan and Dr. M. H. Dwarakanath.

IMAGE IV  
**INTENTIONALLY BLANK**

## TABLE OF CONTENTS

	<u>Page</u>
<b>1.0 INTRODUCTION</b>	1
1.1 SIMWEST OVERVIEW	2
1.2 SIMWEST LIBRARY	3
1.2.1 Storage Subsystems	8
1.2.2 Logic Components	13
1.3 SIMWEST OUTPUT	15
1.4 TESTING	16
1.5 PROGRAM USAGE	18
<b>2.0 SOLAR PHOTOVOLTAIC COMPONENT MODELS</b>	21
2.1 PHOTOVOLTAIC MODEL TEST CASE	23
2.2 FLAT PLATE COLLECTOR MODEL	23
2.3 FRESNEL LENS COLLECTOR MODEL AND INCREMENTAL COSTS	29
<b>3.0 HYBRID SOLAR TEST CASE</b>	43
3.1 SYSTEM DESCRIPTION	43
3.2 DAILY SYSTEM PERFORMANCE	51
3.3 MONTHLY POWER GENERATION	60
3.4 LOAD SERVICE PERFORMANCE	63
3.5 SUMMARY	69
<b>4.0 TECHNICAL APPROACH FOR POWER DYNAMICS LIBRARY</b>	71
4.1 BACKGROUND	71
4.2 GENERAL PROBLEM FORMULATION	74
4.3 LOAD FLOW INITIALIZATION	77
4.4 NETWORK COMPONENT MODEL	82
4.5 SYNCHRONOUS MACHINE MODEL	85
4.5.1 Synchronous Machine Model	85
4.5.2 Current Injection Component	88
4.6 INDUCTION MACHINE MODEL	89
4.6.1 Current Injection for Induction Machine	93
4.7 WIND TURBINE MODEL	94
4.8 SUMMARY CONCLUSIONS	98
<b>5.0 REFERENCES</b>	101

## LIST OF FIGURES AND TABLES

	<u>Page</u>
1.1-1 SIMWEST Program Organization	4
1.2-1 Pneumatic Storage Subsystem	9
1.2-2 Pumped Hydro Storage Subsystem	10
1.2-3 Flywheel Storage	11
1.2-4 Battery Storage	11
1.2-5 Thermal Storage	12
1.2-6 Example of Power Divider and Accumulator Use	14
1.3-1 Cost Monitor Output for Fresnel Lens Model	17
2.1-1 PV Test Case Input Data	24
2.1-2 Solar Array Characteristic Current - Voltage Curves	25
2.1-3 Solar Array Output Power Versus Voltage	26
2.2-1 Flat Plate Collector Model Input Data	27
2.2-2 Flat Plate Model Schematic	28
2.2-3 Global Horizontal Radiation Versus Time	30
2.2-4 Tilt Angle Versus Time for Horizontal E-W Axis Tracking	31
2.2-5 Solar Cell Temperature Versus Time	32
2.3-1 Fresnel Lens Model Input Data	33
2.3-2 Fresnel Lens Model Schematic	35
2.3-3 Solar Cell Temperature for One Week Simulation	36
2.3-4 Photovoltaic Array Output for One Week Simulation	37
2.3-5 Thermal Load Demand for One Week Simulation	38
2.3-6 Thermal Storage Temperature for One Week Simulation	39
3.1-1 Hybrid Solar Test Case Model	44

## FIGURES (Continued)

	<u>Page</u>
3.1-2 Hybrid Model Generation Input Data	46
3.1-3 Line Printer Model Schematic	47
3.1-4 Daily Load Profiles for Hybrid Model	49
3.2-1 Collector Solar Insolation Time History	52
3.2-2 Wind Speed Time History	53
3.2-3 Battery Energy Storage - Hybrid Model	54
3.2-4 Flywheel Energy Storage - Hybrid Model	55
3.2-5 Thermal Energy Storage - Hybrid Model	56
3.2-6 Battery Energy Storage - Solar P-V Model	57
3.2-7 Flywheel Energy Storage - Solar P-V Model	58
3.2-8 Thermal Energy Storage - Solar P-V Model	59
3.3-1 Average Monthly Output Power for Hybrid Model	61
3.3-2 Histogram of Wind Turbine Output Power - May	62
3.3-3 Histogram of Solar Array Output Power - May	62
3.3-4 Average Monthly Output Power - Wind Model	64
3.3-5 Average Monthly Output Power - Solar P-V	65
3.4-1 Average Monthly Power Distribution	66
3.4-2 Monthly Thermal Load Service - Hybrid Model	67
4.2-1 Example Power Network Schematic	76
4.2-2 Example SIMWEST Model Schematic	78
4.3-1 Control Schematic to Initialize Example Model	82
4.5-1 Network and d-q Axis Coordinates	86
4.6-1 Steady State Circuit for Induction Machine	91

## **FIGURES (Continued)**

	<u>Page</u>
4.7-1 Wind Turbine/Generator Model Schematic	95
4.7-2 Coefficient of Power Design Curves	96
4.7-3 Turbine Shaft Dynamics	97

## **TABLES**

	<u>Page</u>
1.1-1 SIMWEST User Oriented Features	5
1.2-1 SIMWEST Library Components	6
1.2-2 Partial List of Component Inputs and Outputs	12
2.0-1 Solar-Photovoltaic Components	22
2.3-1 Incremental Cost Calculations	42
3.1-1 Hybrid Model System Description	48
3.1-2 Test Case Load Matching Parameters	50
3.4-1 Average Storage System Statistics	68
4.4-1 EASY Program Analysis Capability	73

## 1.0 INTRODUCTION

The need for computer models of energy storage for solar energy systems (wind, thermal, heating and cooling, and photovoltaic) is generally recognized. Although a number of computer programs have been developed for specific solar applications, these programs generally have lacked flexibility or comprehensive modeling capability. A general purpose, user oriented, and highly adaptable software program was needed for solar systems research and concept evaluation. In November of 1976, NASA-Lewis as project manager for the Energy Research and Development Administration, awarded a contract to Boeing Computer Services (BCS), to develop such a model. It is called SIMWEST (Simulation Model for Wind Energy Storage). SIMWEST was required to have the capability of modeling wind energy/storage systems utilizing any combination of five types of storage (pumped hydro, battery, thermal, flywheel and pneumatic). The level of detail specified was consistent with evaluating long term economic feasibility and performance of wind energy systems.

To meet these requirements BCS developed SIMWEST based upon an existing dynamic simulation program (EASY). It consists of a library of system components and a precompiler program which allows these components to be put together in building block form. A simulation program is then used for system evaluation. SIMWEST was originally developed to run on the UNIVAC 1100 series of computers.

In July 1978, BCS was awarded a follow-on contract to expand the capabilities of the SIMWEST computer codes. Three areas were selected for further development:

- Expansion of the SIMWEST component library, to include solar-photovoltaic in addition to wind-energy generation systems,
- Extension of program availability and support for both CDC and UNIVAC program versions.

- Specification of dynamic library components and additional analyses for evaluation of wind energy and storage system power transients,

An initial evaluation of the power transient requirements indicated that to achieve the required degree of generality and user capability was not within the scope of the present contract. Subsequent program effort was then focused on the first two areas. The expanded SIMWEST codes enable a user to model a large variety of solar systems utilizing;

- Solar-photovoltaic and/or wind power generation
- Five types of energy storage
- User specified system and control logic
- Utility and backup generation

The simulation program has proven to be efficient and versatile for performing parametric studies and for evaluating concept feasibility. SIMWEST is now available and documented for use on the UNIVAC 1100, CDC 6000 and CDC Cyber series computers.

This report provides an overview of the SIMWEST program and a technical discussion of the work accomplished under the SIMWEST follow-on contract DEN3-42. Section 1 presents a general overview of SIMWEST modeling and simulation capability. Section 2 describes the solar-photovoltaic components and presents several test case models illustrating their usage. Section 3 provides test case results which illustrate the capability of the SIMWEST library to model complex wind or solar systems including storage, loads, and system logic. Section 4 describes the technical approach recommended for power transient analyses and presents details of the component models formulated for the dynamic library.

## 1.1 SIMWEST OVERVIEW

SIMWEST consists of two basic programs, and a library of generation, storage, environmental, and load components. The first program, the Model Generation

Program, is a precompiler which generates computer models (in FORTRAN) of complex energy generation/storage systems, from user specifications using SIMWEST library components. The second program utilizes the resulting computer model to perform cost and power utilization analysis. It handles input, output, integration of system dynamics, and iterates to obtain convergence of implicit variables. The combination of these two programs provides a powerful tool for analyzing alternate generation and storage system designs.

Figure 1.1-1 shows the general organization of the SIMWEST program. In addition to the two programs described above, there is a third which performs file maintenance. It is used to incorporate user supplied data for new subsystem models. Although the program is shown as a number of subprograms, it can be executed as a single batch program by supplying the model description cards and the control cards describing the desired analysis to be performed and the desired tabular and/or plotted output.

The SIMWEST model generation and simulation programs have a number of user oriented features which greatly enhance the value of the codes. Some of the more prominent features are shown in Table 1.1-1. These features and the supplemental components described in 1.2 enable the user to quickly build, debug, simulate and interpret alternative system designs.

## 1.2 SIMWEST LIBRARY

The SIMWEST library is listed in Table 1.2-1. It is made up of six types of components: environmental, generation, load, logical, storage and supplemental. The two character mnemonic names are used to identify components in the users model.

The degree of detail in the component models is based upon two design criteria. First, all models should contain sufficient detail to simulate all physical characteristics and constraints having significant impact on system cost effectiveness. Second, the models should be designed to minimize computer time

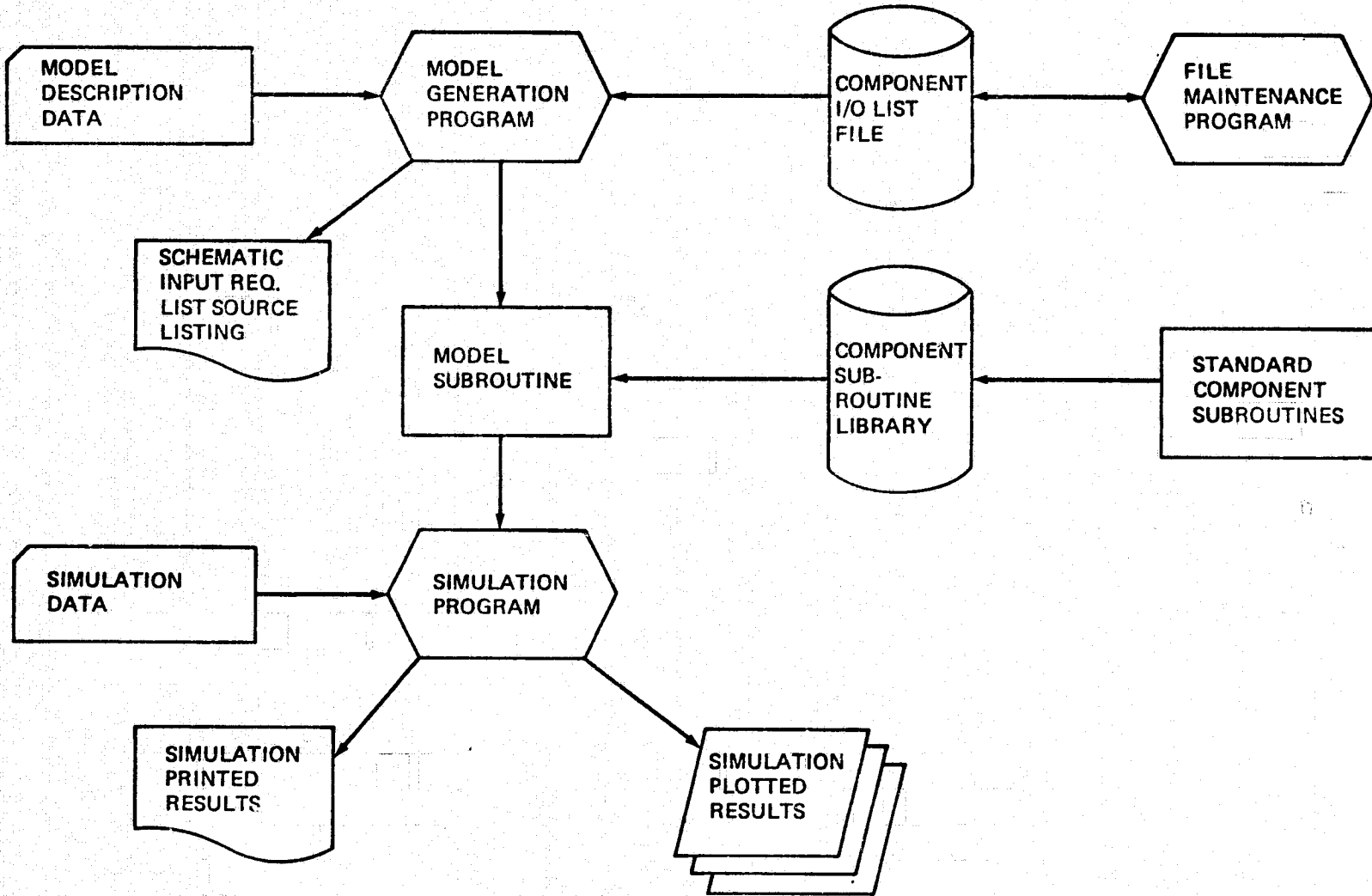


Figure 1.1-1 SIMWEST Program Organization

**Table 1.1-1 SIMWEST User Oriented Features**

**MODEL GENERATION PROGRAM**

- Simplified Component Connections
- Availability of all Input Parameters for Connection
- Fortran Insertion Capability Between Components
- Line Printer Schematic of User's Model Provided
- Automated Naming of Parameters and Variables
- Built-in Diagnostic Capabilities

**SIMULATION PROGRAM**

- Free Field Data Inputs, Including Tables
- Diagnostics on Data Inputs
- Default Values Assigned to Unspecified Parameters
- Optional Levels of Line Printer and Diagnostic Output
- Multiple, Back-to-back Simulation Capability
- Printer Plotter Output of Time Histories and Crossplots

Table 1.2-1 SIMWEST Library Components

<u>ENVIRONMENTAL</u>		<u>BATTERY STORAGE</u>		<u>IV</u> <u>RE</u> <u>BA</u> <u>AD</u>
WIND	WD	INVERTER		
AMBIENT TEMP	TP	RECTIFIER		
TMY WEATHER TAPE	ED	BATTERY		
		ADMITTANCE		
<u>WIND POWER GENERATION</u>		<u>FLYWHEEL STORAGE</u>		<u>MO</u> <u>TR</u> <u>FL</u>
TURBINE/GENERATOR	WP	AC MOTOR		
WIND TURBINE	WT	VARIABLE RATIO TRANSMISSION		
FIXED RATIO TRANSMISSION	GR	FLYWHEEL/CLUTCH		
AC GENERATOR	GE			
<u>SOLAR POWER GENERATION</u>		<u>HYDRO STORAGE</u>		<u>PU</u> <u>HT</u> <u>HS</u>
SOLAR ORIENTATION (TRACKING)	SO	HYDRO PUMP		
FLAT PLATE COLLECTOR	FP	HYDRO TURBINE		
FOCUSING LENS COLLECTOR	FO	HYDRO STORAGE		
PHOTOVOLTAIC ARRAY	PV			
<u>UTILITY GENERATION</u>		<u>PNEUMATIC STORAGE</u>		<u>CO</u> <u>TU</u> <u>HX, HY</u> <u>BN</u> <u>CS</u>
UTILITY	UT	COMPRESSOR		
		TURBINE		
		ADIABATIC HEAT EXCHANGER		
		BURNER		
		PNEUMATIC STORAGE		
<u>LOGIC</u>		<u>Thermal Storage</u>		<u>TS</u>
POWER DIVIDER	PD			
POWER ACCUMULATOR	PA			
PRIORITY INTERRUPT	PI	STORAGE VESSEL		
SWITCHES	SW.SX.SY.SZ			
<u>SUPPLEMENTAL</u>		<u>LOAD</u>		<u>LO</u> <u>TL</u>
SATURATION	SA	ELECTRICAL LOAD		
RANDOM NUMBER GENERATOR	RN	Thermal Load		
TEST FUNCTIONS	AF			
TABLE LOOKUPS	FU,FV			
TRANSFER FUNCTIONS	IT,LA,LL,TF			
<u>SUPPLEMENTAL</u>		<u>Arithmetic Elements</u>		<u>MA, MB, MC</u> <u>CM</u> <u>HG</u> <u>TA</u> <u>TI</u>
		COST MONITOR		
		HISTOGRAM		
		TAPE READ		
		TIME CONVERSION		

and required user specification. It is assumed that a SIMWEST simulation might cover a time span of one year. Thus, from a computer run time and economic impact point of view a simulation step size of between 15 minutes and one hour was established as a design goal.

As a result of the above design criteria, many physical components, such as the electrical components, were modeled mainly in terms of power flow and steady state response. This level of detail is consistent with a 15 minute time step and with the concept that important transients are on the time scale of demand curves or weather patterns, i.e., an hour or more, rather than on the time scale of electric motor transients of a few seconds. If short time transients were to be modeled, additional detail would be required in the component models which would greatly increase the user's task of specifying the model. Further, the simulation time step would have to be reduced and computer runs would be much costlier.

The environmental components listed in Table 1.2-1 simulate environmental conditions. In the present SIMWEST library a user can generate wind speed and ambient temperatures, or can use selected inputs from the recorded weather and insolation data on the Typical Meteorological Year (TMY) tapes for one of 26 U.S. locations. These variables are generally used as inputs to physical components.

The generation components consist of wind generation, solar-photovoltaic and utility routines. The wind turbine-generation components are fairly simple models for computing the power output of a conventional, horizontal axis wind machine given basic machine parameters. The solar-photovoltaic components are somewhat more sophisticated, especially in the collector thermal analysis, and have a number of modeling options which a user may employ, e.g., active or passive cooling.

The storage components encompass such things as motors, generators, transmissions, and flywheels. These components model actual physical hardware

which might be used in a wind or solar energy system. The selection of the particular SIMWEST library set of storage components was based on the requirement that it be capable of modeling the five types of energy storage systems mentioned previously: thermal, flywheel, battery, pumped hydro and pneumatic.

The load components in the SIMWEST library are used to simulate various types of power demand. They also monitor how well the system meets the simulated demand and compute the value of the energy delivered to the load. Like the environmental components, these components may be computed from actual measurement data or from randomly generated data based on user furnished load profiles.

The library's logical components are the power dividers, power accumulators, switches and priority interrupts. Although physical hardware or logic devices could be built to serve the function of the logical components, they are not meant to represent any particular existing hardware. Instead, they are idealized components that allow the user flexibility in modeling a wide variety of system and control logic for operational evaluation of energy storage systems. In practice, the control function might be performed by a control room operator using a predefined control strategy or by use of a process computer.

Finally, the supplemental components include such things as the tape read, the histogram and the cost monitor. These components serve to help the user run the simulation and analyze its results.

### 1.2.1 Storage Subsystems

Figures 1.2-1 through 1.2-5 give possible configurations of the five types of storage subsystems which can be modeled with the present SIMWEST library. For illustrative purposes the number of variables shown passed between components is limited. A description of the variables being passed is given in Table 1.2-2.

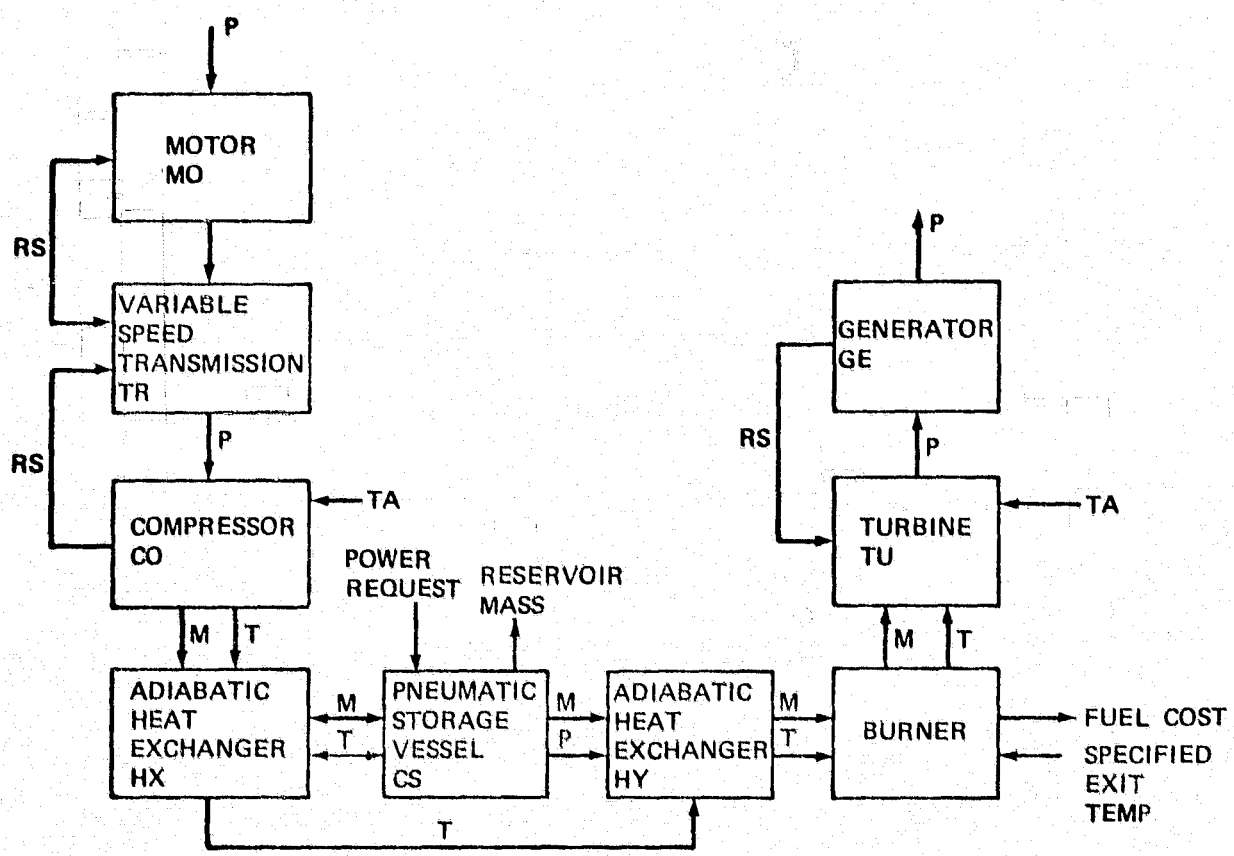


Figure 1.2-1 Pneumatic Storage Subsystem

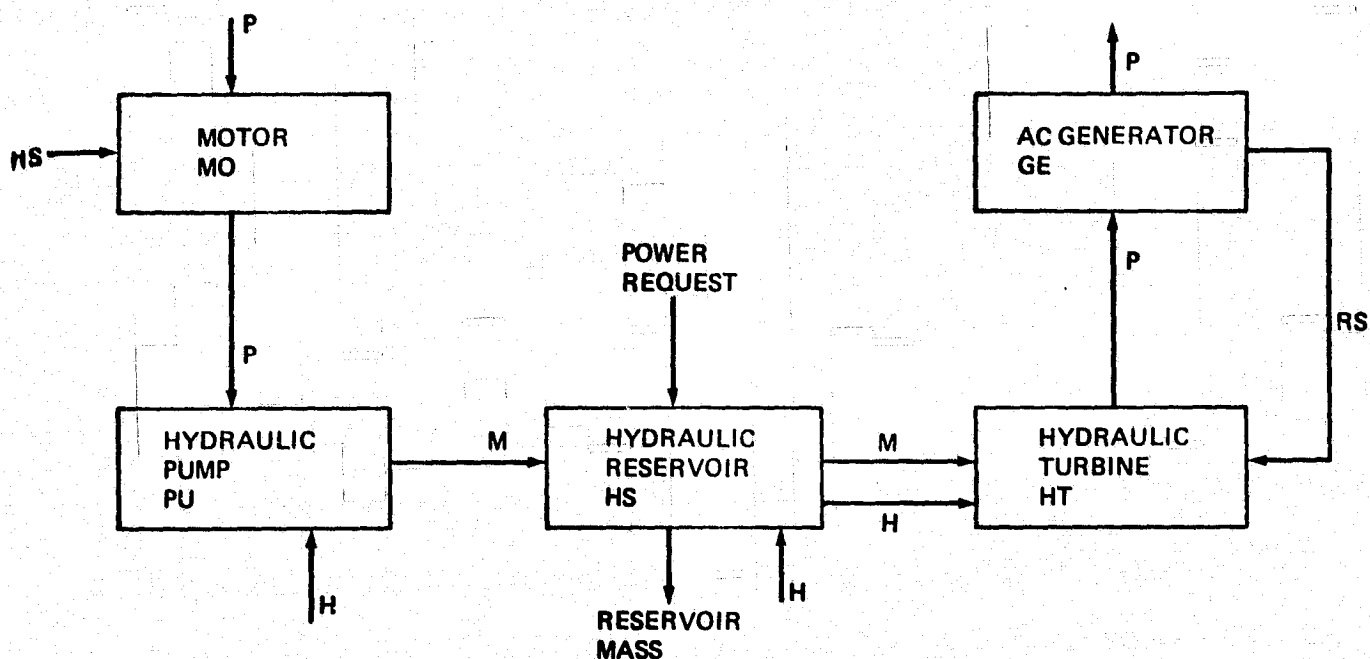
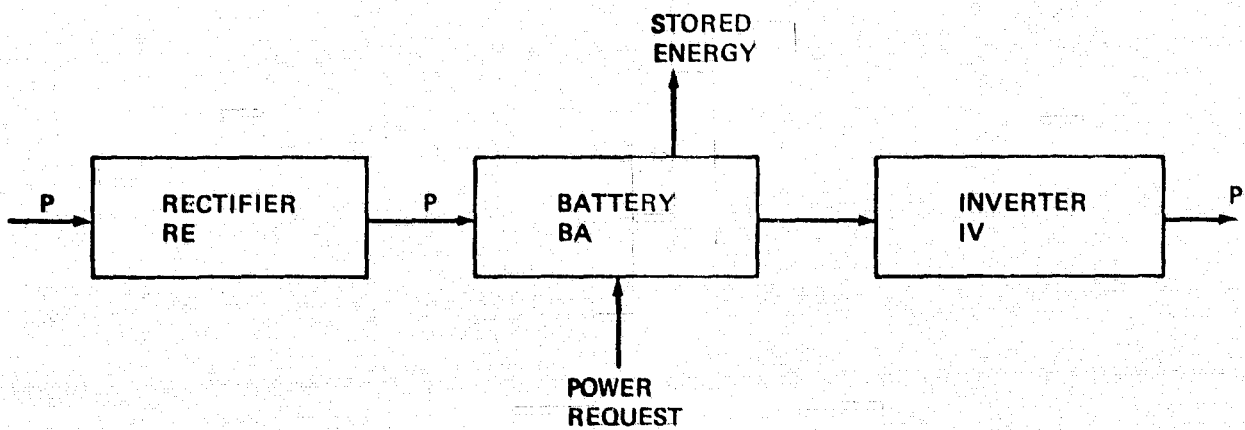
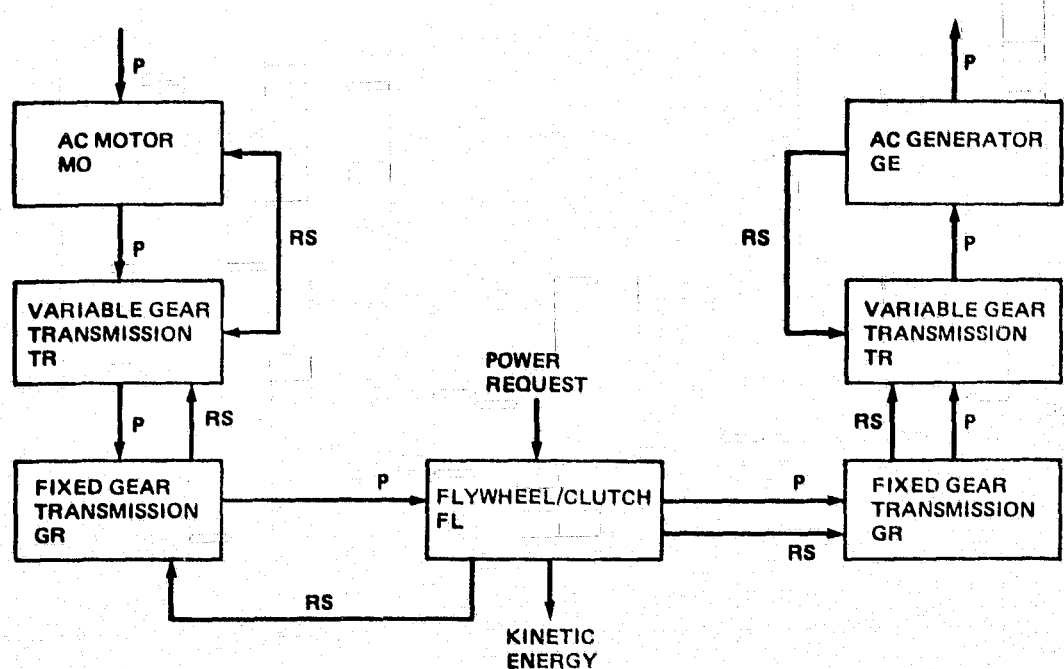
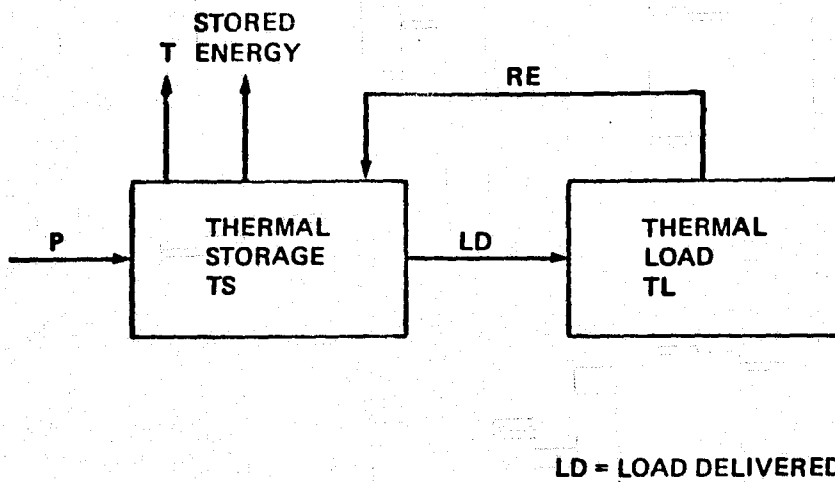


Figure 1.2-2 Pumped Hydro Storage Subsystem





**Figure 1.2-5 Thermal Storage**

**Table 1.2-2 Partial List of Component Inputs and Outputs**

<u>SYMBOLS</u>	
P	POWER
RE	POWER REQUEST
MP	MAXIMUM POWER
RS	ROTOR SPEED
T	TEMPERATURE
TA	AMBIENT TEMPERATURE
M	MASS FLOW RATE
H	RESERVOIR HEIGHT
LD	THERMAL LOAD DELIVERED
WV	WIND VELOCITY
GR	GEAR RATIO
EF	EFFICIENCY
INT	INTERRUPT FLAG
PR	PRESSURE
PS	PRIORITY SEQUENCE
WY	WEEK OF YEAR
DW	DAY OF WEEK
TD	TIME OF DAY
SP	SURPLUS POWER

A total energy system will generally be made up of elements from a number of different subsystems (see Figure 1.2-6). In addition, the SIMWEST program can be used for models which include networks of storage subsystems of the same type or a network of wind or solar generators.

### 1.2.2 Logic Components

The capability for modeling complex system control logic is provided by the power divider, power accumulator and priority interrupt components. Both the divider and accumulator operate on a priority basis. The priority interrupt is used by other system components to change the priority setting of the divider and accumulator.

The power divider has one input power port and four output power ports (not all output ports need be used for a given simulation). The divider also has an input request associated with each of its output ports. A power request originates with a component which is directly or indirectly connected to an output port. The user specifies priorities of either 0, 1, 2, 3, or 4 to be associated with each of the output ports. If the input power exceeds that requested of the port with highest priority (priority 1) then the excess power goes to the port with the next priority. This process continues until either all power is distributed or all requests of non-zero priority ports are met. A port with zero (0) priority does not receive power. Such ports are included to model backup or switch operated components. In these situations, the connected component would change the zero priority setting of the power divider by use of a priority interrupt. Two or more ports may be assigned the same priority in which case the user may specify weights to be associated with each port. Then if there is not enough power available to satisfy all requests of equal priority, the power is divided between them in proportion to the user specified weights.

The power accumulator is similar to the divider except that instead of distributing power from a single input port among four output ports, it accumulates

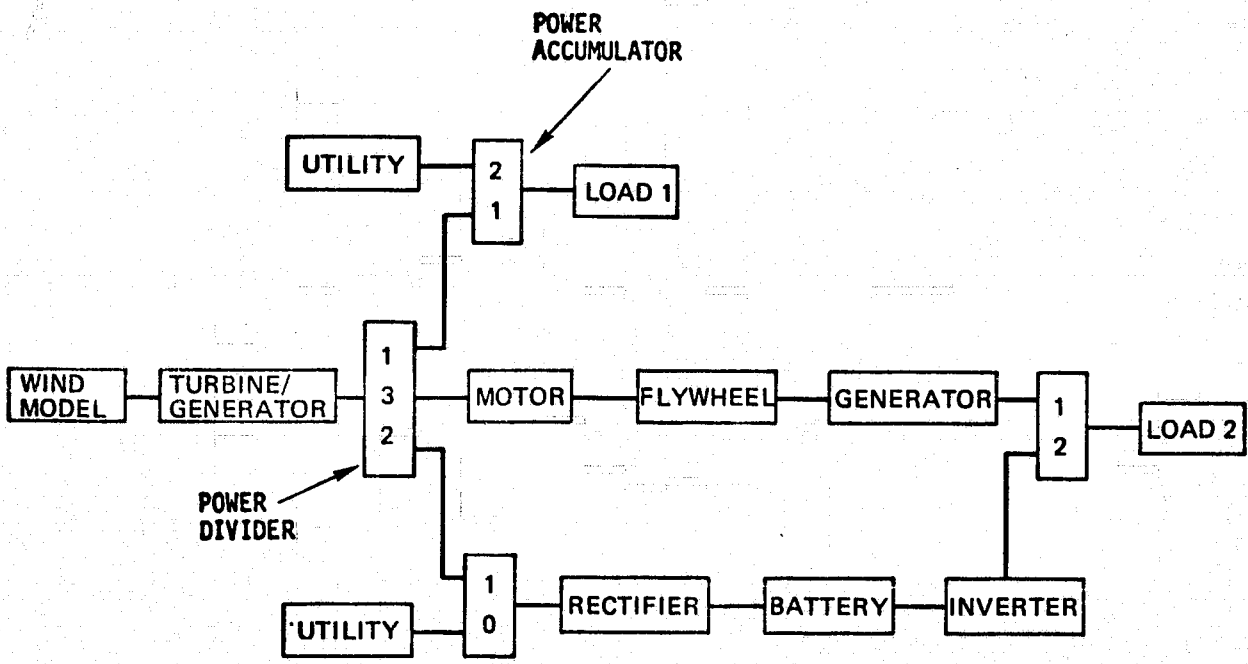


**Figure 1.2-6 Example of Power Divider and Accumulator Use**

power from four input ports and sends it out through a single output port. The power accumulator accepts power requests from the downstream component and allocates requests to each of its input ports in order to service the downstream component.

An example illustration of the use of power dividers and power accumulators is given in Figure 1.2-6. It is seen that power from the turbine/generator is distributed with highest priority (priority 1) going to the power accumulator that services load 1. Since the power accumulator servicing load 1 has its priority 1 input port connected to the power divider, it will try first to satisfy load 1 from the turbine/generator and then from the utility. If the power divider satisfies load 1 and there is power left over, it will be used to satisfy the request from the battery. Finally, if the battery is full or if its charging rate is met, then the excess power goes to the flywheel. The battery also has a priority zero connection to the utility. If the battery remains in a discharge state for more than a specified amount of time, it can change the utility priority (from 0 to 1) to receive needed power.

Also in Figure 1.2-6, we see that load 2 prefers to draw power from the flywheel before turning to the battery. This configuration tends to keep the flywheel as discharged as possible, using it primarily as a means to absorb large influxes of power.

### 1.3 SIMWEST OUTPUT

There are three basic forms of SIMWEST output to facilitate the analysis of wind and solar energy storage systems; line printer plots, histograms of system variables and time sequenced output of variable values. Each SIMWEST library component is associated with a number of output variables. Prior to simulating a given system the user may select any of these outputs for plotting or tabular output. For example, he may want to plot the energy of pneumatic storage as a function of time and/or as a function of temperature. If the user wants a time sequenced listing of all variable values, he may specify the time step between

printouts. The listing of all variables has proven to be a useful tool in understanding the performance of the system under consideration and a valuable aid in validating the system design.

SIMWEST also provides a special output which computes life cycle and leveled energy costs per kwh. This output is produced by the cost monitor component and is illustrated in Figure 1.3-1. The leveled energy costs are based on energy delivered to the loads during a simulation and forecasted to a full years' system operation. This output permits direct comparison of capital and energy costs for alternative system configurations, enabling a user to perform economic trade studies and system sizing.

#### 1.4 TESTING

Reference [1] describes two simulation studies which were used to test the original SIMWEST program. Section 3 describes the NASA-Lewis approved simulation studies for the expanded SIMWEST program. These studies provide an excellent test and illustration of the program's capability to model complex wind/solar energy systems.

Prior to performing the simulation studies and throughout its development the SIMWEST program was systematically tested. First components were grouped into simple systems and simulations were performed. During these simulations system parameters were driven so as to force the individual components through every normal program path and to assure that all component outputs assume a wide range of values. The number of components and the number of ways they can be connected makes it impossible to exercise every combination. However, the subsystem groupings that were used were representative of the expected program usage. Section 2 describes some of the test cases for the solar-photovoltaic generation components.

The test cases and simulation studies revealed that the code is reasonably efficient for system parameter studies. Even on very complex systems, such as

## SOLAR/WIND ENERGY STORAGE COST SUMMARY

20 YEAR LIFE CYCLE

### • YEARLY SYSTEM COSTS

CAPITAL COST (INCLUDING FIXED CHARGES)	526. \$
FIXED O + M COST	107. \$
OPERATING + FUEL COST	14. \$
TOTAL	646. \$

### • ENERGY DELIVERED

ENERGY DELIVERED 7445. KWH

ENERGY COST PER KWH 86.8 MILLS

VALUE OF ENERGY DELIVERED 372 \$  
(VALUE OF FUEL SAVED)

ENERGY VALUE PER KWH 50.0 MILLS

COST PER VALUE DELIVERED 1.74

### • LOAD FACTOR

PERCENT OF LOAD SUPPLIED 100.0  
BY TOTAL SOLAR SYSTEM

PERCENT OF LOAD SUPPLIED 0.0  
BY UTILITY

PERCENT OF SOLAR ENERGY 0.0  
SURPLUSED

COST TO MEET LOAD 86.8 MILLS  
(SOLAR + UTILITY)

Figure 1.3-1 Cost Monitor Output For Fresnel Lens Model  
(Example Only)

represented by the NASA-Lewis test case, convergence of logic variables was quite rapid. Convergence generally took place in less than six iterations per simulation time step. As an example, the year simulations used in the NASA defined parameter study of Reference [1] took less than 420 CPU seconds on the CDC 6600. For comparison, the CPU time on the UNIVAC 1100/40 is approximately two to three times as great as that on the 6600, and CPU time on the Cyber 175 is a factor of two to three times smaller than that of the 6600.

### 1.5 PROGRAM USAGE

During the testing it became clear that while the user need not be a SIMWEST expert or software specialist to make efficient use of the program, he should thoroughly think through and be familiar with the characteristics of the system he wants to simulate. Component models, if not carefully specified, may perform in unexpected ways. If the systems logic is not well thought out, the resulting system may be significantly out of balance and subsystems may not be fully utilized. The test case described in Section 3 illustrates the process of sizing and logic adjustment to satisfy system performance objectives.

A number of useful procedures were developed during the simulation studies. First it was found that when simulating a complex system, it is best to separately develop and test subsystem portions of the model. This allows problems or unexpected results to be isolated and understood prior to the introduction of the more complex characteristics associated with the total system.

It was found during the simulations that the use of Fortran statements in the model definition is very useful for creating special input to system components and for defining special outputs to be plotted or statistics to be printed. For example, Fortran statements enable the user to generate and interpret trade study data by computing component input parameters from user specified system parameters. The use of Fortran statements is simple and should be encouraged early in SIMWEST applications.

Computer simulation costs may be minimized by appropriate tradeoffs between run time and simulation accuracy. Run time is most directly affected by the integration step size, the total simulation length, and the average number of iterations through the model at each time step. For long duration runs, an hour step size is usually acceptable. Models having smaller time constants than the step size may be approximated by implicit steady state conditions and solved by iteration through the model. If a model requires many iterations for convergence then it may be useful to isolate the source of instability in order to modify or simplify that portion of the system model. It has been generally found in the simulation studies that use of a few seasonal weekly simulations is adequate to predict long term performance for system trade studies and design optimization. Based on the results of Section 3, four to six week long simulations are recommended for this purpose.

When making a year simulation run, it is best to break it into twelve monthly simulations. Thus, measures of performance such as plots, histograms and performance statistics are available on a monthly basis. In addition to giving better visibility of the system performance, this helps limit the job core size. The twelve monthly simulations can be submitted as a single run with the results of a given month acting as initial conditions for the next month. The user only needs to submit new data cards for data which changes from one month to the next.

## 2.0 SOLAR PHOTOVOLTAIC COMPONENT MODELS

The solar photovoltaic component models added to the SIMWEST library as a part of contract DEN3-42 are briefly described and test case results illustrating their use are summarized in this section.

Table 2.0-1 summarizes the characteristics of the solar-photovoltaic components. The environmental data component is designed to read Typical Meterological Year (TMY) data tapes containing hourly insolation and weather data at 26 U.S. locations. This component can also be used to read other hourly data tapes such as the SOLMET tapes by inputting a user specified format to the model generation program. The solar orientation or tracking component computes the sum of direct beam and global insolation on a flat plate array for fixed orientation and four different beam tracking options. The flat plate and focusing lens collector components provide detailed thermal analyses for determining average solar cell temperature. The collector models, and that of the solar array are based on similar models developed at Sandia Laboratories for the SOLCEL program. (Reference [4]). The array component model is a simplified model based on scaling the characteristics of a single solar cell. Array voltage can either be user specified or determined by a maximum power tracker. It should be observed that the above components are coded in SI (metric) units, whereas most of the SIMWEST components are coded in English units. This is generally not a problem since there are at most only a few interconnection variables between the solar-photovoltaic generation components and other SIMWEST components, and these are easily converted using arithmetic components.

The TMY data tapes are currently the best environmental data sources available for simulating typical yearly solar energy system performance. These tapes were extracted from SOLMET data tapes containing rehabilitated hourly solar and meterological observation data over a period of many years at each observation site. Each Typical Meterological Year was created by statistical selection of a typical meterological month for each calendar month in the long term data base and catenating the 12 months to form a TMY. All of the TMY data files

TABLE 2.0-1 SOLAR-PHOTOVOLTAIC COMPONENTS

<u>COMPONENTS</u>	<u>SYMBOL</u>	<u>PURPOSE</u>
● ENVIRONMENTAL	ED	READ DOE SOLAR INSOLATION AND WEATHER DATA-TYPICAL METEOROLOGICAL YEAR TAPE
● SOLAR ORIENTATION	SO	SOLAR INSOLATION ON TILTED FLAT PLATE ARRAY. (FIVE OPTIONS)
● FLAT PLATE COLLECTOR	FP	FLAT PLATE THERMAL MODEL WITH FLUID AND PASSIVE COOLING OPTIONS
● FOCUSING LENS COLLECTOR	FO	FRESNEL LENS THERMAL MODEL WITH FLUID AND PASSIVE COOLING OPTIONS
● PHOTOVOLTAIC ARRAY	PV	CONVERTS SOLAR INSOLATION TO D.C. ELECTRICAL POWER. MAXIMUM POWER TRACKER OR USER SPECIFIED VOLTAGE

are available for use by a SIMWEST user. He thus has access to a high quality environmental data base for solar energy simulations and system analyses.

## 2.1 PHOTOVOLTAIC MODEL TEST CASE

The input data for the photovoltaic model test case is shown in Figure 2.1-1. The purpose of this model is to obtain characteristic current voltage curves for the default solar array parameters. Fortran statements are used in the model generation data to let the terminal voltage range between 0 and 204 volts for solar insolation values of 5, 20, and 50 suns ( $1 \text{ sun} = 1000 \text{ W/m}^2$ ). Cell temperature is specified at  $25^\circ\text{C}$  for the first simulation and  $55^\circ\text{C}$  for the second. Figure 2.1-2 shows the current voltage curves and Figure 2.1-3 shows power voltage cross plots at the lower cell temperature and for the three solar insolation levels. These curves verify the physical characteristics of the solar cell model. It may be noted in these figures that current and output power become negative when the specified voltage exceeds the array open circuit voltage. Individual cell characteristics may be obtained by dividing voltage by 300 (default number of cells in series) and by dividing current by 500 (default number of cells in parallel).

## 2.2 FLAT PLATE COLLECTOR MODEL

The input data for the flat plate model test case is shown in Figure 2.2-1. The purpose of this model is to illustrate water and wind cooling of the collector and to test the tracking options of the orientation component S0. There are six 1-1/2 day simulation runs. The first run uses water cooling (CMOFP=2), a single glass cover over the front plate and insolation on the back. The second run uses passive cooling (CMOFP=0), no plate insulation and fins on the back to cool the collector. In the first two runs, the collector is tilted and has a fixed, southward facing orientation (MO S0=1). The last four runs are similar to run 2 except different tracking options are utilized.

The model schematic produced by the model generation program is shown in Figure 2.2-2. The component TI is used to furnish time of day and day of year

MODEL DESCRIPTION      PHOTO-VOLTAIC CURRENT VOLTAGE CURVES  
LOCATION=11      TI  
FORTRAN STATEMENTS  
ST PV=5000  
IF(DY TI,GT,1,5)ST PV=20000  
IF(DY-TI,GT,2,5)ST-PV=50000  
VT PV=8,5\*T0 TI  
LOCATION=53      PV  
END OF MODEL  
PRINT

a) Model Generation Input Data

PARAMETER VALUES  
CYCLES=0, T0 TI=0  
DLINES=50  
TC PV=25  
RC PV=1  
PRINTER PLOTS, DISPLAY1  
V PV, VS, TIME  
I PV, VS, V PV  
P PV, VS, V PV  
P PV, VS, TIME  
TINC=.5, TMAX=72, PRATE=24, PRINT CONTROL=3, INT MODE=3, OUTRATE=1  
TITLE=PHOTO-VOLTAIC CELL CURRENT VOLTAGE CURVES  
SIMULATE  
PARAMETER VALUES  
TG PV=55  
SIMULATE

b) Simulation Program Input Data

Figure 2.1-1 PV Test Case Input Data

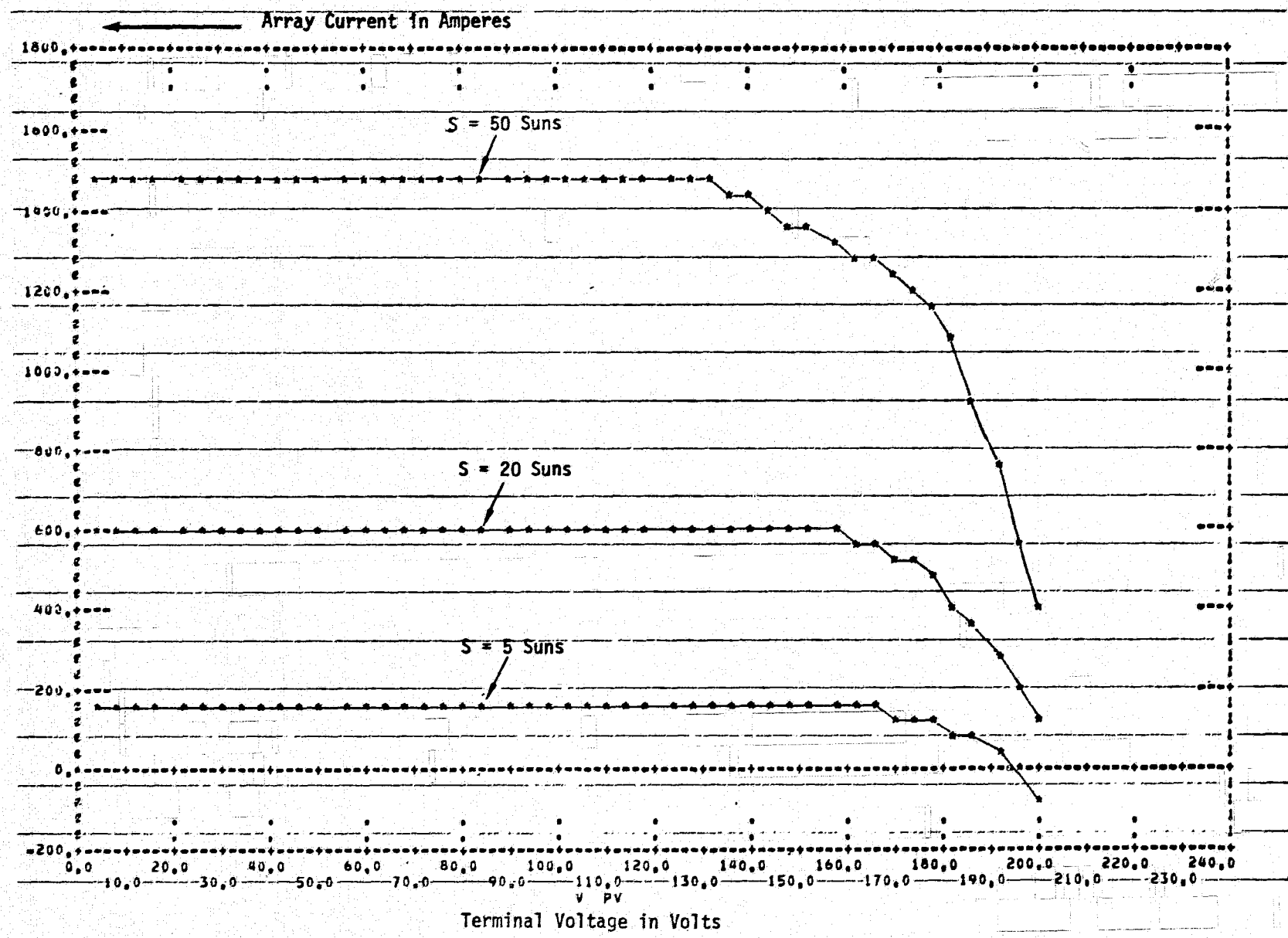


Figure 2.1-2 Solar Array Characteristic Current - Voltage Curves

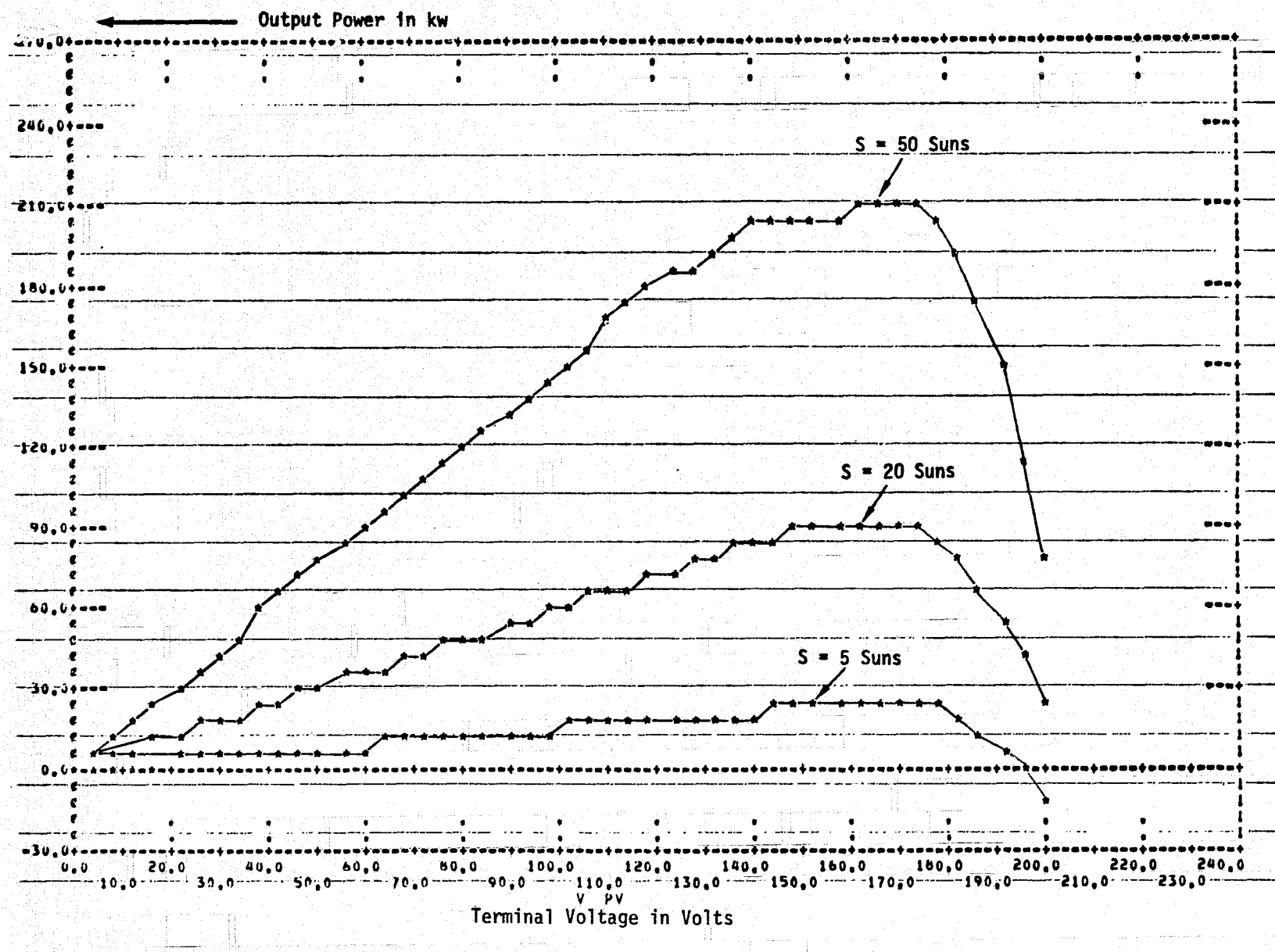


Figure 2.1-3 Solar Array Output Power Versus Voltage

MODEL DESCRIPTION	FLAT PLATE TEST CASE		
LOCATION=11	TI	INPUTS=TI	
LOCATION=35	ED	INPUTS=TI,ED(X1=SB,X2=ST)	
LOCATION=53	SD	INPUTS=SD,ED(X4=WD,X3=TA)	
END-OF-MODEL			
PRINT			

a) Model Generation Input Data

PARAMETER VALUES

CYCLES=2.01,T0 TI=36,TFIFP=10,TFDFP=30,MFMFP=.02,CMOFP=2,NG FP=1,  
DLINES=50  
HI FP=.01  
CW FP=1,CL FP=2,NT FP=10,CC FP=1000,CM FP=10,CPOFP=.01,LA SD=29,733,  
TL SD=29,733,AA SD=2

PRINTER PLOTS, DISPLAY1

TLTSU,VS,TIME

TC FP,VS,TIME

X2 ED,VS,TIME

P1 FP,VS,TIME

TINC=.5,TMAX=36,PRATE=6,PRINT CONTROL=3,INT-MODE=3,OUTRATE=1

TITLE=FLAT PLATE COLLECTOR TEST CASE

SIMULATE

PARAMETER VALUES

CMOFP=0,HI FP=1,E9,FIRFP=4

SIMULATE

PARAMETER VALUES

MO SD=2

SIMULATE

PARAMETER VALUES

MO SD=3

SIMULATE

PARAMETER VALUES

MO SD=4

SIMULATE

PARAMETER VALUES

MO SD=5

SIMULATE

b) Simulation Program Input Data

Figure 2.2-1 Flat Plate Collector Model Input Data

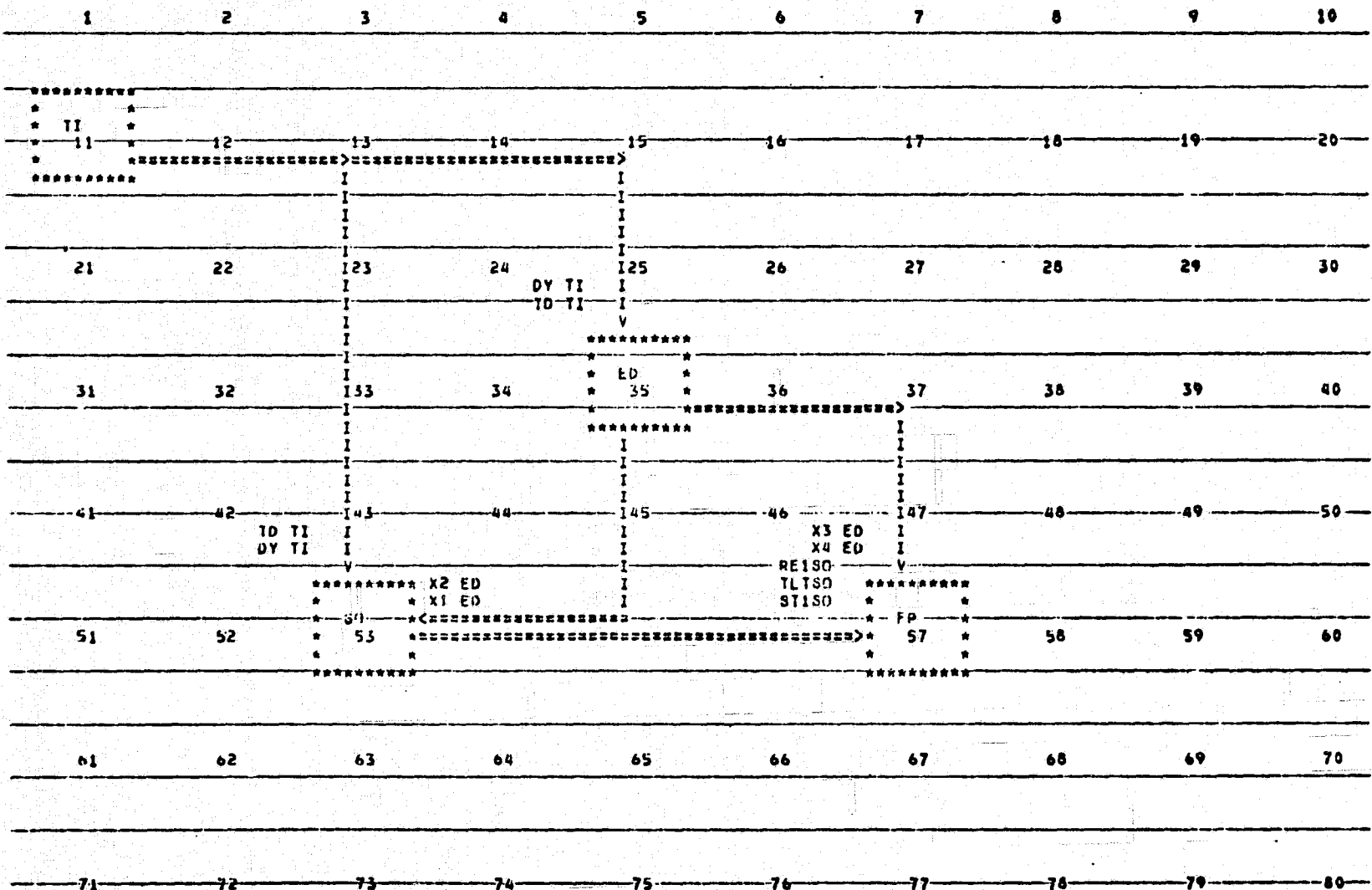


Figure 2.2-2 Flat Plate Model Schematic

information to **SO** and to the TMY read component **ED**. **ED** supplies direct beam and global insolation to **SO**, and ambient temperature and wind speed to the collector component **FP**. Based on collector orientation, **SO** supplies solar insolation incident to the array, collector tilt angle, and tracking power to **FP**.

Typical results of the flat plate model runs are shown in Figures 2.2-3 through 2.2-5. Figure 2.2-3 shows the global horizontal insolation obtained from **ED** during the 36 hour simulation period. The data period was during mid-winter and the daily peak levels are thus low to moderate. The array tilt angle daily pattern for horizontal E-W axis tracking is shown in Figure 2.2-4. At noon the array is oriented normal to the sun's incident rays and thus maximizes the insolation gathered during the mid-day peak. The tilt angle approaches  $90^{\circ}$  as the sun approaches the horizon, and remains fixed at  $90^{\circ}$  overnight. Comparison of the solar insolation peaks with the various tracking options showed that horizontal E-W axis tracking gave the best results of the single axis tracking systems, and was only slightly inferior to two-axis beam tracking. Solar cell temperature for this case is shown in Figure 2.2-5. The cell temperature is within a few degrees of ambient most of the day and rises in mid-day proportional to the solar insolation received. The results with water cooling are quite similar.

### 2.3 FRESNEL LENS COLLECTOR MODEL AND INCREMENTAL COSTS

The input data for the Fresnel Lens test case is shown in Figure 2.3-1. The purpose of this model is to illustrate a Fresnel Lens collector model with thermal fluid loops for collector cooling and for solar heating. Three week long simulations are used to demonstrate incremental cost calculations for subsystem economic design. A variable speed pump is assumed for the collector fluid loop with the flow rate adjusted so that the outlet temperature is  $5^{\circ}\text{C}$  greater than the inlet. The collector consists of a rectangular grid of 120 Fresnel lenses each of which focuses solar radiation on a  $5 \times 5$  array of solar cells. Excess thermal energy is conducted to a heat sink surface and then dissipated by natural convection, radiation and heat exchange to the coolant fluid. The collector parameters are chosen for a lens concentration ratio of

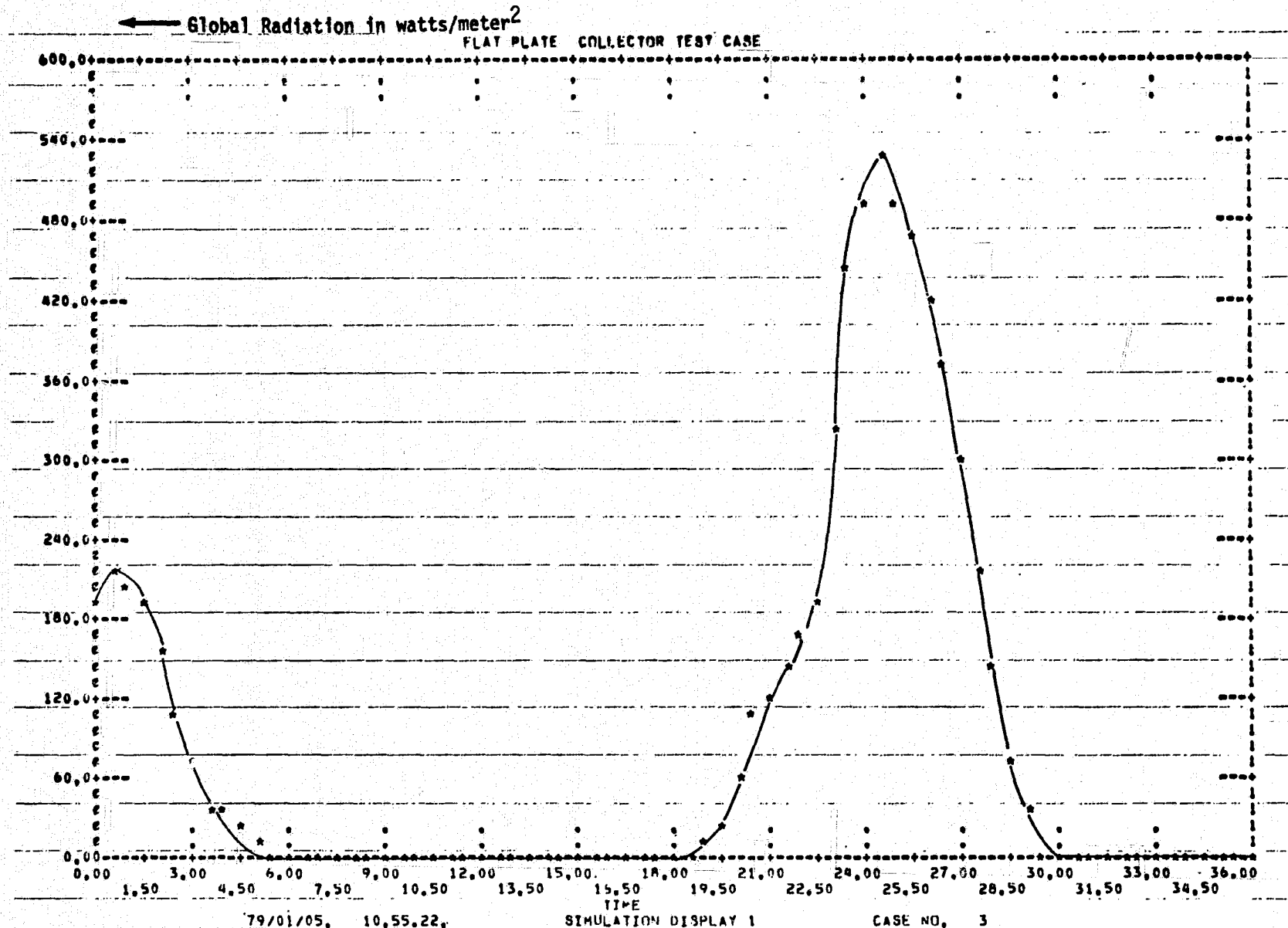


Figure 2.2-3 Global Horizontal Radiation Versus Time

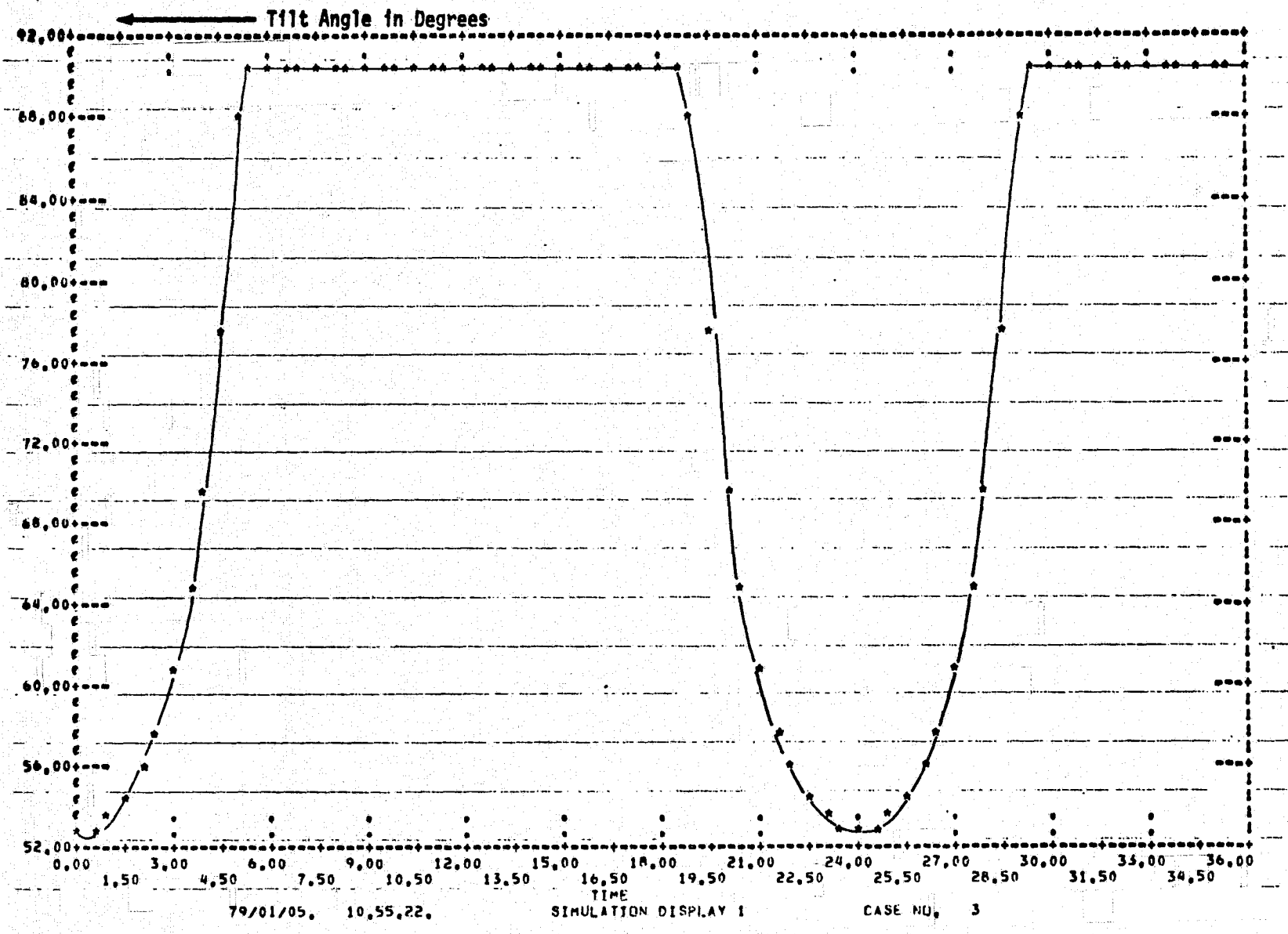


Figure 2.2-4 Tilt Angle Versus Time for Horizontal E-W Axis Tracking

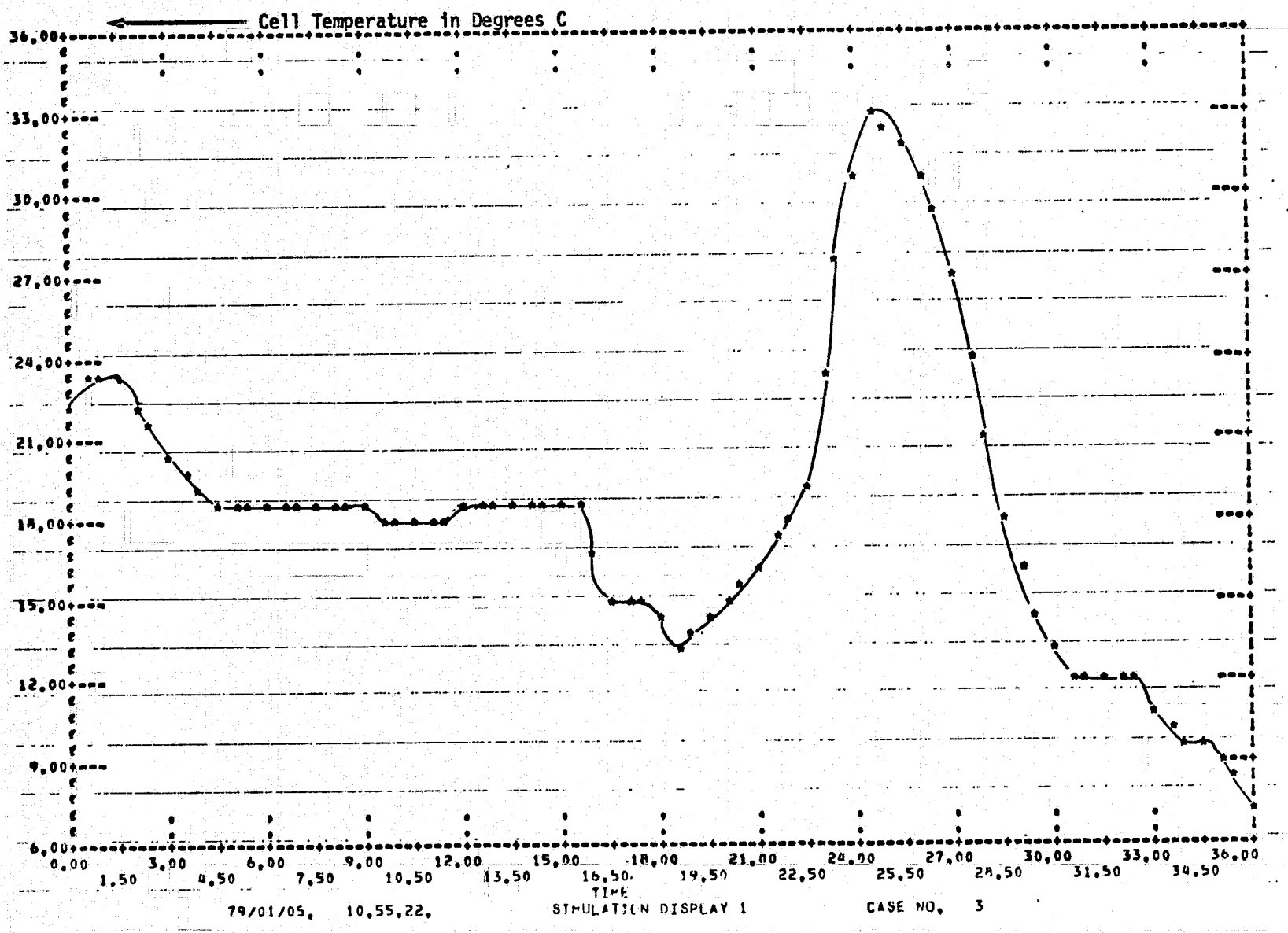


Figure 2.2-5 Solar Cell Temperature Versus Time

MODEL DESCRIPTION : FRESNEL LENS COLLECTOR WITH THERMAL STORAGE AND LOAD  
 LOCATION=11 TI  
 LOCATION=71 ED INPUTS=TI  
 LOCATION=45 MA INPUTS=TS(T=FIN)  
 FORTRAN STATEMENTS  
 $TF0FO = FO \cdot MA + 5.$   
 LOCATION=33 FO INPUTS=ED(X1=ST,X3=TA,X4=WD),MA(FO=TFI)  
 LOCATION=73 PV INPUTS=ED(X1=ST),FO  
 LOCATION=47 TS INPUTS=FO(P,1=P),TL  
 LOCATION=27 TL INPUTS=TI,ED(X3=TA)  
 LOCATION=77 LO INPUTS=PV(P=P,1,P=LO,1)  
 LOCATION=79 CM  
 END OF MODEL  
 PRINT

a) Model Generation Input Data

TITLE=FRESNEL LENS COLLECTOR (INCREMENTAL COST COMPUTATION)  
 PARAMETER VALUES  
 CYCLES=4.01,T0 TI=0,CMOFO=2,CW FO=3.75,CL FO=3.9,DLINES=50  
 NL FO=120,NF FO=24,MFMFO=0.5,CC FO=6.,CM FO=50,HI FO=.01,RC FO=.06  
 TS TS=5,DH TS=.00879,PD TS=12,LE TS=30,NU TS=.01,NC TL=0.2  
 C1 MA=.55556,C2 MA=-17.778, COPFO=0.5  
 CC PV=100,CM PV=50,LE TS=30,CR CM=15,LE CM=20  
 AA PV=0.6,NS PV=600,NP PV=5,RAPPV=1.3  
 VE LO=-.05,VE TL=.05  
 TABLE,HT TS=4  
 .00879,.025491,.047371,.064072  
 90,147,147,204  
 TABLE,TL0TL=4  
 -10,0,10,25  
 4,2,1.5,1  
 TABLE,TWTTL=4  
 0,6,18,24  
 .4,1,1,.4  
 PRINTER PLOTS,DISPLAY1  
 RE TL,VS,TIME  
 E TS,VS,TIME  
 P1 FO,VS,TIME  
 FMDFO,VS,TIME  
 DISPLAY2  
 TC FO,VS,TIME  
 P PV,VS,TIME  
 FO MA,VS,TIME  
 INITIAL CONDITIONS=E TS=80  
 TINC=.5,TMAX=168,PRATE=12,PRINT CONTROL=3,INT MODE=3,OUTRATE=1  
 SIMULATE  
 PARAMETER VALUES, TS TS=5.5  
 SIMULATE  
 PARAMETER VALUES  
 TS TS=5.,NL FO=126,CW FO=3.94,AA PV=0.63,NS PV=630  
 SIMULATE

b) Simulation Program Input Data

Figure 2.3-1 Fresnel Lens Model Input Data

25 and series connection of the output from each array. At maximum output the array collects about 10kw of solar radiation and produces about 1.7kw of electrical power.

The model schematic produced by the model generation program is shown in Figure 2.3-2. The collector thermal loop is formed by the connections between the collector **F0**, the thermal storage **TS**, and the multiply and add component **MA**. The **MA** component is used to convert the thermal storage outlet temperature from degrees fahrenheit to degrees centigrade. The output temperature from **MA** is supplied as the inlet temperature to **F0**. The total thermal power gathered by the coolant fluid is computed in **F0** and supplied to **TS**. Similarly, the thermal load fluid loop is represented by a power request from the load component **TL** to **TS** and by thermal power delivered from **TS** to **TL**. The electrical output of the array is computed by **PV** and supplied to a load component **LO** which monitors the electrical energy collected.

Results of the first week simulation run are summarized in Figures 2.3-3 through 2.3-6. The weather was fairly constant during this run and solar insolation was fairly strong all week. Figure 2.3-3 shows that with water cooling cell temperature was held to less than 70°C at peak insolation. In fact, about 60% of the solar energy incident on the array is exchanged to the coolant fluid during peak insolation. The electrical output of the array is shown in Figure 2.3-4. The fluid flow rate of the pump and thermal energy collected exhibit very similar daily patterns. The thermal load for this week is shown in Figure 2.3-5. This load is dependent on both time of day and ambient temperature which yields the complex load pattern shown. Figure 2.3-6 shows the temperature of the thermal storage vessel resulting from the collector and load thermal loops. The daily cycles are predominant with the periods of strong insolation providing sufficient energy to satisfy the load and compensate for thermal losses. Average load is fairly well matched to solar generation during the week since the temperature remains within a 15° channel and does not have an apparent trend away from this range.



Figure 2.3-2 Fresnel Lens Model Schematic

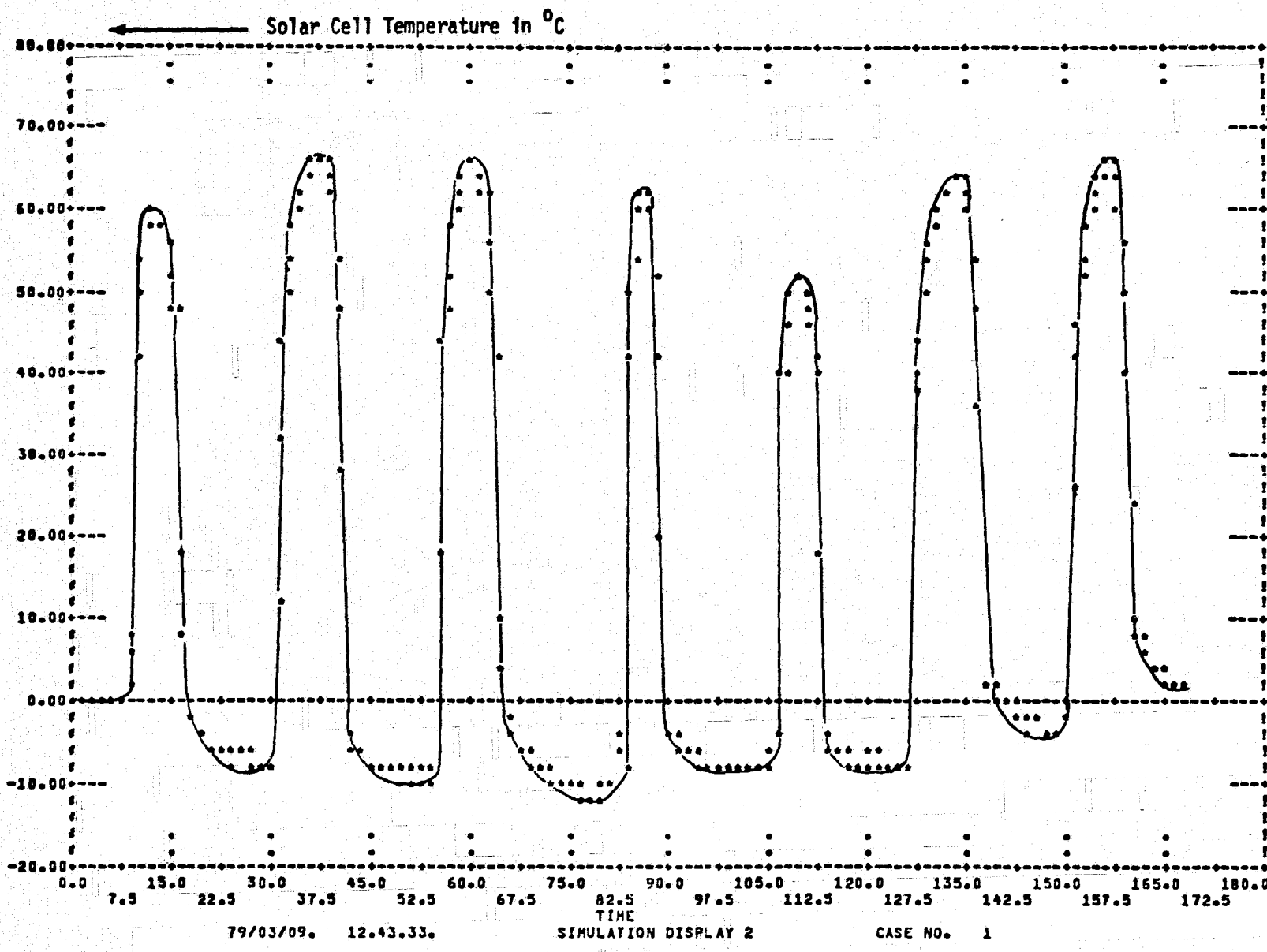


Figure 2.3-3 Solar Cell Temperature for One Week Simulation

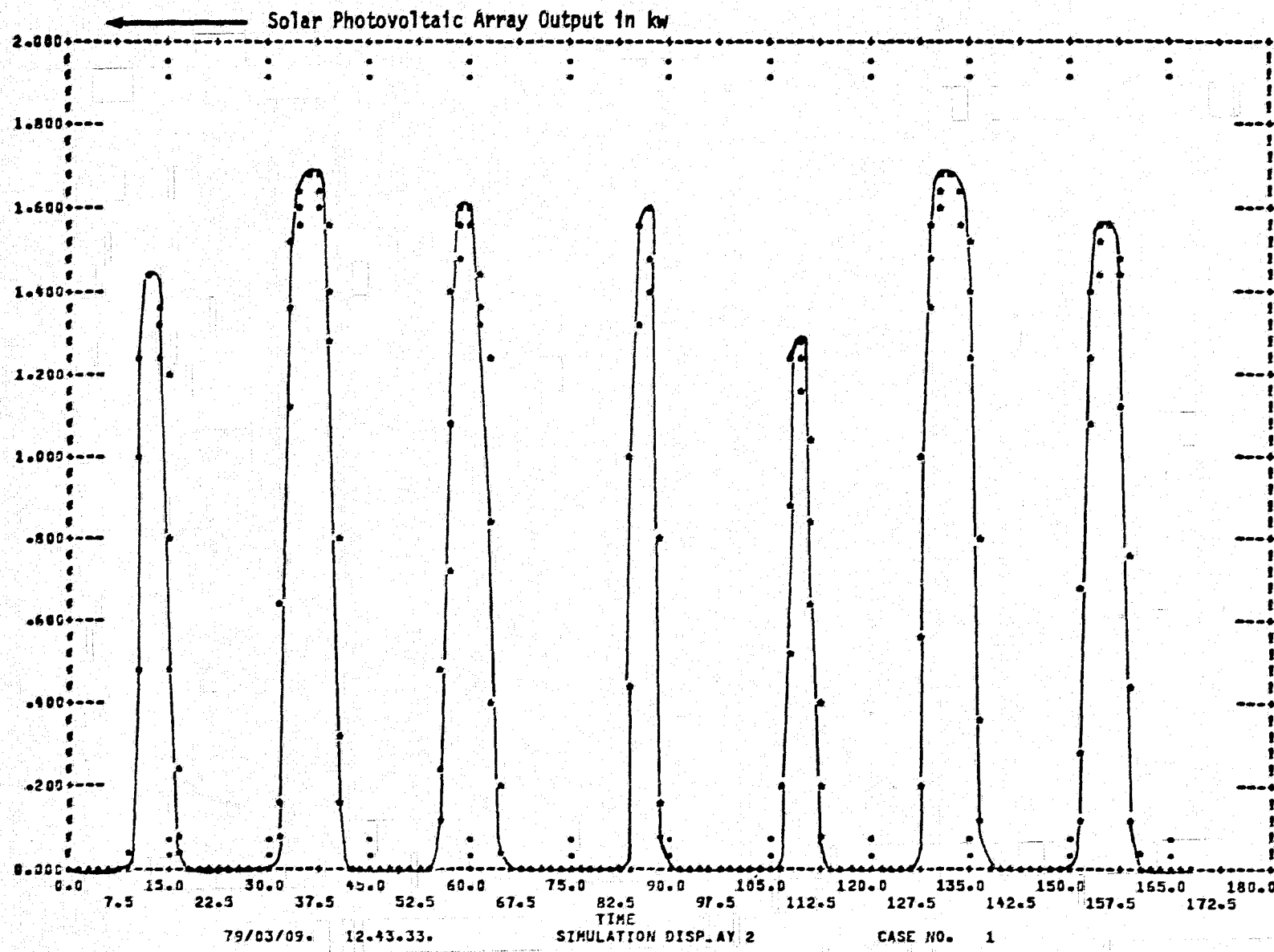


Figure 2.3-4 Photovoltaic Array Output for One Week Simulation

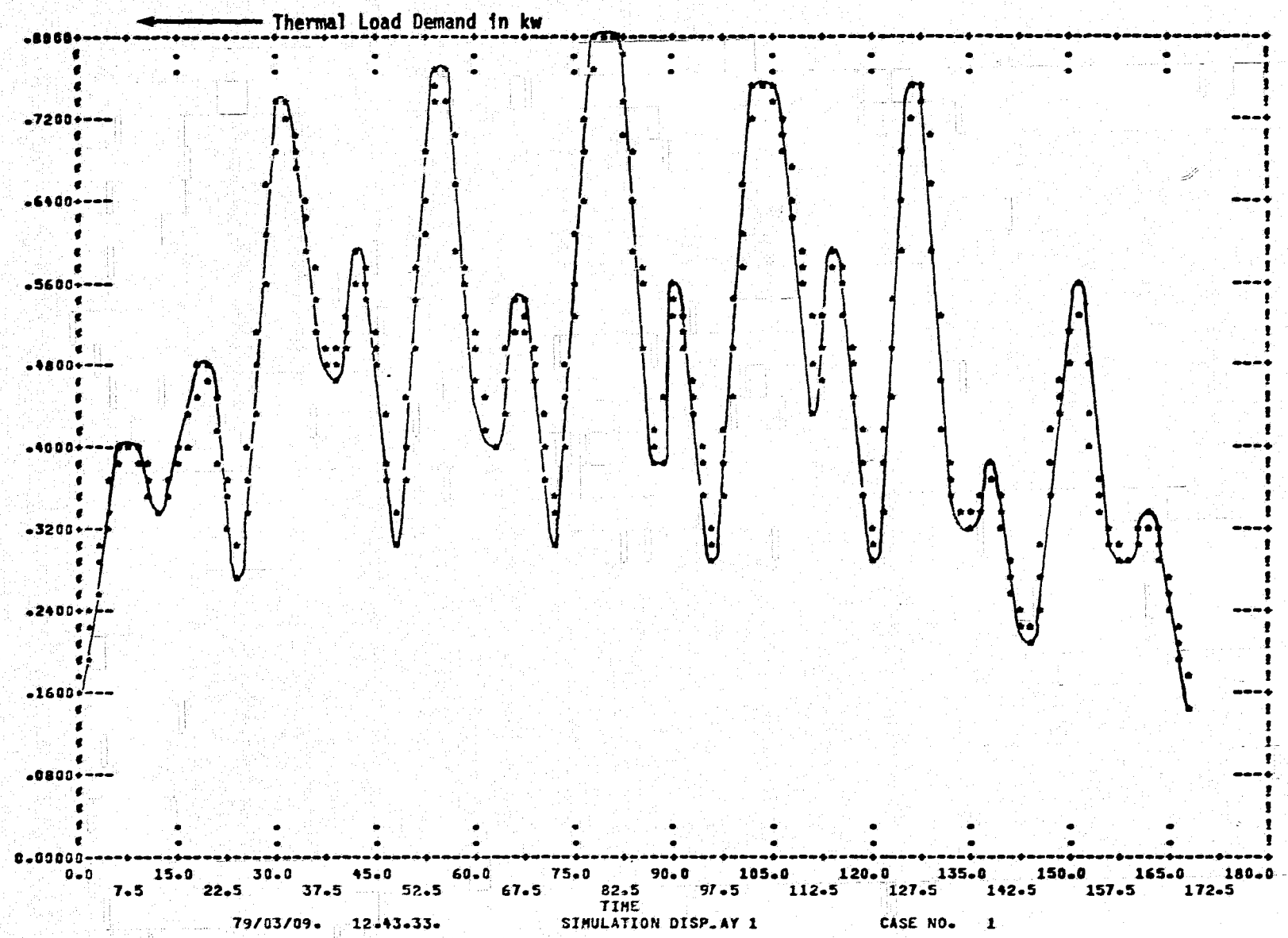


Figure 2.3-5 Thermal Load Demand for One Week Simulation

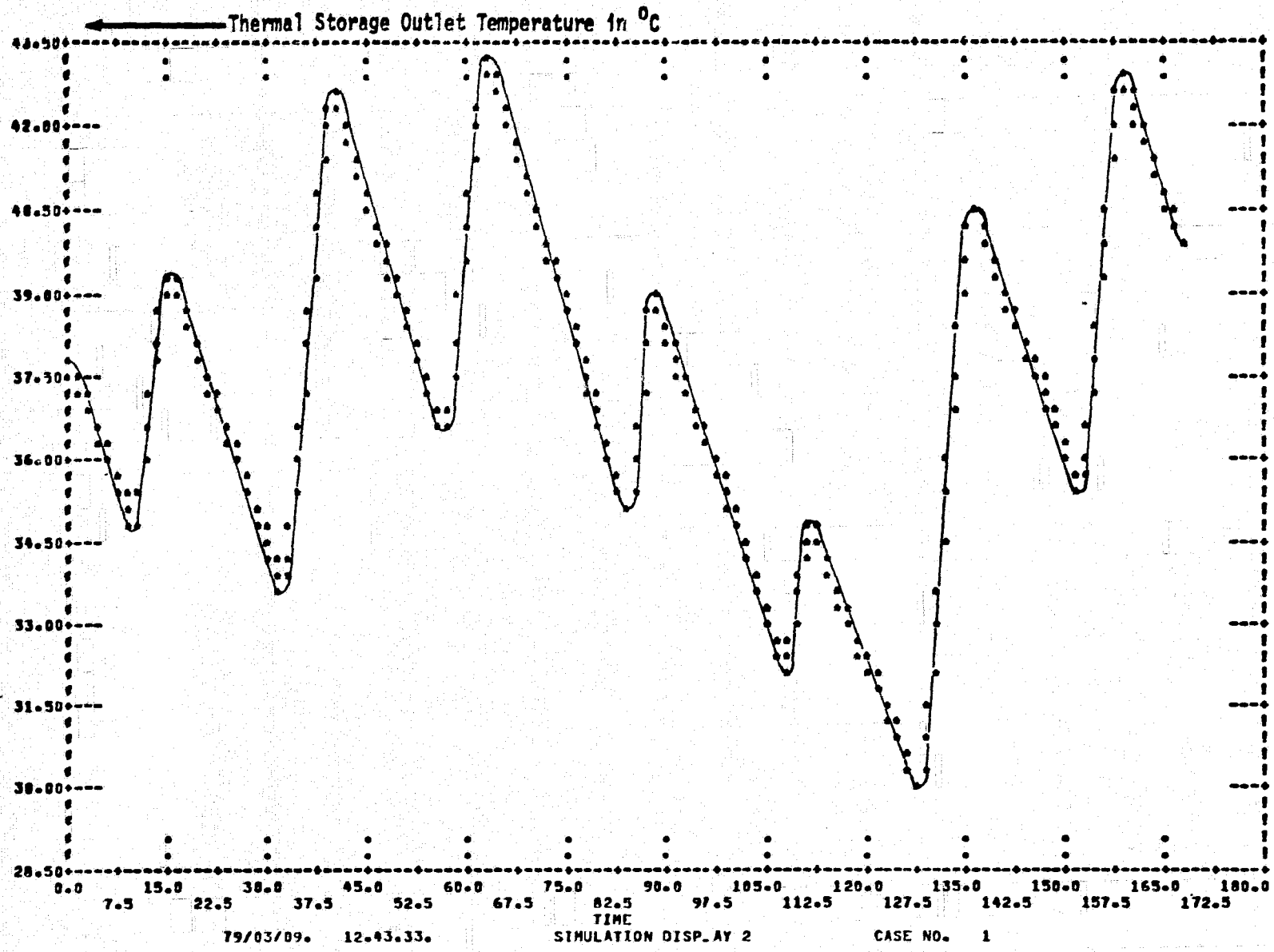


Figure 2.3-6 Thermal Storage Temperature for One Week Simulation

One of the most important measures of performance for a solar energy system is the leveledized cost of energy, i.e., the life cycle cost to produce one unit of usable energy including generation, storage, transmission and conversion subsystems. Energy cost may be used to size components and select most promising system alternatives, i.e., minimum energy cost is used as a selection or optimization principle. Although SIMWEST does not provide user optimization capability, optimal sizing of a few key parameters, such as the ratio of solar to utility generation and the size of storage relative to generation, is possible and may be accomplished quickly using the concept of incremental energy cost. The idea is to compute the incremental change in leveledized energy cost per incremental change in capital cost, for the system parameters of interest. Given an initial system configuration and M sizing parameters to be selected, optimization proceeds as follows:

- 1) Perform M+1 back to back simulations to compute the cost and energy performance of the baseline configuration and M incremental configurations from the baseline.
- 2) Calculate the incremental energy costs for each parameter variation. Then select a new baseline configuration. Since the incremental costs are equal at the minimum cost point, increase or decrease the sizing parameters so as to equalize the new baseline incremental costs.
- 3) Go to 1) and continue adjusting subsystem parameters until either a performance limit is reached or until the incremental costs of the remaining parameters are equalized. (If two incremental costs are unequal, one can always lower the system energy cost by increasing the subsystem with the smallest incremental cost at the expense of the other subsystem.)

This procedure is recommended as more efficient and economical than using a series of parametric trade studies for subsystem optimization.

The process of computing incremental costs is illustrated for the Fresnel Lens model. In the first simulation the baseline system performance and costs are computed. The second simulation differs from the first in that thermal storage capacity has been increased by 10%, and the third simulation differs from the first in that the solar collector and photovoltaic array area have been increased by 5%. Table 2.3-1 summarizes the incremental cost and simulation results for these runs. Column 1 shows the initial capital cost of the baseline system and the incremental capital costs for the thermal storage and solar array increases. (These costs are meant to be illustrative rather than representative.) Column 2 shows the results of a 20 year leveled cost analysis of the three systems, including maintenance and operating costs, e.g., the change in thermal storage increases costs by \$9.10 per year. Column 3 shows the energy delivered to the loads in a year as estimated from the one week simulations. (Note: the change in storage capacity lowers the average coolant temperature, thus increasing output power.) Column 4 shows the leveled energy costs of the baseline system and of the increments in storage and generation. This column shows that the leveled energy cost will decrease as thermal storage or generation are increased, and that thermal storage is undersized relative to generation since a fixed \$ increase in storage will lower the system energy cost more than the same \$ increase in array area. Column 5 shows the % change in leveled energy cost given a 1% increase in capital investment. This column contains the same basic information as column 4 but provides a better quantitative measure of the economic value of increased storage capacity.

Table 2.3-1 Incremental Cost Calculations

	CC	LC	ED	EC	NIC
Baseline	7392.	1272.	7829.	16.2	----
10% Inc. in Thermal	61.	9.10	110.5	8.2	-.84
5% Inc. in Solar	319.	47.90	365.0	13.1	-.21

NOMENCLATURE:

CC = Initial Capital Cost in \$

LC = Levelized Total Cost/Yr. in \$

= Capital Cost\*Life Cycle\*Charge Rate +  
Maintenance Cost + Operating Cost

ED = Useful Energy Delivered/Yr. in KWH

= Electrical Load + Thermal Load +  
Net Change in Thermal Storage

EC = Levelized Energy Cost in ¢/KWH

= LC\*100/ED

NIC = Normalized Incremental Costs

= % Change in EC Per % Change in CC

≈  $(\Delta LC/LC - \Delta ED/ED)/(\Delta CC/CC)$

### 3.0 HYBRID SOLAR TEST CASE

This section illustrates the capability of the expanded SIMWEST library for modeling complex wind or solar systems including storage, loads, and system logic. A test case model was chosen utilizing:

- Typical Meteorological Year (TMY) environmental inputs
- Hybrid generation - wind turbine plus solar array
- Battery, flywheel and heat storage systems
- Three user specified loads plus control loads
- Complex system logic including utility tie-ins.

The model and data inputs were debugged and roughly sized using week long simulations. Four seasonal week long simulations were used to balance generation to loads and power distribution to storage. Full year long simulations were then run to measure typical year system performance. This task utilized about three manweeks from model inception to completed year long simulations.

#### 3.1 SYSTEM DESCRIPTION

An overview schematic of the hybrid solar test case model is shown in Figure 3.1-1. Each box or function is represented by one or more components from the SIMWEST library, and the arrows between boxes show information and power flow through the model. In this model, all the power generated by the wind turbine and solar array are distributed to the storage devices with any remaining power surplus to a utility. The DC load is met from battery storage, the control loads from flywheel storage, and the heating load from thermal storage. The AC load has been segmented into baseload and peak load portions to illustrate utility type unit commitment to load demand. The baseload is met from battery storage and the peak load from flywheel storage with a utility backup if either storage unit has insufficient capacity. Utility backups are also provided for the storage devices.

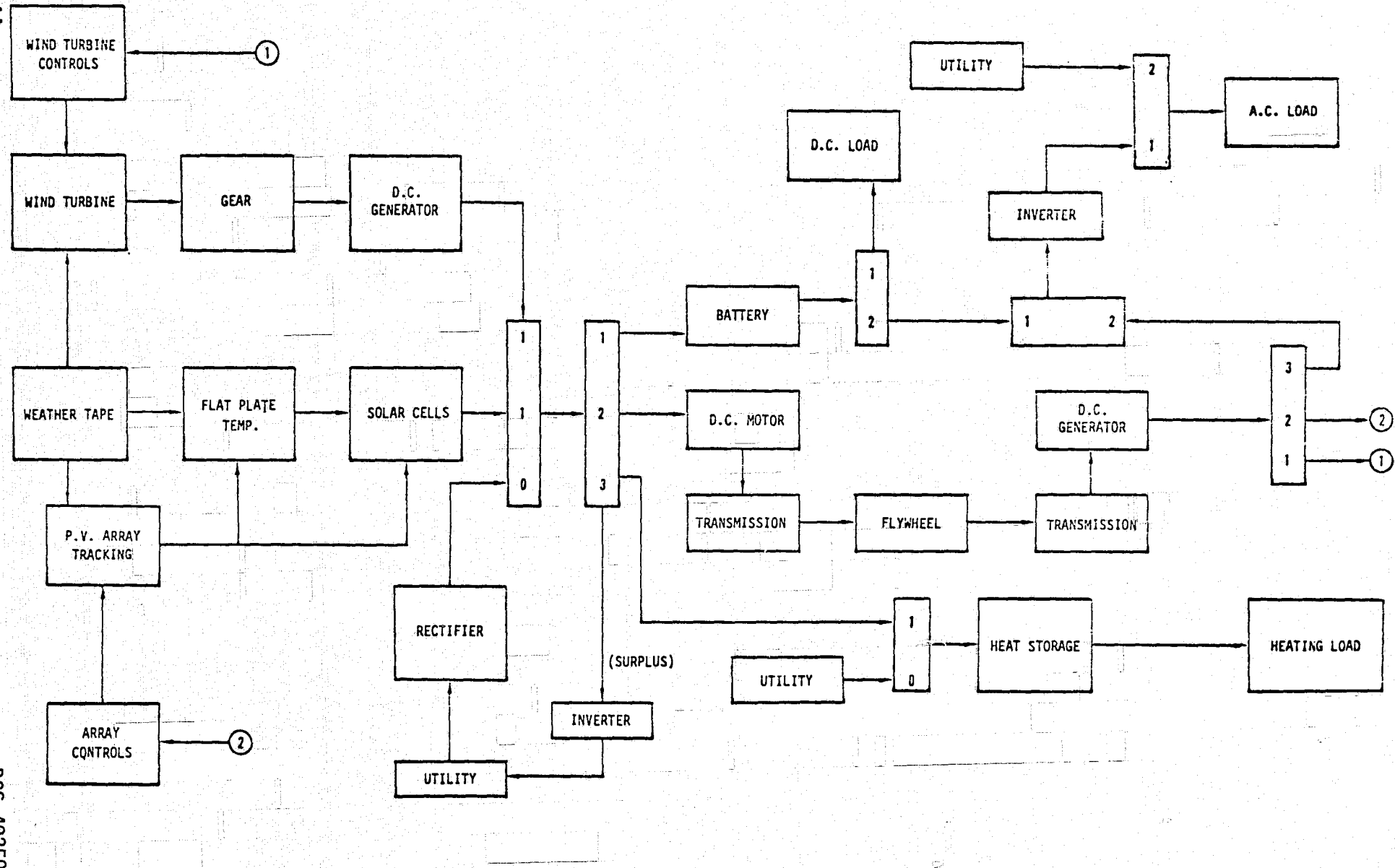


Figure 3.1-1 Hybrid Solar Test Case Model

The boxes with numbers in Figure 3.1-1 represent power divider and power accumulator logic controllers. The flow of power in these multi-port components is regulated by the priority numbers with 1 = highest priority, 2 = second priority, 3 = third priority, 0 = no priority (used for back-up or switch regulated components). For example, the power divider component preceding the battery allocates the power generated by the wind turbine and the solar array to the battery first (up to its maximum charging level), to the flywheel second, and to heat storage third, with any remaining power being surplused to a utility. These logic components have proven to be quite versatile for specifying and modifying model control logic.

Once an overall system model has been defined, the user may construct a Fortran system model using the SIMWEST model generation program. Figure 3.1-2 shows the model generation input for the hybrid model. This program produces a line printer schematic of all the component model interconnections which enables the user to quickly debug and verify his system model. Figure 3.1-3 shows the line printer schematic for the generation portion of the hybrid model. The symbols within the boxes are two or three character mnemonics for library components, i.e., WT represents a wind turbine component, GR a fixed gear ratio transmission, and GE1 the first generator component in the model (there are several). The four to six character symbols between boxes are the formal names of interconnection variables, i.e., P2 WT is the power output from the wind turbine into the gear box.

The most important system characteristics of the hybrid test model are summarized in Table 3.1-1. Dodge City, Kansas TMY inputs were chosen since this location has both a favorable wind regime and good solar insolation. The total rated output of the solar array and wind turbine is 50kw, which produces an average output of 14kw at this location. The storage units were sized with sufficient capacity to accommodate most of the variability in output power due to changing weather fronts. Thus the battery and thermal storage units have about 5 days of storage, whereas the flywheel has a 1.4 day storage capacity to accommodate daily load fluctuations. Figure 3.1-4 shows the daily load

**MODEL DESCRIPTION**      **SOLAR TEST CASE**  
 LOCATION=41      TI  
 LOCATION=21      ED      INPUTS=TI  
 LOCATION=43      SO      INPUTS=TI,ED(X1=SB,X2=ST)  
 LOCATION=24      FP      INPUTS=SO,ED(X4=WD,X3=TA)  
 LOCATION=45      PV      INPUTS=SO(ST,1=ST),FP  
 LOCATION=1      MA      INPUTS=ED(X4=FIN)  
 LOCATION=3      WT      INPUTS=MA(F0=HV)  
 LOCATION=5      GR      INPUTS=WT  
 LOCATION=7      GE1      INPUTS=GR  
 LOCATION=74      UT1      INPUTS=IV(P,2=P,0),PA1(RE,3=RE)  
 LOCATION=54      RE      INPUTS=UT1(2,1)  
**FORTRAN STATEMENTS**  
 C      RESET PRIORITY WHEN BATTERY OR FLYWHEEL EMPTY  
 PS3PA1=0  
 IF(INTFL,GT.,1)PS3PA1=2.  
 IF(INTBA,GT.,1)PS3PA1=2.  
 C      WIND TURBINE CONTROL LOAD WHEN WIND SPEED IS NON-ZERO  
 LO1LOW=0.  
 IF(X4 ED,GT.0,)LO1LOW=.2  
 LOCATION=57      PA1      INPUTS=GE1(P,2=P,2,P,2=MP,2),PV(P=P,1,P=MP,1),RE(2,3),  
 LOCATION=131      PD      INPUTS=FL(RE,2=RE,2),PA4(1,3),BA(RE,2=RE,1)  
 LOCATION=103      BA      INPUTS=PD2(RE,0=RE,1),PD(1,1)  
 LOCATION=105      PD2      INPUTS=PA3(1,2),LOD(1,1),BA(P,2=P,0)  
**FORTRAN STATEMENTS**  
 C      BASELOAD POWER TO ELECTRIC LOAD  
 MP2PD2=A MINI(CMP2PD2,4,5)  
 LOCATION=117      FUD      INPUTS=TI(TD=FIN)  
 LOCATION=119      MA3      INPUTS=FUD(F0=FIN)  
 LOCATION=110      LO0      INPUTS=MA3(F0=LO,1)  
 LOCATION=161      MO      INPUTS=PD(2,1)  
 LOCATION=163      TR1      INPUTS=MO,FL(RS=RS,2)  
 LOCATION=144      FL      INPUTS=TR1,PD3(RE,0=RE)  
 LOCATION=165      TR2      INPUTS=FL  
 LOCATION=167      GE2      INPUTS=TR2  
 LOCATION=180      PD3      INPUTS=GE2(2,0),LOW(1,1),SO(1,2),LOP(1,2)  
 LOCATION=260      LOW      INPUTS=SO(RE,1=LO,1)  
 LOCATION=258      LOP      INPUTS=SO(RE,1=LO,1)  
 LOCATION=140      PA3      INPUTS=PA2(RE,1=RE,0),PD3(3,2)  
 LOCATION=201      IV2      INPUTS=PA3(0,1)  
 LOCATION=211      UT2      INPUTS=PA3(0,1)  
 LOCATION=214      PA2      INPUTS=IV2(2,1),UT2(2,2),LO(1,0)  
 LOCATION=206      FVL      INPUTS=TI(TD=FNA,MY=FNB)  
 LOCATION=208      MA2      INPUTS=FVL(F0=FIN)  
 LOCATION=220      LO      INPUTS=MA2(F0=LO,1)  
 LOCATION=221      UT3      INPUTS=PA4(2,2)  
 LOCATION=224      PA4      INPUTS=PI(2,2),TS(RE,2=RE,0)  
 LOCATION=236      TS      INPUTS=TL,PA4(0,1)  
 LOCATION=244      PI      INPUTS=TS  
 LOCATION=240      TL      INPUTS=TI  
 LOCATION=71      IV      INPUTS=PD(SP=P,1)  
 LOCATION=39      CM      INPUTS=PD(P,2=FIN)  
 LOCATION=271      HGI      INPUTS=PD(P,2=FIN)  
 LOCATION=272      HGO      INPUTS=GE2(P,2=FIN)  
 LOCATION=273      HGS      INPUTS=PV(P=FIN)  
 LOCATION=274      HGW      INPUTS=GE1(P,2=FIN)  
**END OF MODEL**  
 PRINT

Figure 3.1-2 Hybrid Model Generation Input Data

PAGE 0

SOLAR TEST CASE										
PO MA			P2 HT		GR HT			P2 GR		
MA			HT		GR			EF2GR		
1			3		5			P2GR		
RS1GR										
RS GE1										
X8 ED										
	12	13	14	15	16	17	18	19	20	
X3 ED										
X4 ED										
ED										
21			FP		24			25		
						26			17	
IST180										
ITLTSO										
IRE180										
TD TI										
DY TI										
32			I		34			I		
			I			I			I	
X2 ED										
X1 ED			TC FP		V			I		
TO TI										
DY TI			ST180		PV			I		
TI			SO		PV			I		
41			43		45			46		
PV										
P2 GE1										
P2 GE1										
MP2RE										
P2 RE										
EF2RE										
RE										
PA1										
51										
52										
53										
54			I		55			I		
			I			I			I	
A										
P2 UT1										
MP2UT1										
PAGE 1										
REOPD										
P2 IV										
IV			RESPA1		UT1			I		
71			74		75			76		
77										
78										
79										
80										

Figure 3.1-3 Line Printer Model Schematic (Page 0 Only)

**Table 3.1-1 Hybrid Model System Description**

**GENERATION**

- Environmental
  - Dodge City, Kansas Inputs
  - Mean Wind Speed = 5.2 m/s
- Solar P-V System
  - Flat Plate Array
  - Horizontal EW Axis Tracking
  - Passive Cooling with Fins
  - Maximum Power Tracker
  - Rated Output = 30 kw  
(189 m<sup>2</sup> Array Area)
- Wind Turbine System
  - Horizontal Axis, Fixed Speed Turbine
  - D.C. Generator
  - Rated Output = 20 kw  
(6.4m Blade Radius)

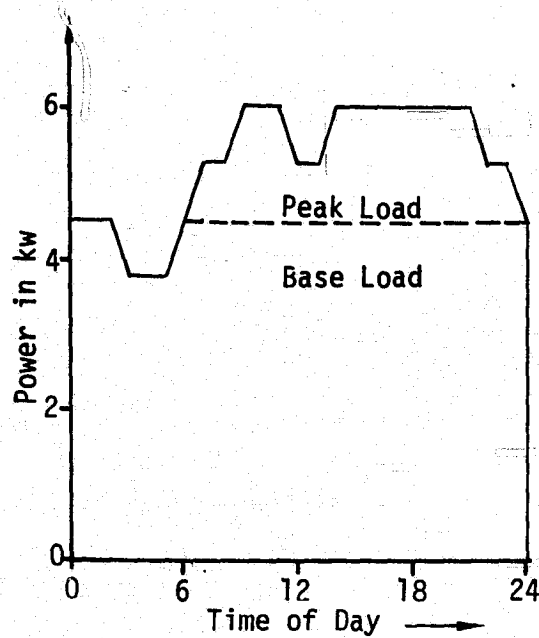
**LOADS<sup>1</sup>**

- AC Electrical Load
  - Plumbrook, Ohio Profile
  - Mean Load = 5 kw
  - Base Load Power = 4.5 kw
- DC Electrical Load
  - Mean Load = 1 kw
  - Peak Load = 4 kw
- Thermal Load
  - Hot Water Heating
  - Mean Load = 4 kw
  - Peak Load = 12 kw

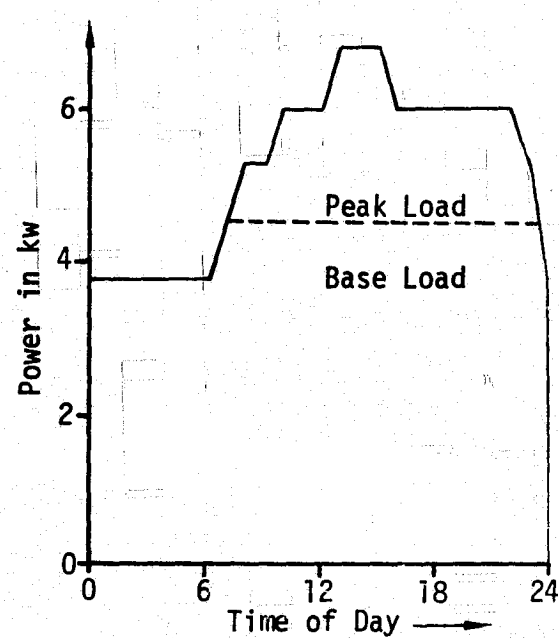
**STORAGE**

- BATTERY
  - Lead-Acid Battery Bank
  - Rated Capacity = 750 kwh
  - Rated Power = 10 kw
- FLYWHEEL
  - Steel Rotor
  - Variable Ratio Transmission
  - Rated Capacity = 50 kwh  
(24,000 pound weight)
  - Rated Power = 20 kw
- THERMAL
  - Parafin Wax Phase Change Media
  - Rated Capacity = 500 kwh
  - Rated Input Power = 50 kw
- LOGIC
  - Priorities for generated power
    - 1 - Battery Storage
    - 2 - Flywheel Storage
    - 3 - Thermal Storage
    - 4 - Surplus to Utility
  - Utility Backup for Storage Media
  - Battery Services AC Base Load and DC Load, Flywheel Services AC Peak Load

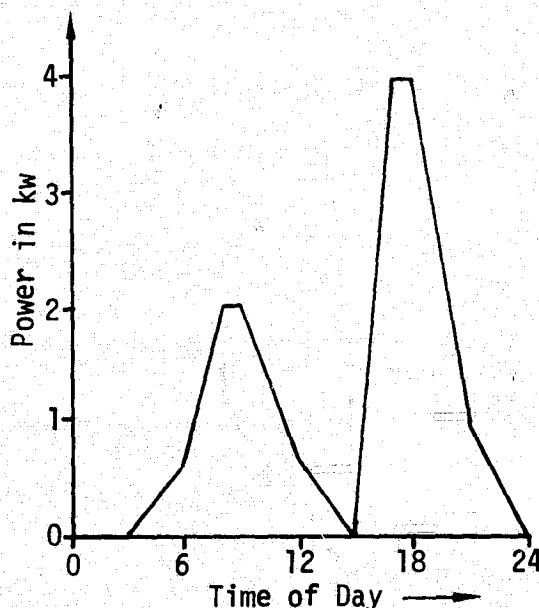
1 See Figure 3.1-3 for Load Profiles



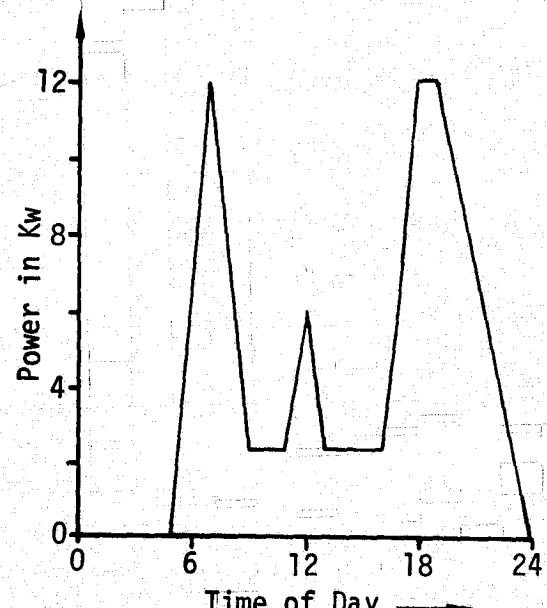
(a) AC LOAD - NOV. TO APR.



(b) AC LOAD - MAY TO OCT.



(c) DC LOAD



(d) THERMAL LOAD

Figure 3.1-4 Daily Load Profiles for Hybrid Model

profiles used for the electrical and thermal loads. Since the AC load is a function of both time of day and month, a two dimension table lookup component was used in the system model to represent the load profiles shown in (a) and (b). The mean value of the combined electrical, thermal, and control loads is 10.8kw. It should be noted that this model was chosen simply to illustrate the capabilities of the SIMWEST program and is not a proposed concept or economic system design.

In addition to the hybrid model simulations, several variations of this model were sized and simulated for comparison purposes. The alternative models use only solar photovoltaic generation and wind power generation, respectively. Table 3.1-2 shows the system parameters used to size each of the models. Generation was sized to the load by increasing rated output until the energy surplus exceeded that required from the utility backup to satisfy the thermal load. Rated input power to the battery was also adjusted, so that the electrical loads are primarily satisfied by solar and wind generation with excess power going to thermal storage. The rated solar P-V parameters are considerably larger than the Hybrid and Wind model parameters since solar energy generation is restricted to an 8-9 hour period each day.

Table 3.1-2 Test Case Load Matching Parameters

MODEL PARAMETER	HYBRID	SOLAR P-V	WIND
Wind Turbine Blade Radius	6.4 m	-----	8.8 m
Rated Wind Output Power	20 kw	-----	36 kw
Solar Array Area <sup>1</sup>	189 m <sup>2</sup>	459 m <sup>2</sup>	---
Rated Solar Output Power	30 kw	75 kw	---
Battery Rated Input Power	10 kw	18 kw	10 kw

1 Number of solar cells and collector dimension parameters varied proportionately.

### 3.2 DAILY SYSTEM PERFORMANCE

In this section daily and short term performance of the energy storage systems is illustrated by analyzing environmental and storage time plots over a weekly period. Figures 3.2-1 and 3.2-2 show the collector solar insolation and wind speed inputs for the week selected. Both the wind and solar inputs are strong during the first three days, and then fall off for several days, gradually increasing toward the end of the week. These inputs are typical for this time of year.

The battery, flywheel and thermal energy storage time plots for the Hybrid model are shown in Figures 3.2-1 to 3.2-5, respectively. Battery storage energy is a rather smooth curve, not responding greatly to the daily fluctuations in generation and electrical load. The total swing in battery storage is in fact less than half of its capacity during this period. Flywheel storage, on the other hand, is quite responsive to daily fluctuations in generation and swings rapidly to full capacity when generation is strong and to fully discharged when generation is weak. Thermal storage is not very responsive to daily fluctuations but absorbs most of the output when generation is strong. Thermal storage tends to become fully discharged during several day periods of weak generation.

For comparison purposes, the energy storage time plots for the Solar P-V model are shown in Figures 3.2-6 to 3.2-8. These plots are similar to those for the Hybrid model except that the daily fluctuations are more pronounced, and more regular than those with wind generation.

It has been found that performance data using four seasonal week long simulations is quite suitable for solar systems trade study and design tasks. For example, the above analysis of the Hybrid model points out several areas in which the system design might be improved: The plots of battery storage tend to indicate that the battery is oversized and its capacity could be reduced. The flywheel seems well sized to its purpose, but frequently calls on a utility

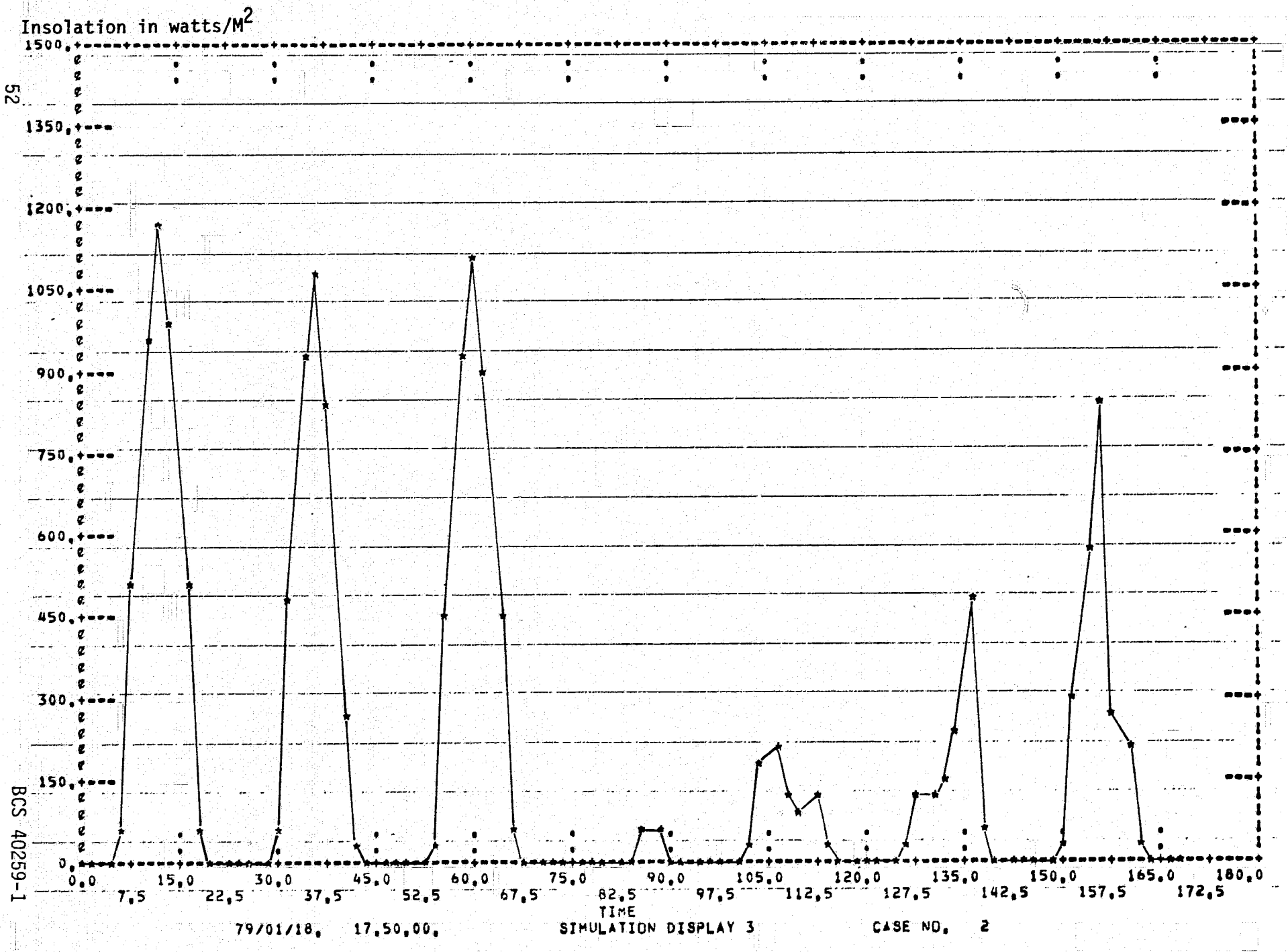


Figure 3.2-1 Collector Solar Insolation Time History

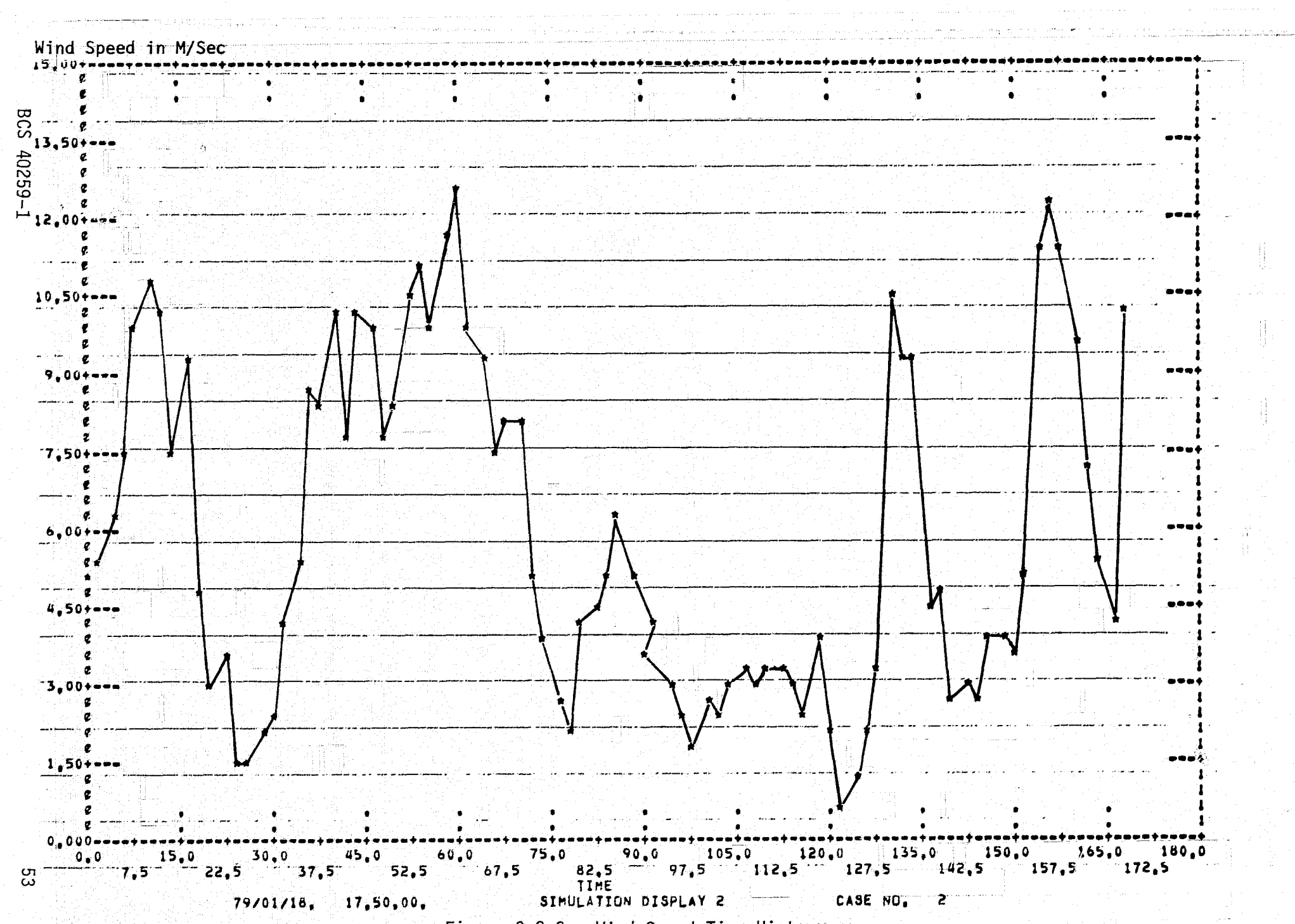


Figure 3.2-2 Wind Speed Time History

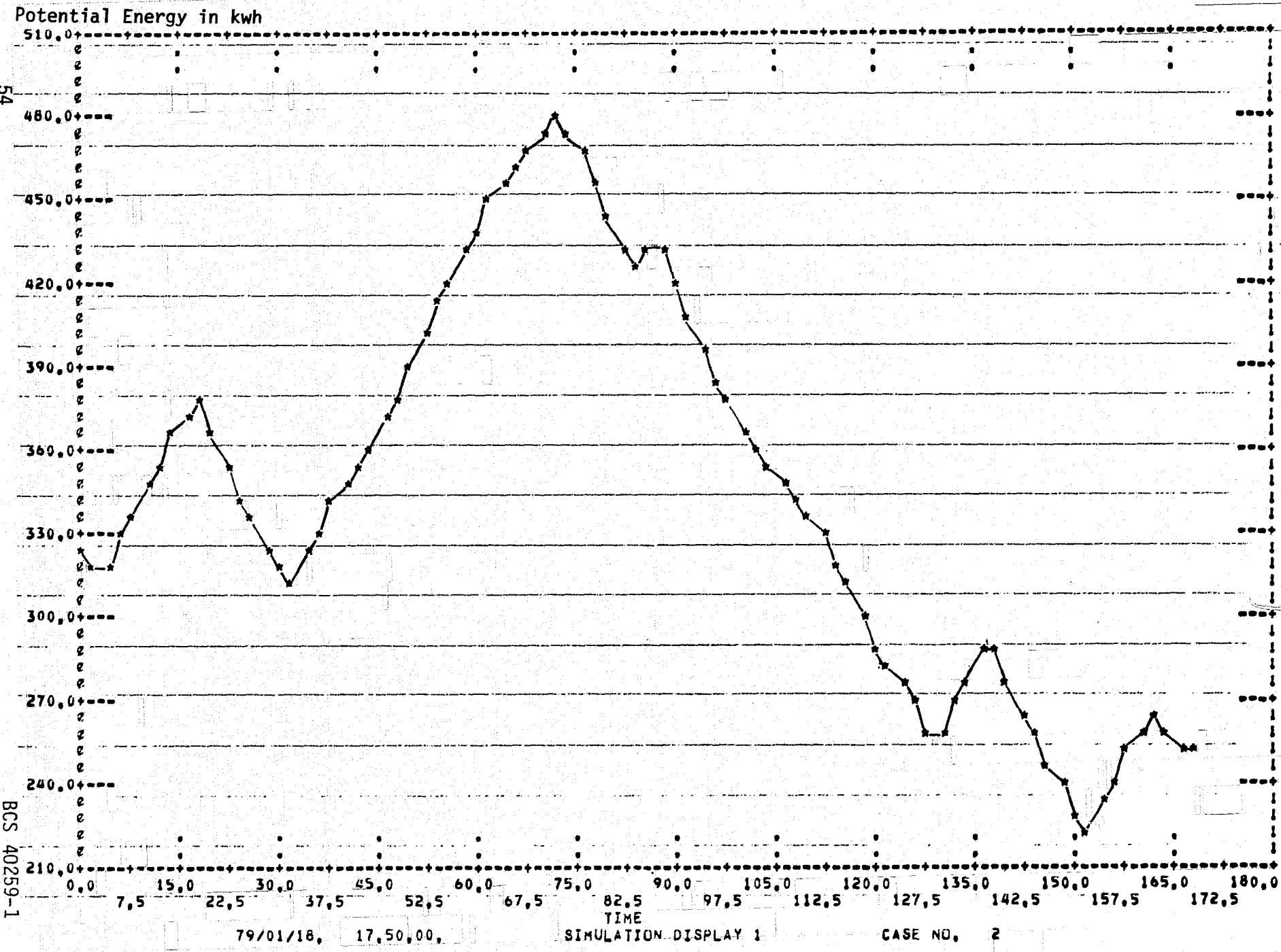


Figure 3.2-3 Battery Energy Storage - Hybrid Model

# Kinetic Energy in kwh

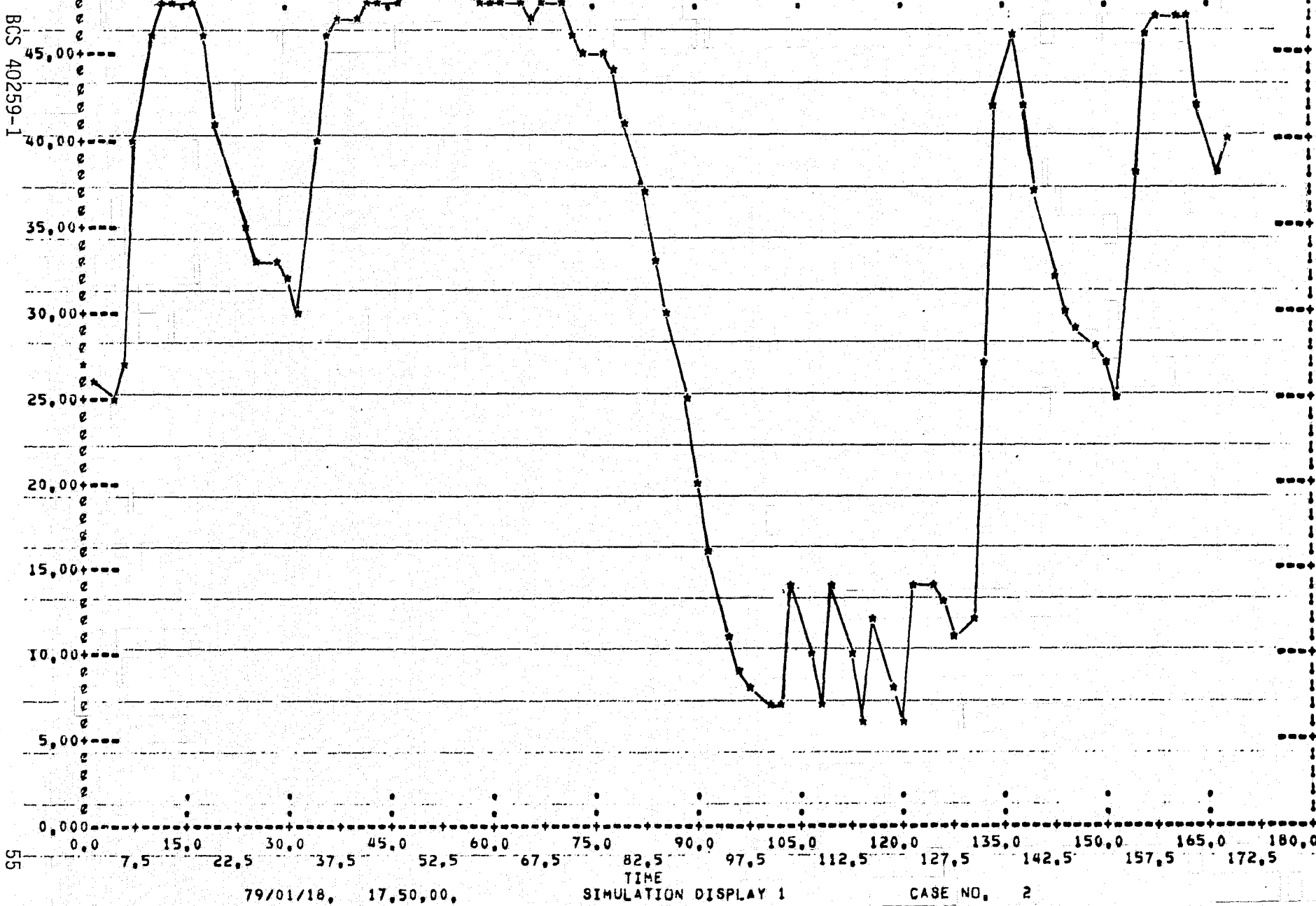


Figure 3.2-4 Flywheel Energy Storage - Hybrid Model

# Thermal Energy in kwh.

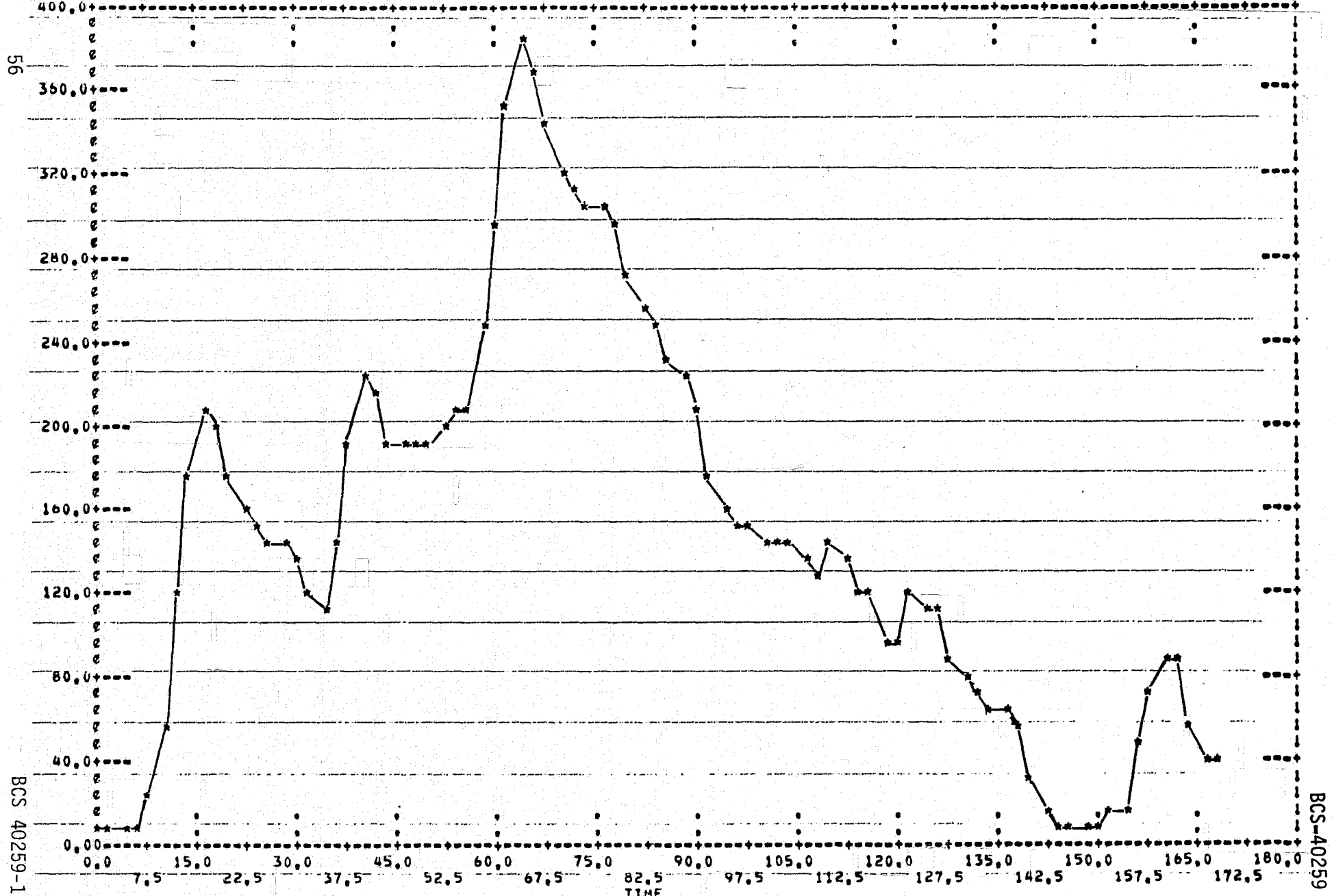


Figure 3.2-5 Thermal Energy Storage - Hybrid Model

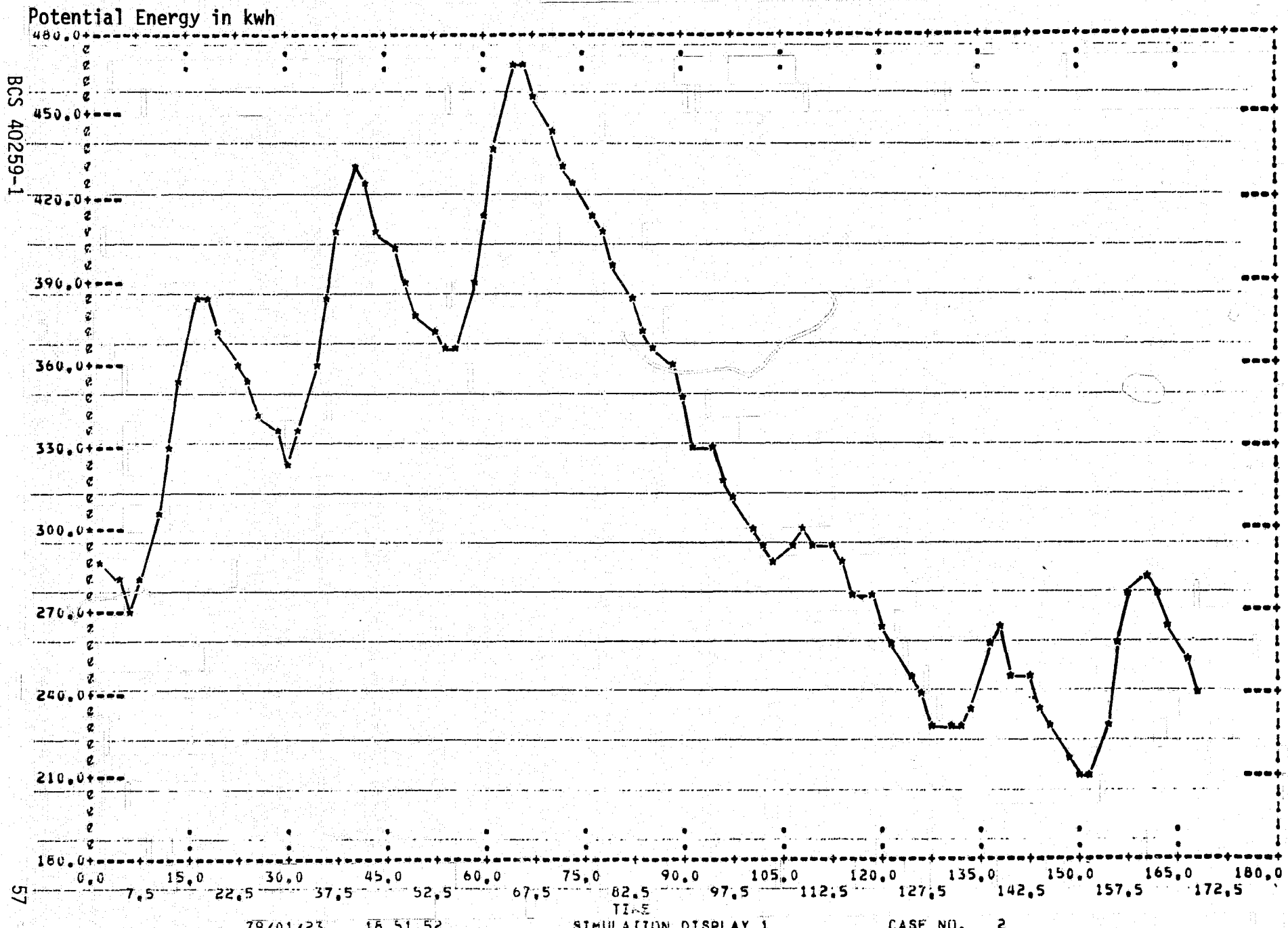
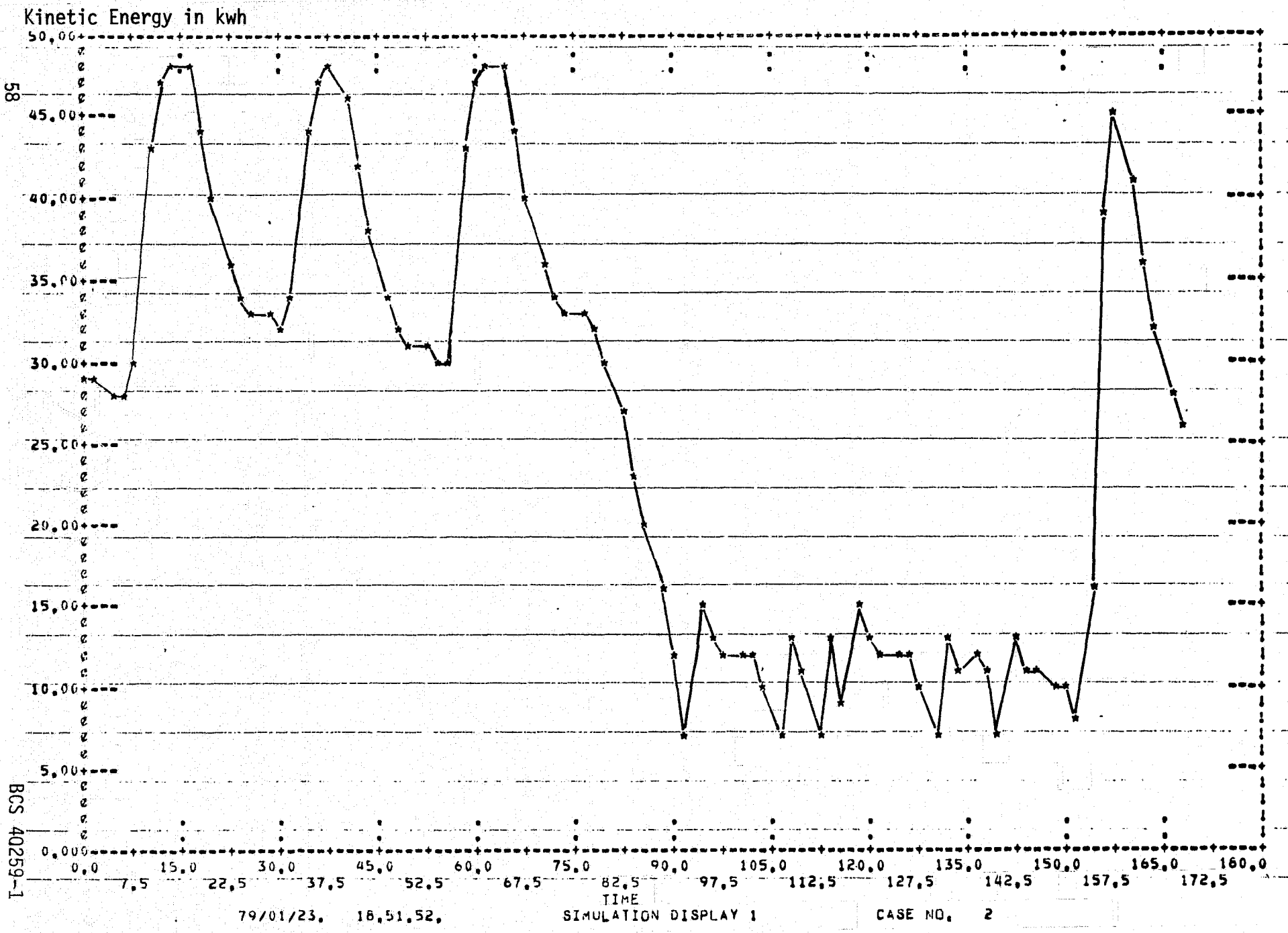


Figure 3.2-6 Battery Energy Storage - Solar P-V Model



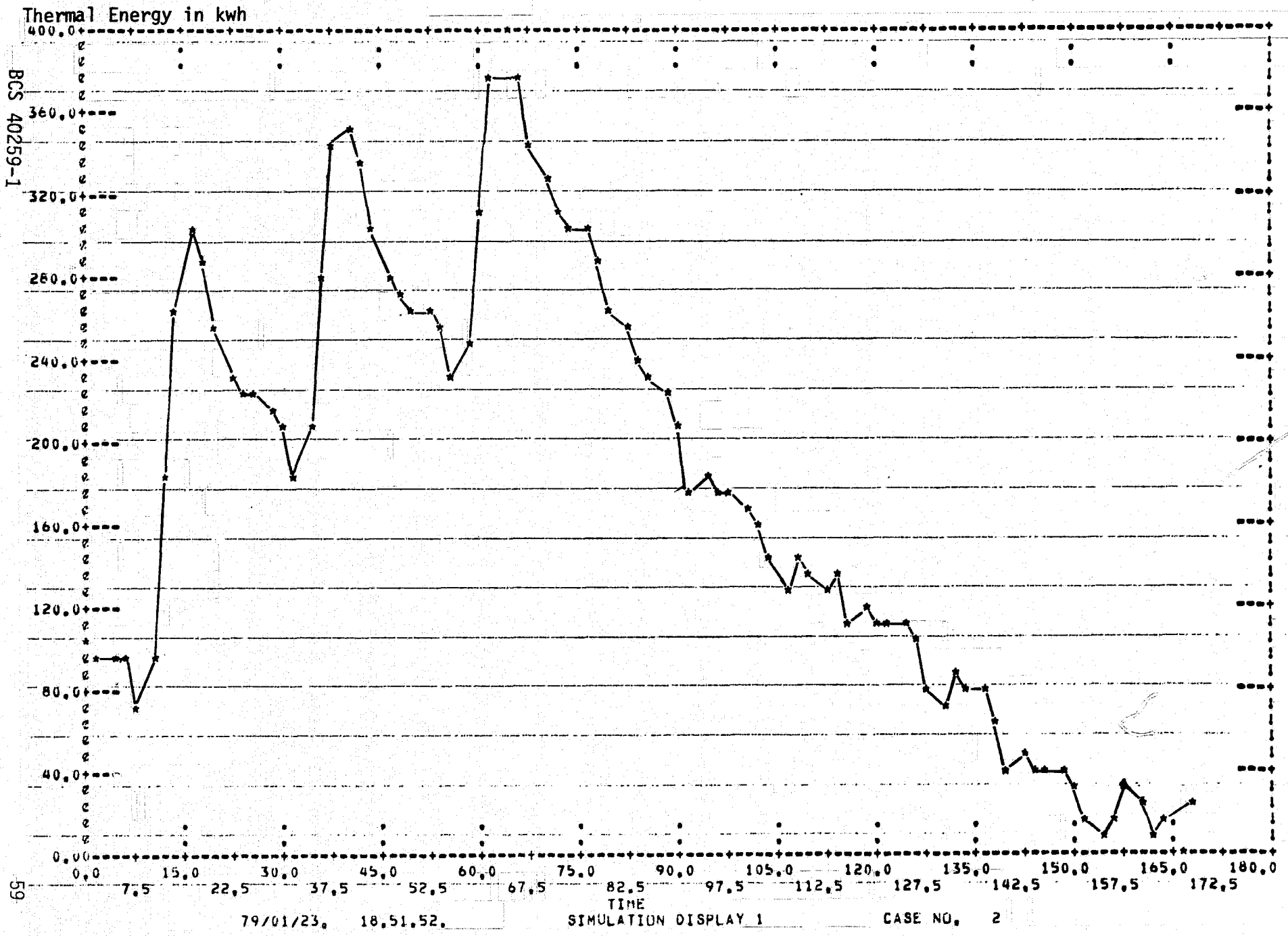


Figure 3.2-8 Thermal Energy Storage - Solar P-V Model

for charging even when the battery has substantial capacity. This suggests that the battery back up the flywheel and service its load whenever the flywheel is fully discharged, rather than calling on a utility. Finally, the thermal storage unit is too small to supply a substantially higher percentage of the load, since increased generation capacity tends to be surplused to the utility.

### 3.3 MONTHLY POWER GENERATION

The yearly wind and solar simulations are best set-up as twelve monthly simulations in order to generate partial results from printer plots, histograms, and numeric tabular output. This section summarizes monthly results from the year long simulations.

Figure 3.3-1 shows the average monthly generation for the Hybrid solar model. The wind turbine output is highly variable from one month to the next and does not show a significant seasonal trend. This may be an artifact, however, resulting from TMY data selection of "typical" meteorological months from different years of SOLMET (Ref.[3]) weather and insolation data. The solar array output, by contrast, is a fairly smooth curve with a distinct mid-summer peak. Utility back-up generation is complementary to the wind and solar generation, with no back-up required for those months with strong wind generation.

Figures 3.3-2 and 3.3-3 show the monthly output histograms for wind and solar generation during May. This was one of the strongest months for wind generation and the wind turbine operated at rated output (20kw) about 30% of the time. The solar array output, although more consistent than the wind, produces substantial output only for a short period each day. Only 20% of the time did the solar array produce more than 50% of its rated capacity. Thus the monthly plant factor or ratio between average output and rated output was 0.55 for the wind turbine and 0.20 for the solar array.

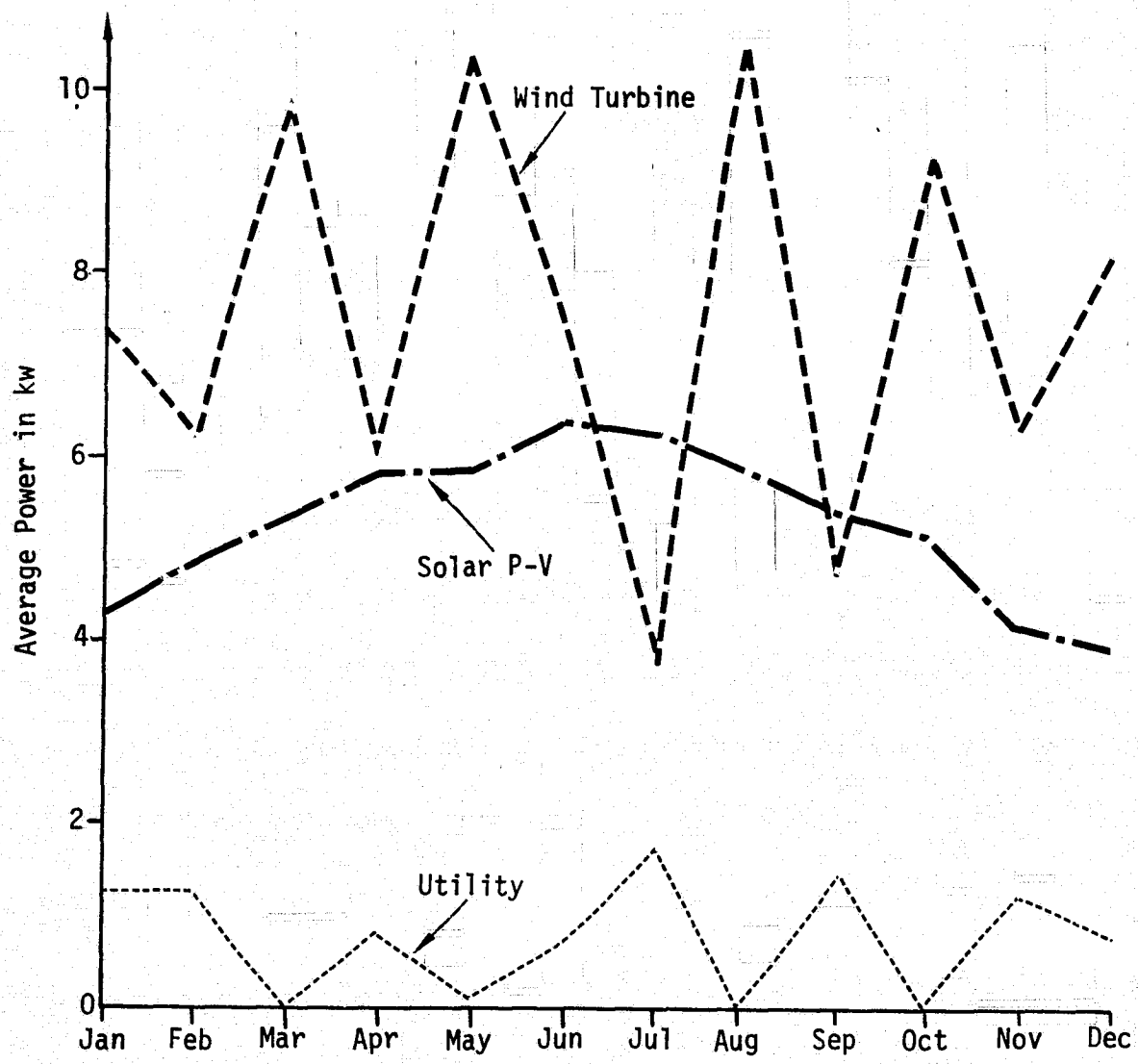


Figure 3.3-1 Average Monthly Output Power For Hybrid Model

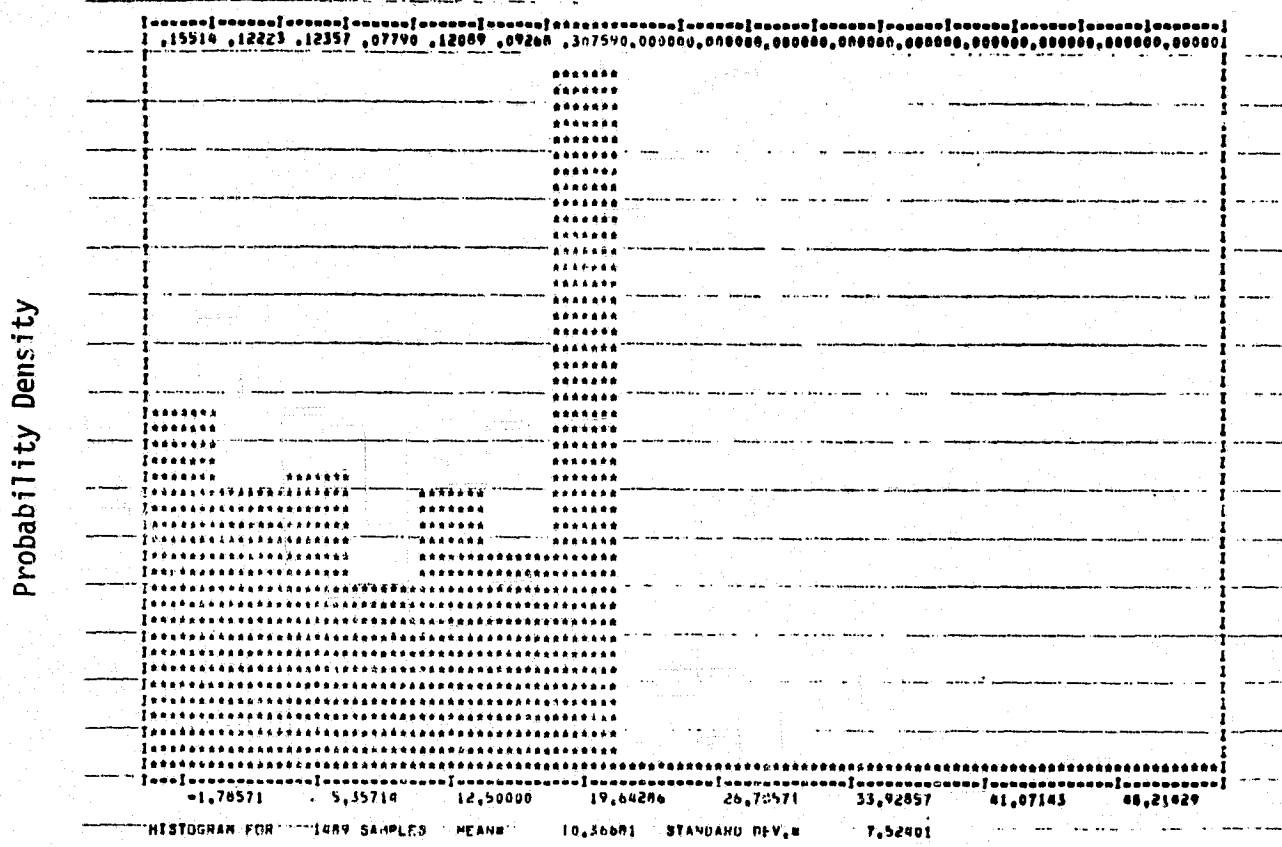


Figure 3.3-2 Histogram of Wind Turbine Output Power - May

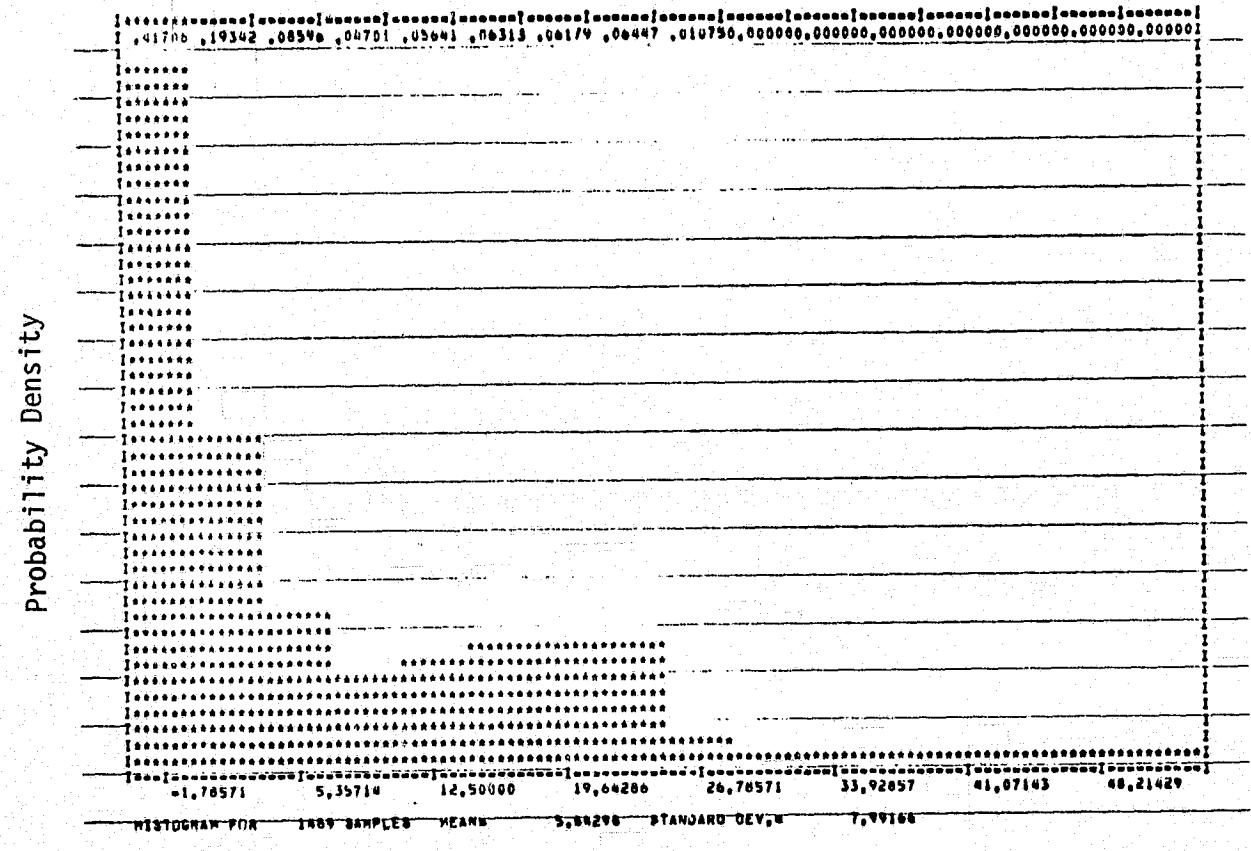


Figure 3.3-3 Histogram of Solar Array Output Power - May

Figures 3.3-4 and 3.3-5 show the average monthly output for the Wind and Solar P-V models. The average output power from the wind turbine in 3.3-4 is higher than the combined wind and solar generation for the Hybrid model, but the average utility power required is also higher due to the larger power deficits during less windy months. The average power surplus is about equal to that demanded from the utility in this case. Figure 3.3-5 shows that the Solar P-V system has a substantial power deficit during the winter months which changes to a small surplus in the summer months. This indicates that the solar array may be undersized for yearly system operation.

### 3.4 LOAD SERVICE PERFORMANCE

Many of the component models monitor power flow statistics, such as total energy into or out of a component since the beginning of simulation. The use of these statistics and histograms enable the SIMWEST user to analyze subsystem and component level performance of a wind or solar simulation. This is illustrated in this section by analyzing the distribution of power flow to the loads, and storage system efficiencies for the Hybrid model.

Figure 3.4-1 shows the average monthly distribution of input power to storage and surplus. The battery input is fairly constant, ranging between 5 and 6kw each month except January. Similarly, the flywheel input is fairly constant, ranging between 1.5 and 2kw each month. The thermal vessel, and to a lesser extent surplus power follows the ups and downs of the wind based generation. It should be noted that this figure simply confirms the analysis of daily and short term performance obtained with weekly time plots of energy storage, i.e., Figures 3.2-3 to 3.2-5.

The monthly distribution of power flow to the electrical loads is not of much interest since the battery supplies the DC load and the flywheel and battery supply the AC load in proportion to the peakload and baseload demand, respectively, except for a small amount of power supplied by a utility when the flywheel is discharged. Figure 3.4-2 shows the monthly percentage of power

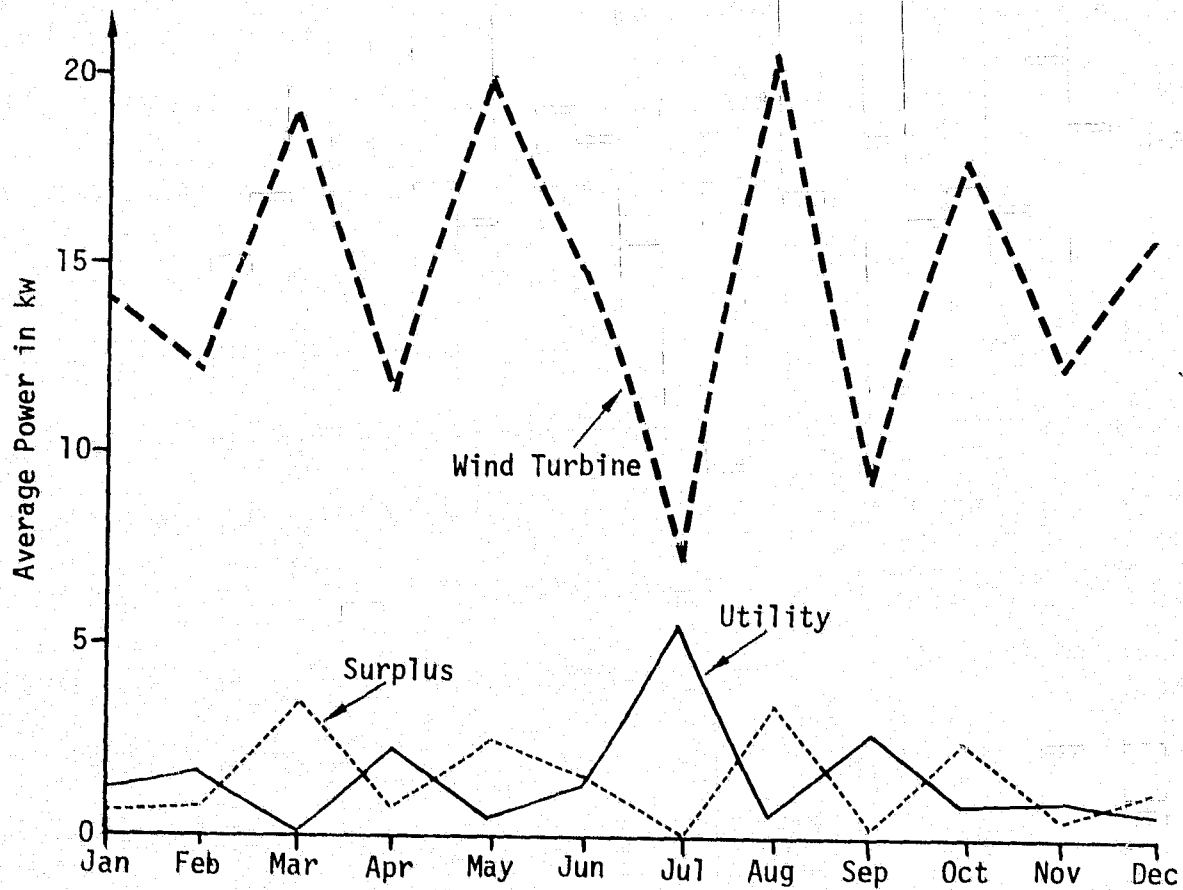


Figure 3.3-4 Average Monthly Output Power- Wind Model

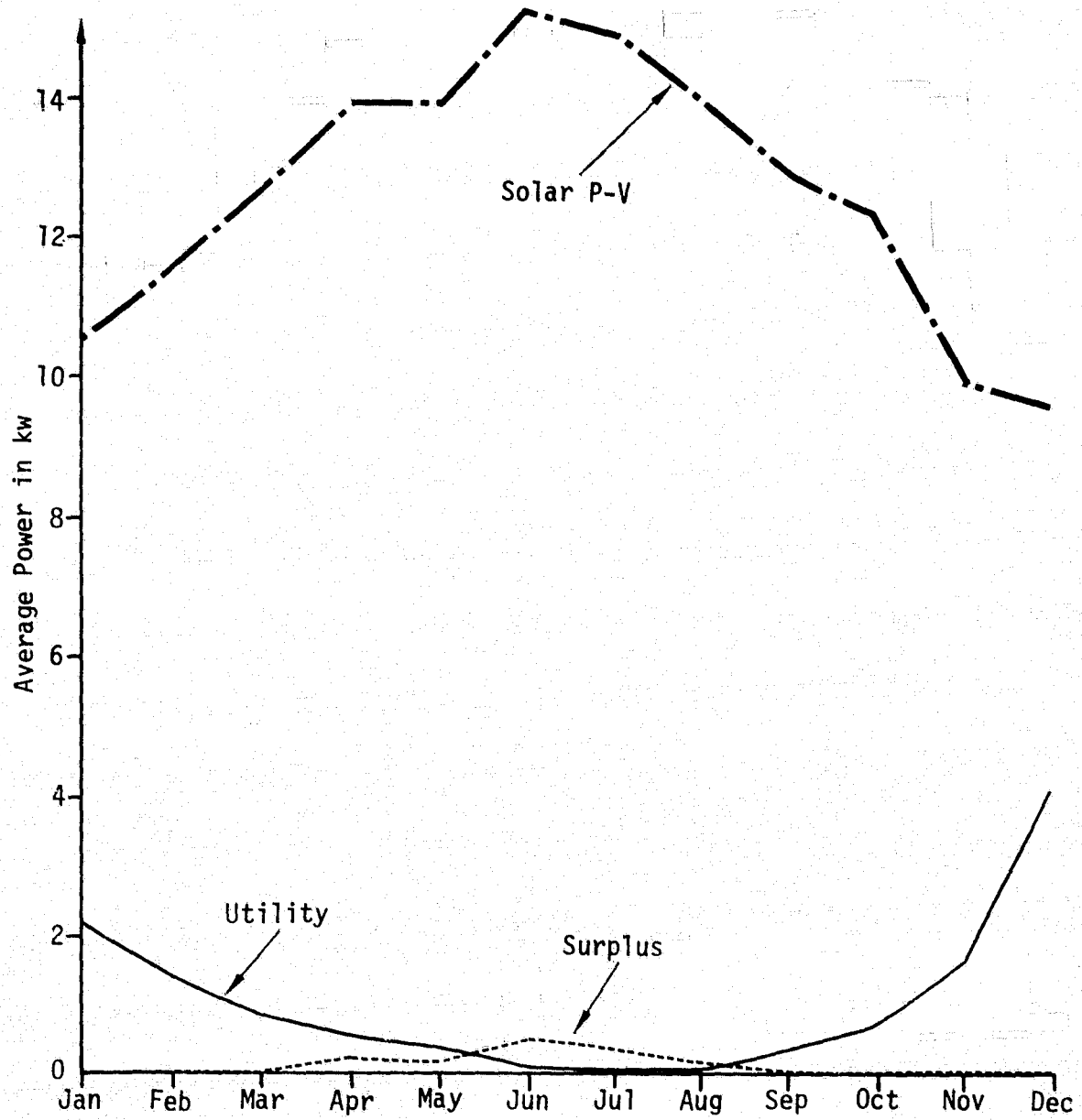


Figure 3.3-5 Average Monthly Output Power - Solar P-V

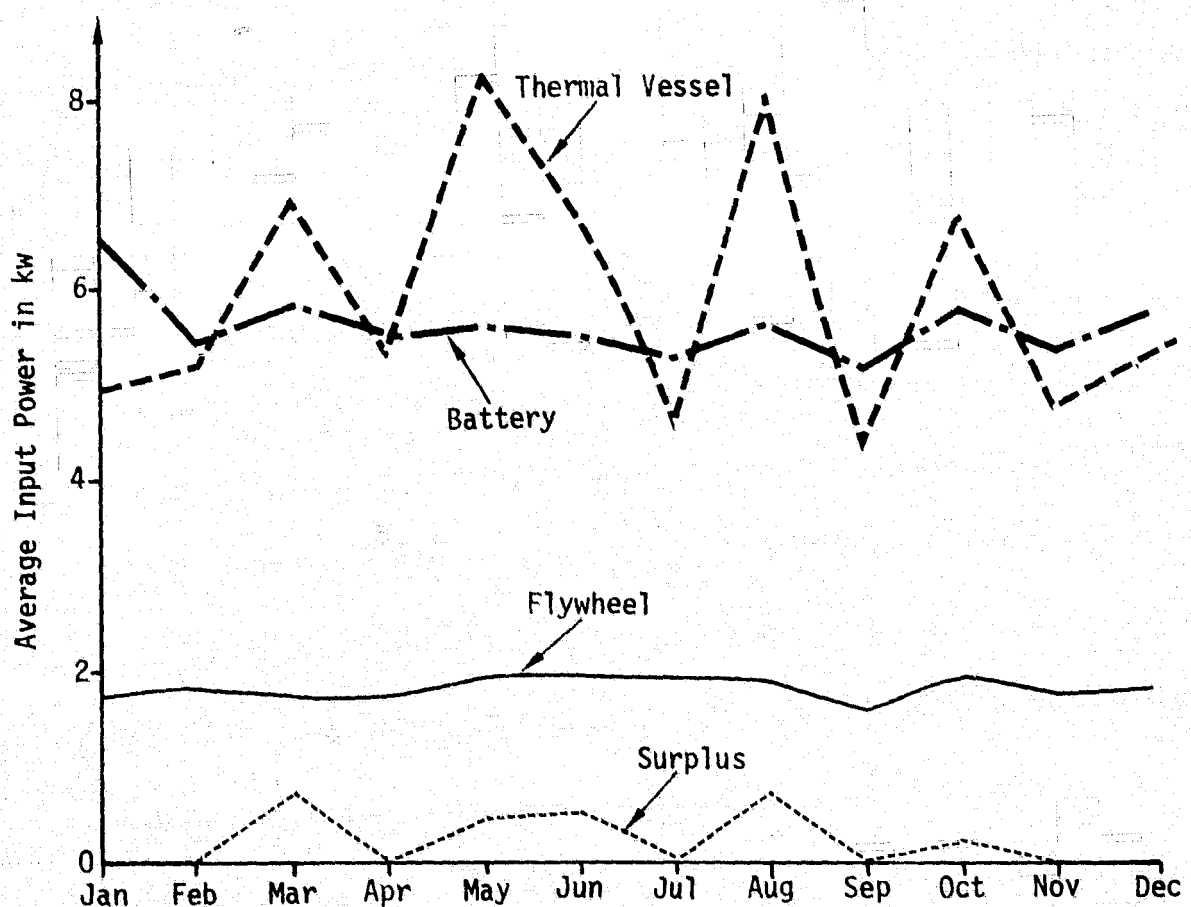


Figure 3.4-1 Average Monthly Power Distribution

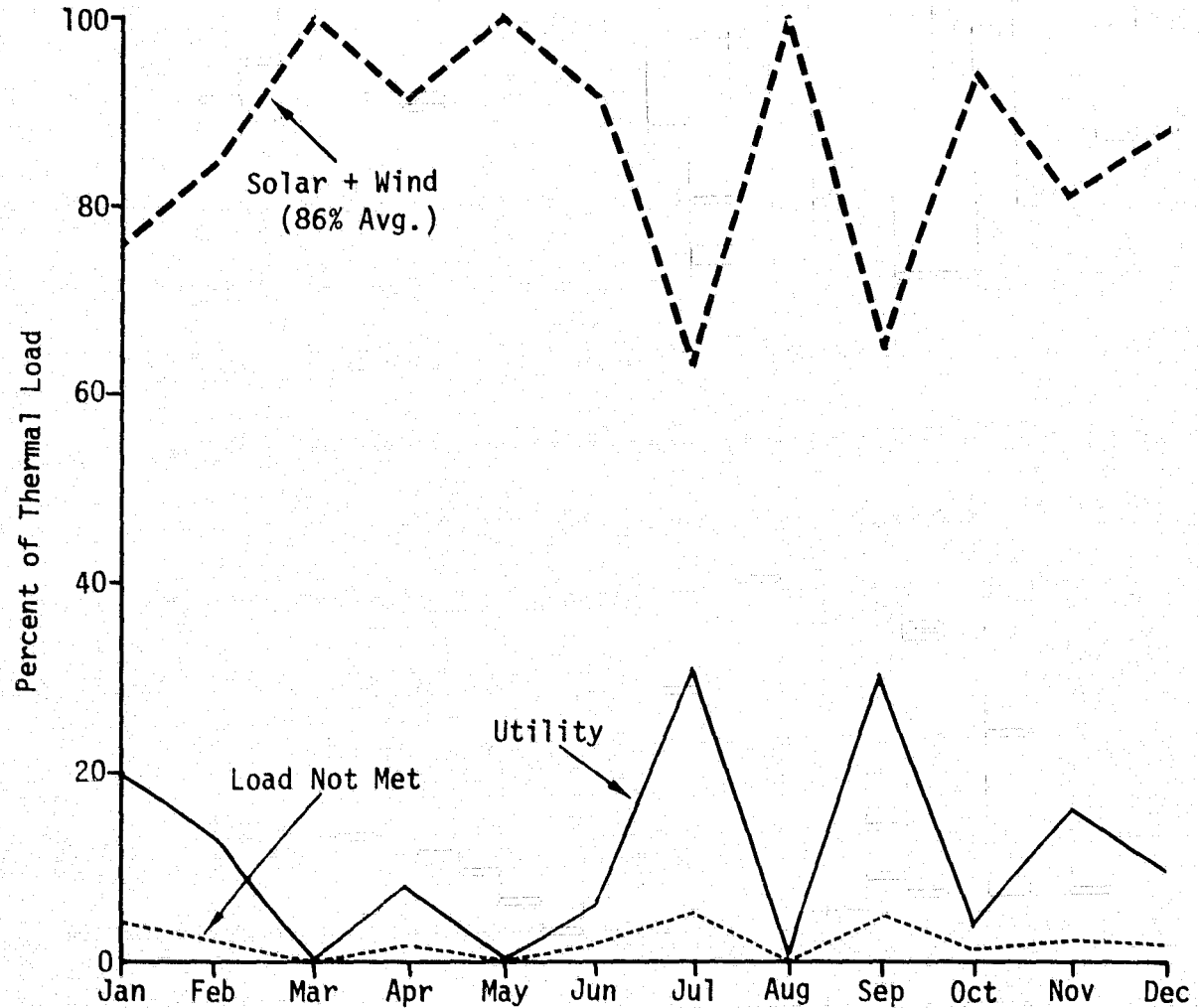


Figure 3.4-2 Monthly Thermal Load Service - Hybrid Model

to the thermal load from solar and wind generation, the percentage from a utility, and the percentage of thermal load not met. Solar and wind generation supply at least 75% of the thermal load each month except July and September when wind generation is low. This suggests increasing the solar generation capacity, relative to the wind in order to reduce the utility supplied load during the summer months. The small percentage load not met is due to an assumed temperature deadband when thermal storage temperature drops below a minimum useful level.

Table 3.4-1 summarizes the storage system performance in meeting the loads. The values shown represent total subsystem level performance, i.e., input power to the flywheel is the DC power to the motor and output power is the power delivered to the loads by the generator and inverter. The battery efficiency is higher than would be expected for a conventional lead-acid battery, but this is easily corrected by appropriate scaling of the battery terminal resistance parameter. This would lower the overall storage efficiency and thus require greater total generation to meet the load.

Table 3.4-1 Average Storage System Statistics

	Input Power <sup>1</sup>	Output Power	Turnaround Efficiency
Battery	5.6	5.2	0.94
Flywheel	1.8	1.3	0.75
Thermal	5.9	4.2	0.71
Total	13.3	10.8	0.81

<sup>1</sup> Adjusted for net change in energy storage

### **3.5 SUMMARY**

The Hybrid solar test case simulations have illustrated the general ability of the SIMWEST program to model and analyze complex solar and wind system models. These studies have shown that using four seasonal week long simulations rather than expensive year long simulations gives an adequate data base for system level design and trade study analyses. Year long simulations are then recommended for final confirmation of the selected system designs. For simplicity, we have neglected cost economics constraints associated with an actual system application. However, the economic and life cycle cost analysis described in Section 1 could have been used to investigate system economics.

## **4.0 TECHNICAL APPROACH FOR POWER DYNAMICS LIBRARY**

### **4.1 BACKGROUND**

The technical approaches studied for development of a dynamic component library to model transient effects on generation, distribution, and storage of power are summarized in this section. The objective of this library development was to provide component models for analysis of transients such as wind gusts, transmission line faults and generation or storage switching on an electrical network. Only those phenomena with physical time constants on the order of hundredths of a second to ten seconds were envisioned as within the scope of the component modeling. This is the primary region of interest for power system transient stability analyses. Most of the dominant machine time constants for power generation and load distribution fall within this region. The component models formulated do not model detailed control and design phenomena such as wind turbine structural vibrations or synchronous generator excitation voltage modeling. Similarly, system phenomena with time constants on the order of minutes to hours were not modeled, except to the extent necessary to specify steady state operating conditions.

One of the primary considerations in formulating the dynamic library was to make the codes easy to use. Simplified dynamic models were envisioned for this purpose so that a user could create and debug a simulation quickly, and run simulations with reasonable cost expectations. Other user related factors such as model generality, documentation clarity, output capability and model adaptability were also considerations during the model definition effort. Within this framework, a primary objective of the model definition effort was to obtain component models which could be easily modified or augmented to incorporate control system interaction with the network, i.e., excitation regulation on a synchronous generator. A user would build up a control system from transfer function, algebraic operations, saturation, and other library components and link the control system to the affected physical components. Such control system modeling would be desirable, for example, to provide

damping for electrical machine transients or lightly damped DC transmission lines with series inductors. In addition, control system modeling is important for evaluating system stability under fault current and over voltage conditions.

The analysis capabilities of the EASY program for control system design and evaluation were to be incorporated into SIMWEST as part of the dynamic library development effort. (Table 4.1-1 summarizes these analysis capabilities.) The proposed marriage of the EASY program analysis capabilities and components for power generation, transmission, and distribution would provide a unique research tool for dynamic analysis of solar energy/utility/energy storage systems. The resulting program would thus provide the capability of evaluating control system designs as well as performing transient stability analyses.

During the formulation of the dynamic component library it became evident that initializing the user's model to steady state power flow conditions is a more difficult technical problem than originally anticipated. In general, when simulating a dynamic system for the purpose of investigating stability, steady state operating conditions are a prerequisite for investigating system transient behavior. The EASY program has a steady state analysis capability which yields a steady state configuration given user specified initial conditions. However, this capability is not sufficient for steady state power flows since there are voltage and power angle operating constraints which are necessary when modeling power system operation. For a system with more than a modest number of busses, or for a user not familiar with power system behavior, specification of appropriate initial conditions to balance real and reactive power within these constraints could be an arduous task. Consequently, a technical approach for initializing the user's model was formulated which employs a classical load flow analysis, and a separate set of parameter computations at each network bus. An EASY steady state analysis would also be required in order to initialize the dynamics of other components such as wind turbines and utility steam driven turbines.

TABLE 4.1-1 EASY PROGRAM ANALYSIS CAPABILITY

<u>ANALYSIS</u>	<u>PURPOSE</u>
● SIMULATION	CONCEPT VERIFICATION, SYSTEM OPTIMIZATION AND DESIGN
● MODEL LINEARIZATION	
● STEADY STATE CALCULATIONS	INITIALIZE TRANSIENT SIMULATIONS, INVESTIGATE STEADY STATE CONDITIONS AND SYSTEM STABILITY
● ROOT LOCUS	
● STABILITY MARGIN	CONTROL SYSTEM DESIGN, SYSTEM STABILIZATION AND SYNTHESIS
● OPTIMAL CONTROLLER	
● EIGENVALUES	
● TRANSFER FUNCTION	FREQUENCY DOMAIN ANALYSIS, SYSTEM STABILITY

This technical approach for initializing a transient power simulation was considerably beyond that originally anticipated. Since the estimated increase in funding to implement this approach exceeded the project scope, further development in this area was terminated. It was decided, however, to document the technical approach and component models formulated, since the capabilities envisioned through development of such a program would provide a unique research tool for investigation and design of innovative power system generation and storage technologies.

The SIMWEST dynamic component models which were studied in depth during the model formulation effort included a load flow component, network solver, synchronous machine models, induction machine models, and a wind turbine component. Descriptions of these components and the general problem formulation summarized above are provided in subsequent sections. These components describe all the network related components originally contemplated, except for an AC/DC converter model. The simplified converter model described in reference [5] appears to be compatible with this problem formulation. However, the model formulation effort was terminated before this model could be evaluated for inclusion in the dynamic library.

#### 4.2 GENERAL PROBLEM FORMULATION

A power system model for transient stability simulations consists of the physical machines or subsystems which generate power into an electrical network, the transmission grid which allocates power flow between the network busses, and the machines or subsystems which constitute the loads. From a modeling viewpoint, the power network consists of a set of busses or nodes which are connected by transmission lines, and which is characterized by (complex) voltage and power at each node. A power simulation consists of four basic calculation steps:

- 1) Calculation of the machine dynamics or differential equations, given the current state of the power system.

- 2) Numerical integration of the system dynamics to the next time step.
- 3) Calculation of two of the nodal electrical states for each bus, based on the current machine dynamics.
- 4) Solution of the electrical network equations for the remaining two electrical states at each bus.

Steps 3) and 4) may involve iteration, depending on the complexity of the system models. The component models which were selected for the dynamic library do not require iteration and thus would economize on computer time for transient simulations.

Three types of busses are modeled in the network component which computes step 4) above:

- Busses which provide a specified current injection into the network. This includes machine busses such as generators, motors and converters.
- Reference or infinite busses which specify a known bus voltage and act as infinite power sources or sinks and thus stabilize the network.
- Internal or passive busses used to provide power flow branching in the transmission network and to represent loads.

Figure 4.2-1 shows a power network model illustrating all of the above types of network busses. The reference bus is used to model an interconnection with an external utility network. The branching bus is used to furnish redundant transmission capability to the loads. The other busses all inject current into the network and result in positive power flow for generation and negative power flow for the loads.

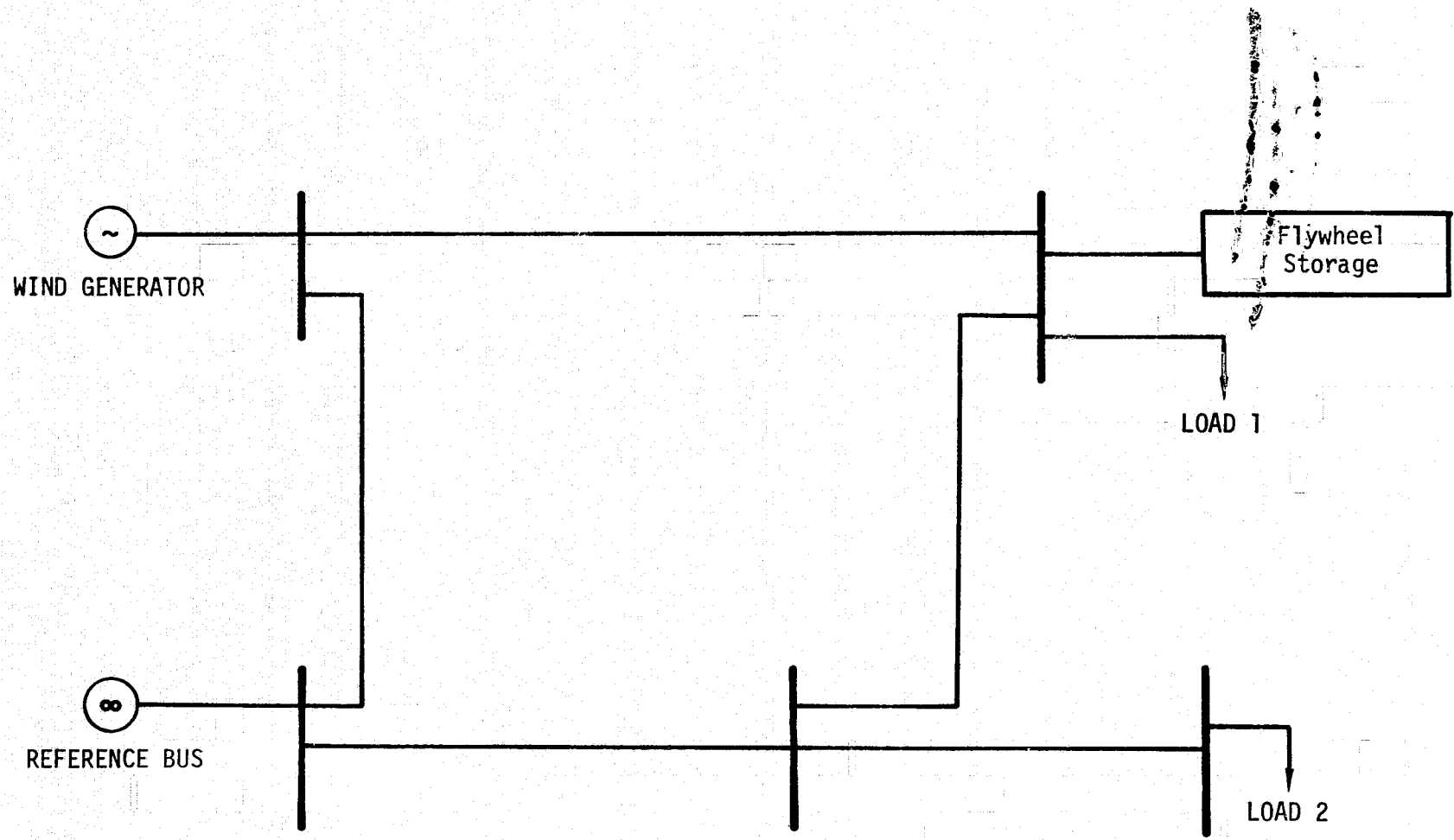


Figure 4.2-1 Example Power Network Schematic

The general flow of power calculations for the components formulated in this section is illustrated by Figure 4.2-2 for the five bus model of Figure 4.2-1. Following integration of the system dynamics, the first calculations in the model are the Norton current injections into the network (blocks ① and ②) for the induction and synchronous machine busses. The reference bus furnishes a constant voltage into the network component. The internal bus and the two load busses have been replaced by an equivalent circuit in the network and thus are transparent to the solution process. The network component (block ③) solves the circuit equations for bus voltage at all current specified busses and for current flow at the reference bus. The wind turbine-generator components (blocks ④, ⑤ and ⑥) then compute the mechanical torque into the generator and the differential equations of the machine dynamics. (Feedback connections are denoted by dashed lines in Figure 4.2-2.) Finally power flow and machine dynamics of the motor-transmission-flywheel components are computed (blocks ⑦ and ⑧).

At the beginning of each simulation the system model is initialized by a load flow computation for specified steady state power flow at each bus node, and by a steady state analysis to obtain initial conditions for the machine dynamics. The load flow output and initialized state variables are stored for use in later simulations or later runs. During a given simulation run the network topology remains constant, i.e., no switching in or out of generators, loads, or transmission lines. The user introduces such transients by running a simulation prior to the switch, then beginning a new simulation with changes in the network, and running a subsequent simulation to analyze power transients.

#### 4.3 LOAD FLOW INITIALIZATION

A load flow calculation is a nonlinear equation solution method for obtaining the steady state real and reactive power at each nodal bus. This calculation procedure is widely used in the electric utility industry, and is the standard method for initializing transient stability programs. Its purpose in the problem formulation above is to provide appropriate shunt constants for the load busses and to provide initial conditions for synchronous and induction

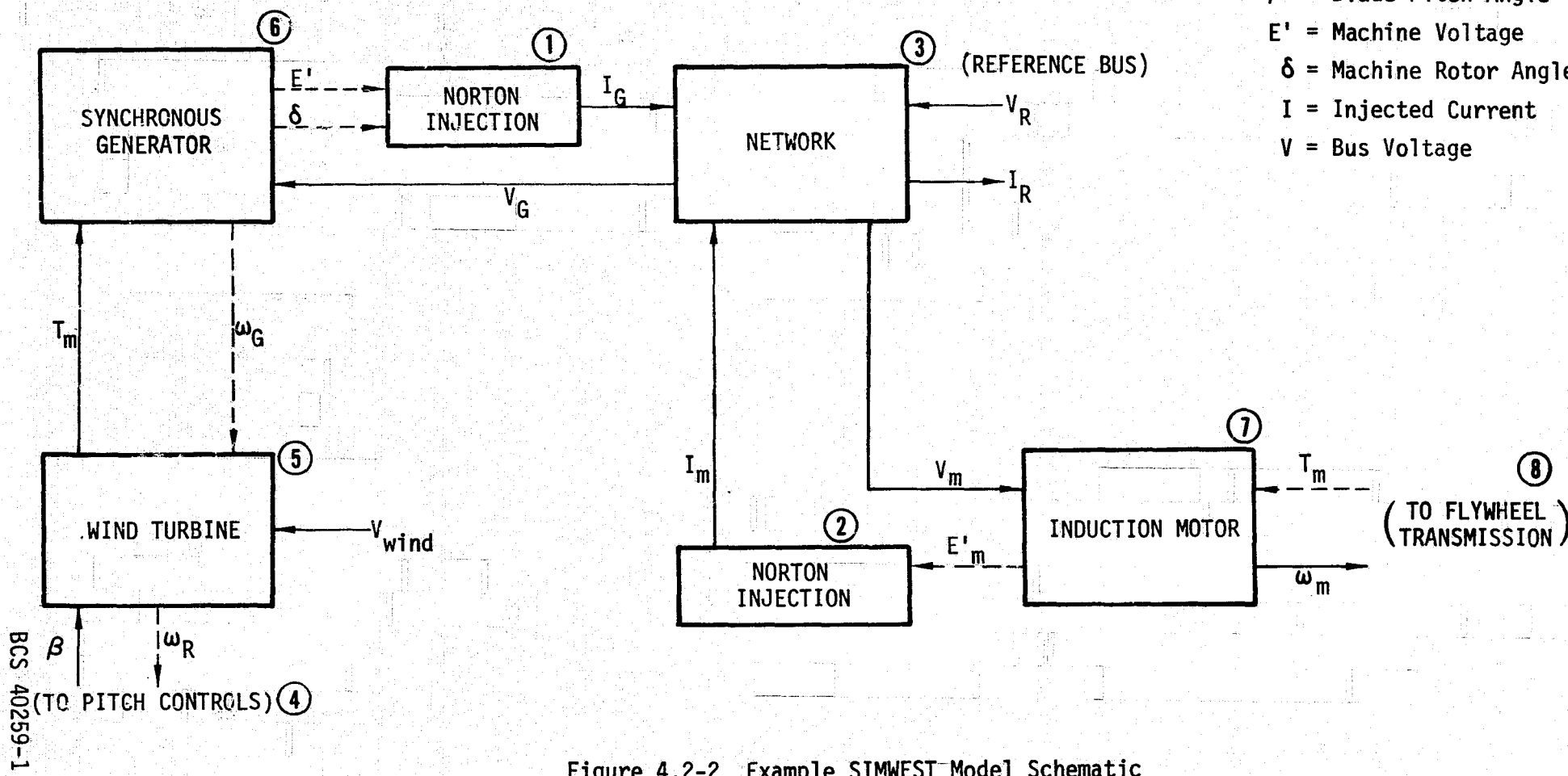


Figure 4.2-2 Example SIMWEST Model Schematic

machine injections. If one were to use the EASY program steady state analysis and nominal shunt parameters to balance real power flow, it might be possible to obtain steady state power flows without a load flow calculation. However, such solutions would generally have poorly balanced reactive power generation resulting in large voltage magnitude differences throughout the network. Thus a load flow calculation is essential in order to balance both real and reactive generation to the loads.

Three types of busses are modeled in load flow calculations:

- 1) load busses (including induction machines) where the net real and reactive power injections  $P$  and  $Q$  are specified and the load flow solves for voltage magnitude  $|V|$  and angle  $\delta$ ,
- 2) Voltage controlled busses such as synchronous machines where the voltage magnitude  $|V|$  and real power  $P$  are specified and the load flow solves for reactive power  $Q$  and voltage angle  $\delta$ ,
- 3) Reference busses where  $|V|$  and  $\delta$  are specified and the load flow computes power injections  $P$  and  $Q$  which balance real and reactive power flow throughout the network.

Passive busses may be ignored since a network reduction may be performed to eliminate such busses prior to the load flow.

Mathematically, the load flow is a procedure for solving the  $n$  nodal power flow equations

$$S_m \triangleq P_m + jQ_m = V_m * I_m^* \quad (4.1)$$

where the (complex) currents  $I_m$  satisfy the network equations

$$I_m = \sum_k Y_{mk} V_k \quad (4.2)$$

and  $(Y_{mk})$  denotes the complex valued admittance matrix of the transmission network. Using the polar representations

$$V_k \triangleq |V_k| e^{j\delta_k}, \quad Y_{mk} \triangleq |Y_{mk}| e^{j\theta_{mk}},$$

and substituting (4.2) into (4.1) yields

$$S_m = \sum_k |V_m V_k Y_{mk}| e^{-j(\theta_{mk} + \delta_k - \delta_m)} \quad (4.3)$$

Separating (4.3) into real and imaginary parts, one obtains

$$0 = P_m - \sum_k |V_m V_k Y_{mk}| \cos(\theta_{mk} + \delta_k - \delta_m) \quad (4.4)$$

$$0 = Q_m - \sum_k |V_m V_k Y_{mk}| \sin(\theta_{mk} + \delta_k - \delta_m). \quad (4.5)$$

Equations (4.4) and (4.5) represent a nonlinear system of equations of the general form

$$0 = g(x, y) \quad (4.6)$$

where  $x$  represents the  $2n$  unknowns to be solved,  $y$  represents the  $2n$  nodal conditions which are specified, and  $g$  represents the  $2n$  equations (4.4) and (4.5).

Given an initial estimate  $x_0$ , (4.6) may be solved by Newton-Raphson iterations

$$\frac{\partial g}{\partial x}(x_i, y) \cdot \delta x_i = g(x_i, y) \quad (4.7)$$

$$x_{i+1} = x_i - \delta x_i \quad (4.8)$$

Although a number of advanced techniques exist for efficiently updating the Jacobian matrix  $\frac{\partial g}{\partial x}$  and for solving the linear equations (4.7), these methods are probably not warranted for the small dimension networks envisioned for SIMWEST transient stability simulations. Consequently, the Jacobian matrix would be evaluated each iteration with the particular structure of equations

(4.4) and (4.5) used to reduce the evaluation effort, and Gaussian elimination then used to compute  $\delta x_i$ .

Once a load flow solution to (4.4) and (4.5) is obtained, appropriate network constants and bus states may be supplied to the network and machine components. The current injections for each bus may be obtained by solving (4.1), i.e.,

$$I_m = S_m^* / V_m^* = (P_m - jQ_m) e^{j\delta_m} / |V_m| \quad (4.9)$$

Similarly, the shunt impedance for constant load busses satisfies  $V = Z_s I$ , and thus

$$S = V^* I^* = |I|^2 \cdot Z_s$$

or equivalently

$$Z_s = (P + jQ) / |I|^2 \quad (4.10)$$

After these quantities are computed, the Y admittance matrix, the nodal current and voltage quantities  $I_m, V_m$  and the shunt impedances  $Z_s$  are output to disc storage for later use in initializing transient simulations.

In order to fully initialize a transient simulation, the initial conditions of all state variables must be selected consistent with the steady state load flow. This is easily done using the EASY steady state analysis, but requires adding new state variables to the model whenever a specified load flow condition is the output of other components. For example, in the model illustrated in Figure 4.2-2, the output power of the generator is a function of wind speed whenever  $V_{WIND}$  is less than rated wind speed. In this case a feedback controller is used during the steady state analysis to obtain the value of  $V_{WIND}$  corresponding to the specified output power  $P_{GEN}$  (See Figure 4.3-1). The steady state routine will iterate until  $P_G$  converges to  $P_{GEN}$ , solving for the corresponding  $V_{WIND}$  value. This part of the model can be switched off after model initialization so that  $V_{WIND}$  is independent of the output power  $P_G$ .

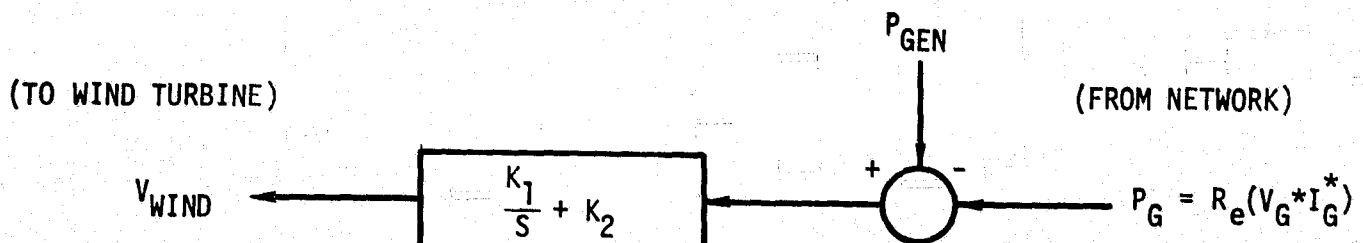


Figure 4.3-1 Control Schematic to Initialize Example Model

#### 4.4 NETWORK COMPONENT MODEL

This component provides solutions for the voltage and power flow at each bus, given the injected current for machine busses and the reference voltage for reference or infinite busses. On the first pass through the model during a simulation or steady state analysis, the network admittance matrix is constructed and a triangular decomposition is performed. The admittance matrix may be constructed either from the load flow matrix, or from user specified input data, and includes a shunt impedance for load busses and machine busses. During each subsequent pass through the model the linear network equations are solved and bus power and voltage variables are output.

##### 1) Admittance Matrix Calculations (First Pass Only)

The network admittance matrix may be constructed either from the load flow admittance matrix or from user specified inputs:

- Load Flow Initialization

Read in the load flow admittance matrix  $Y$  and shunt impedances  $Z_m$  for all load busses. Recompute the diagonal elements of  $Y$  such that

$$Y'_{mm} = Y_{mm} + 1/Z_m.$$

- User Specified Initialization

$$Y_{1m} = -1/Z_{1m} \quad 1 \neq m$$

$$Y_{mm} = -\sum_{1 \neq m} Y_{1m} + \sum_1 (j\omega C_{1m}/2) + 1/Z_m$$

where

$Z_{1m}$  = Impedance of the transmission line between nodes 1 and m

$\omega C_{1m}$  = Line capacitance to ground between nodes 1 and m,  
multiplied by synchronous frequency ( $120\pi$   
radians/second).

$Z_m$  = Shunt impedance of a load or machine bus.

2) Network Reduction (to eliminate passive busses)

Partition the admittance matrix into external or injection busses and internal or passive busses:

$$Y = \begin{pmatrix} Y_{EE} & Y_{EI} \\ Y_{EI}^T & Y_{II} \end{pmatrix}$$

The equivalent reduced network for the external busses is given by

$$Y' = Y_{EE} - Y_{EI} Y_{II}^{-1} Y_{EI}^T ,$$

where the matrix  $X = Y_{EI} Y_{II}^{-1}$  is obtained by Gaussian elimination of the linear matrix equation

$$Y_{II} \cdot X = Y_{EI}$$

3) Solution of the Network Equations

Partition the admittance matrix  $Y'$  into current injection busses denoted by the symbol P and reference busses denoted by R:

$$\mathbf{Y} = \begin{pmatrix} Y_{PP} & Y_{PR} \\ Y_{PR}^T & Y_{RR} \end{pmatrix}$$

Let  $\tilde{\mathbf{I}}_P$ ,  $\tilde{\mathbf{I}}_R$  and  $\tilde{\mathbf{V}}_P$ ,  $\tilde{\mathbf{V}}_R$  denote the complex valued current and voltage vectors corresponding to the current injection busses and the reference busses. Then the network equations may be written as

$$\begin{pmatrix} \tilde{\mathbf{I}}_P \\ \tilde{\mathbf{I}}_R \end{pmatrix} = \begin{pmatrix} Y_{PP} & Y_{PR} \\ Y_{PR}^T & Y_{RR} \end{pmatrix} \begin{pmatrix} \tilde{\mathbf{V}}_P \\ \tilde{\mathbf{V}}_R \end{pmatrix} \quad (4.11)$$

We may expand (4.11) into partitioned equations for  $\tilde{\mathbf{I}}_P$  and  $\tilde{\mathbf{I}}_R$  and formally solve these equations for  $\tilde{\mathbf{V}}_P$  and  $\tilde{\mathbf{I}}_R$ :

$$\tilde{\mathbf{V}}_P = Y_{PP}^{-1} (\tilde{\mathbf{I}}_P - Y_{PR} \tilde{\mathbf{V}}_R) \quad (4.12)$$

$$\tilde{\mathbf{I}}_R = Y_{PR}^T \tilde{\mathbf{V}}_P + Y_{RR} \tilde{\mathbf{V}}_R \quad (4.13)$$

It is more efficient and accurate to solve (4.12) using a triangular factorization of  $Y_{PP}$ :

$$Y_{PP} = L \cdot U \quad (4.14)$$

This factorization is performed during the first pass and then stored to solve (4.12) by forward and backward substitution, i.e., we solve the two sets of equations

$$LX = \tilde{\mathbf{I}}_P - Y_{PR} \tilde{\mathbf{V}}_R \quad (4.15)$$

$$U\tilde{\mathbf{V}}_P = X \quad (4.16)$$

Once  $\tilde{\mathbf{V}}_P$  is obtained,  $\tilde{\mathbf{I}}_R$  is computed from (4.13). The complex power flow at each bus is then computed from the bus current and voltage variables:

$$P_m + jQ_m = V_m I_m^* \quad (4.17)$$

## 4.5 SYNCHRONOUS MACHINE MODEL

The synchronous machine model selected for the SIMWEST dynamic library is a compromise between the simple classical machine which models only the machine rotor mechanics, and more detailed machine models which may include excitation control, rotor transient and subtransient dynamics, and stator transients. Specifically, rotor electric and mechanical dynamics are modeled, field voltage is constant, and stator and subtransient dynamics are ignored. The model is sufficiently detailed to enable a user to add excitation or governor controls to the system model, and is simple enough to minimize the computations required to solve the network equations. The synchronous model may be used to represent either a motor or a generator, depending on the algebraic sign of injected power into the network. Another component is also needed with the synchronous machines to compute the Norton equivalent current into the network. These models are described below.

### 4.5.1 Synchronous Machine Model

The model given here is a simplified version of the machine model in reference [6]. The model is most easily described in terms of the machine direct and quadrature rotating coordinate system (d-q axes). Four state variables are used to represent the machine dynamics:

- $\delta$  = rotor angle in radians
- $\omega$  = rotor shaft speed in radians/second
- $e'_d, e'_q$  = d-q axis representation of the machine internal voltage  $E'$  (See Figure 4.5-1)

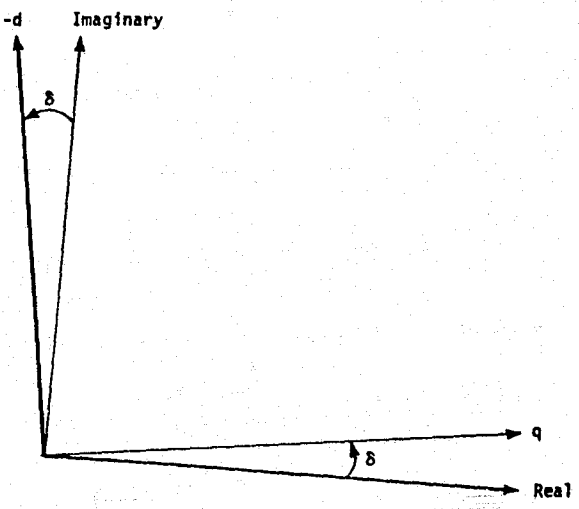


Figure 4.5-1 Network and d-q Axis Coordinates

The basic equations for this model are:

### 1) Stator Electrical Equations

$$\begin{pmatrix} e'_d - V_d \\ e'_q - V_q \end{pmatrix} = \begin{pmatrix} R_s & -x'_d \\ x'_d & R_s \end{pmatrix} \begin{pmatrix} I_d \\ I_q \end{pmatrix} \quad (4.18)$$

where

- $I_d, I_q$  = bus injected current in d-q axes
- $V_d, V_q$  = bus terminal voltage in d-q axes
- $R_s$  = stator resistance
- $x'_d$ , = transient reactance

### 2) Machine Dynamics

$$T_E = (e'_d \cdot I_d + e'_q \cdot I_q)/\omega \quad (4.19)$$

$$J\dot{\omega} = T_M - T_E - D\omega \quad (4.20)$$

$$\dot{\delta} = \omega - \omega_0$$

where

$T_E$  = electrical torque output

$J$  = rotor drive shaft inertia  
 $D$  = machine damping  
 $T_M$  = mechanical input torque  
 $\omega_0$  = synchronous frequency (120 $\pi$  radians/second)

### 3) Internal Voltage Dynamics

$$\dot{e}'_d = (I_q(x_d - x'_d) - e'_d)/T'_q \quad (4.21)$$

$$\dot{e}'_q = (E_f - e'_q - I_d(x_d - x'_d))/T'_d$$

where

$x_d$  = synchronous reactance

$T'_d, T'_q$  = open circuit transient time constants

$E_f$  = field voltage of excitation system

During a simulation the terminal voltage  $V$  from the network is transformed to d-q axes using the rotation equations:

$$V_d = \sin\delta \cdot \operatorname{Re}(V) - \cos\delta \cdot \operatorname{Im}(V) \quad (4.22)$$

$$V_q = \cos\delta \cdot \operatorname{Re}(V) + \sin\delta \cdot \operatorname{Im}(V)$$

Equations (4.18) and (4.19) for current and electrical torque are then solved and the differential equations (4.20) and 4.21) are computed.

- Initialization (First Pass Only)

When load flow initialization is desired the state variables  $\omega$  and  $\delta$  are computed using

$$\begin{aligned} \omega &= \omega_0 \\ \tan \delta &= (\operatorname{Im}(V) + R_s \cdot \operatorname{Im}(I) + x_d \cdot \operatorname{Re}(I)) / \\ &\quad (\operatorname{Re}(V) + R_s \cdot \operatorname{Re}(I) - x_d \cdot \operatorname{Im}(I)) \end{aligned}$$

where  $I$ ,  $V$  denote the bus current and terminal voltage from the load flow. Given the angle  $\delta$ , the d-q axis components for  $I$  and  $V$  may be computed using the rotation equations (4.22). Initial values of  $e'_d$  and  $e'_q$  are then obtained from (4.18), i.e.,

$$e'_d = V_d + R_s \cdot I_d - x'_d \cdot I_q$$

$$e'_q = V_q + x'_d \cdot I_d + R_s \cdot I_q$$

The field voltage  $E_f$  and mechanical torque  $T_M$  values driving (4.20) and (4.21) to zero are then computed:

$$T_M = (e'_d \cdot I_d + e'_q \cdot I_q) / \omega_0 + D\omega_0$$

$$E_f = e'_q + I_d \cdot (x_d - x'_d)$$

If the machine is being used as a generator, the input torque  $T_M$  may require initialization by the procedure indicated in the last part of Section 4.3. On the other hand, if the model is being used as a synchronous motor then  $T_M$  may be a state variable feedback from a downstream component. In this case the above computation for  $T_M$  initializes this state.

The admittance matrix  $Y'$  for the network is also modified to represent the Norton equivalent stator circuit, i.e.,

$$Y'_{mm} = Y_{mm} + 1/(R_s + jx'_d)$$

where  $m$  is the index of the synchronous machine bus.

#### 4.5.2 Current Injection Component

The current injection component computes the Norton current  $I$  into the network given the state variables  $E'$  and  $\delta$ . The stator equations (4.18) neglecting  $V_d$

and  $V_q$  are used to solve for d-q axis components  $I_d$  and  $I_q$  and then a transformation is performed to obtain the synchronous frame components. Specifically, solving (4.18) for  $I_d$  and  $I_q$  yields

$$I_d = (R_s \cdot e'_d + x'_d e'_q) / (R_s^2 + x'_d \cdot x'_d)$$

$$I_q = (-x'_d e'_d + R_s e'_q) / (R_s^2 + x'_d \cdot x'_d)$$

and thus

$$I_{re} = +\sin \delta \cdot I_d + \cos \delta \cdot I_q$$

$$I_{im} = -\cos \delta \cdot I_d + \sin \delta \cdot I_q$$

#### 4.6 INDUCTION MACHINE MODEL

The induction machine model is a simplified model which neglects stator transients and includes rotor electrical and mechanical dynamics. The machine model may be used to represent either a motor or a generator depending on the algebraic sign of the input torque. A current injection component is also required to compute the Norton equivalent current into the network.

Three state variables are used to represent the machine dynamics:

$\omega$  = rotor shaft speed in radians/second

$e'_d, e'_q$  = d-q axis representation of the machine internal voltage  $E'$ .

The axes are chosen such that the direct axis coincides with the network frame real axis and the quadrature axis coincides with the network frame imaginary axis. Torque and slip are positive for a motor, negative for a generator.

The basic equations for this model in d-q axes are

## 1) Stator Equations

$$x' = x_s - x_m^2/x_r$$

$$\begin{pmatrix} e'_d - v_d \\ e'_q - v_q \end{pmatrix} = \begin{pmatrix} -R_s & x' \\ -x' & -R_s \end{pmatrix} \begin{pmatrix} I_d \\ I_q \end{pmatrix} \quad (4.23)$$

where

$x_s$  = stator reactance

$x_m$  = magnetizing reactance between stator and rotor

$x_r$  = rotor reactance

$R_s$  = stator resistance

$V_d, V_q$  = d-q axis components of bus terminal voltage  $V = V_d + jV_q$

$I_d, I_q$  = d-q axis components of injected current  $I = I_d + jI_q$

## 2) Machine Dynamics

$$T_E = (e'_d \cdot I_d + e'_q \cdot I_q)/\omega \quad (4.24)$$

$$J\ddot{\omega} = T_E - T_M - D\dot{\omega} \quad (4.25)$$

where

$T_E$  = electrical torque

$J$  = rotor drive shaft inertia

$D$  = machine damping

$T_M$  = mechanical torque (input variable)

$\omega_0$  = synchronous frequency (120  $\pi$  radians/second)

## 3) Electrical Dynamics

$$\dot{e}'_d = (\omega_0 - \omega) e'_q - \frac{1}{T_0} (e'_d + (x_s - x') I_q) \quad (4.26)$$

$$\dot{e}'_q = (\omega - \omega_0) e'_d - \frac{1}{T_0} (e'_q - (x_s - x') I_d) \quad (4.27)$$

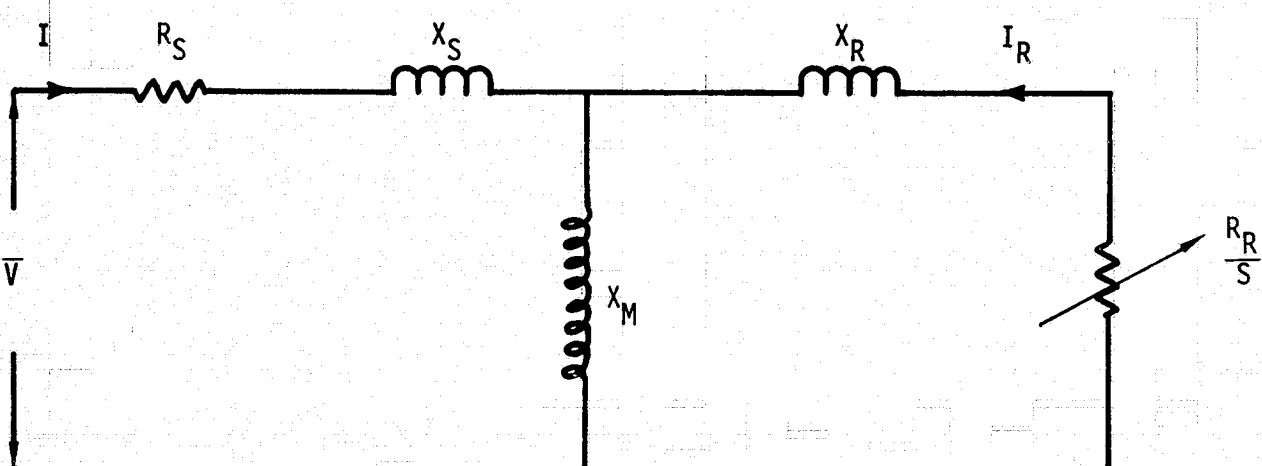
where

$$T_0 = \frac{x_r}{\omega_0 \cdot R_r}, \quad R_r = \text{rotor resistance}$$

During a simulation, (4.23) is solved for  $I_d$  and  $I_q$ , and then equations (4.24) to (4.27) are used to compute the differential equations for  $\omega$ ,  $e'_d$  and  $e'_q$ .

- Load Flow Initialization (First Pass Only)

Given the load flow  $P_e + jQ$  and bus voltage  $V$ , the steady state slip or rotor speed corresponding to real power output is computed. Then a shunt reactance balancing reactive power flow is obtained. Finally,  $I_d$  and  $I_q$  are obtained in order to compute the initial states  $e'_d$  and  $e'_q$ . The equations below are based on the circuit model shown in Figure 4.6-1.



$$S = 1 - \frac{\omega}{\omega_0}$$

Figure 4.6-1 Steady State Circuit for Induction Machine

1) Steady State Slip

$$C_2 s^2 + C_1 s + C_0 = 0 \quad (4.28)$$

where

$$\begin{aligned} C_0 &\triangleq R_r^2 P_e \left( R_s^2 + x_s^2 \right) - R_r^2 R_s |v|^2 \\ C_1 &\triangleq 2R_r R_s P_e x_M^2 - R_r x_M^2 |v|^2 \\ C_2 &\triangleq P_e \left( R_s^2 x_r^2 + (x_M^2 - x_s x_r)^2 \right) - R_s x_r^2 |v|^2 \end{aligned}$$

The classical quadratic formula may be used to solve (4.28) for  $s$ .  $\omega$  is then given by

$$\omega = (1 - s)\omega_0 \quad (4.29)$$

2) Shunt Reactance and Admittance Matrix Update

$$Q_e = \frac{|v|^2}{A^2 + B^2} \left( x_s \left( R_r^2/s^2 + x_r^2 \right) + x_r x_M^2 \right) \quad (4.30)$$

with

$$\begin{aligned} A &\triangleq R_s R_r/s - x_s x_r + x_M^2 \\ B &\triangleq R_s x_r + R_r x_s/s \end{aligned}$$

$P_e + jQ_e$  represents the power flow from the induction machine. Since the load flow power  $Q$  is in general not equal to  $Q_e$ , a shunt reactance is used to balance reactive power:

$$j(Q - Q_e) = v \cdot (v^*/ - jx_0) = j |v|^2/x_0$$

Thus

$$x_0 = |v|^2 / (Q - Q_e) \quad (4.31)$$

The admittance matrix  $Y$  for the network is then modified such that

$$Y'_{mm} = Y_{mm} + 1/(R_s + jx') - j/x_0$$

### 3) Initial Voltage States and Torque

The current components  $I_d$  and  $I_q$  are obtained by solving

$$(P_e + jQ_e) = V^* I^*$$

i.e.,

$$\begin{pmatrix} P_e \\ Q_e \end{pmatrix} = \begin{pmatrix} V_d & V_q \\ V_q & -V_d \end{pmatrix} \begin{pmatrix} I_d \\ I_q \end{pmatrix} \quad (4.32)$$

$e'_d$  and  $e'_q$  are then obtained from (4.23). Mechanical Torque is given by

$$T_M = T_E - D\omega \quad (4.33)$$

where  $T_E$  is computed from (4.24)

#### 4.6.1 Current Injection for Induction Machine

The current injection to the network for the Norton equivalent of the induction machine is obtained by solving (4.23) for  $I_d$  and  $I_q$ , neglecting the bus voltage terms:

$$I_d = -(R_s \cdot e'_d + x' \cdot e'_q) / (R_s^2 + (x')^2)$$

$$I_q = (x' \cdot e'_d - R_s \cdot e'_q) / (R_s^2 + (x')^2)$$

#### 4.7 WIND TURBINE MODEL

The wind turbine model is a simplified model of the turbine dynamics and blade pitch controls, ignoring the structural dynamics of the tower and flexing motions of the rotor blades. This model is based on a wind turbine simulation developed for studying pitch control effectiveness of the Mod-2 wind turbine under development for DOE. The model includes a twice-per-revolution disturbance due to passage of a blade through the tower wind shadow, and damping of the rotor hub oscillations by use of a flexible shaft or hydraulic coupling to the generator.

Figure 4.7-1 shows the main components and variables for the wind turbine/generator system. The blade aerodynamics are summarized by coefficient of power ( $C_p$ ) curves as functions of wind tip speed ratio ( $\lambda$ ) and blade pitch ( $\beta$ ). The torque output at the hub ( $T_{HUB}$ ) is computed based on  $C_p$  and a blade angle dependent torque disturbance. The shaft dynamics consist of differential equations for rotor reference angle and speed at the hub ( $\theta_H, \omega_H$ ), differential equations for shaft flexing angle and speed ( $\delta_s, \omega_s$ ) at the gearbox coupling, and calculation of output torque ( $T_s$ ) to the gearbox. The gearbox model is a simple table lookup used to compute power loss in the output torque ( $T_m$ ) to the alternator. The pitch controller is a linear control system for  $\beta$  which includes integral and proportional feedback of hub speed error and generator output power error, and a notch filter to attenuate twice-per-revolution disturbances. Basic equations for these components are outlined below:

- Blade Aerodynamics

Given  $V_{WIND}$  and  $\omega_H$  the tip speed ratio  $\lambda$  is computed:

$$\lambda = r \cdot \omega_H / V_{WIND} \quad (4.34)$$

where  $r$  = rotor blade radius.

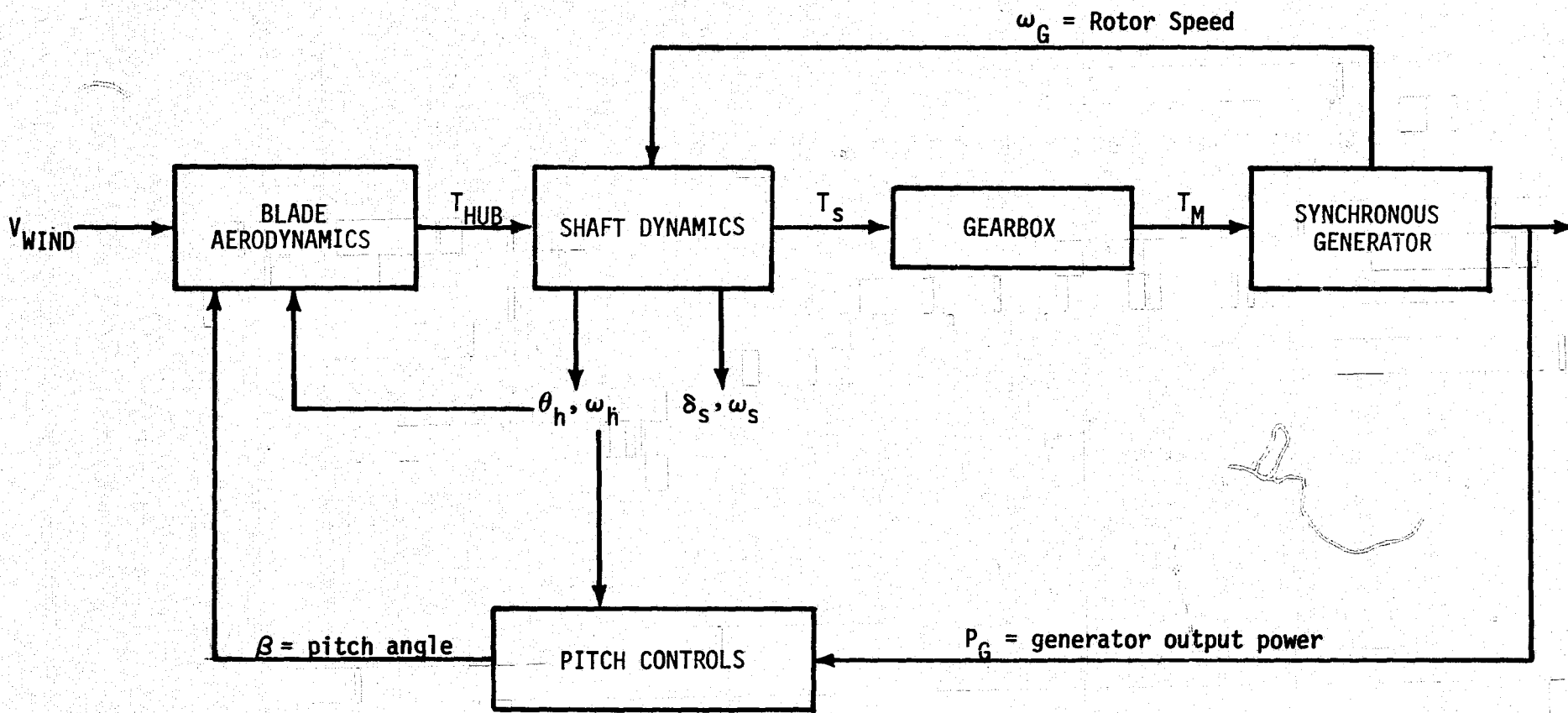


Figure 4.7-1 Wind Turbine/Generator Model Schematic

The wind power generated at the hub is then given by

$$P_{WIND} = C_p(\beta, \lambda) \cdot \pi r^2 \cdot \rho V_{WIND}^3 / 2 \quad (4.35)$$

where  $\rho$  = air density

$C_p(\beta, \lambda)$  is obtained by interpolation of  $C_p$  curves versus  $\lambda$  for fixed  $\beta$   
(See Figure 4.7-2).

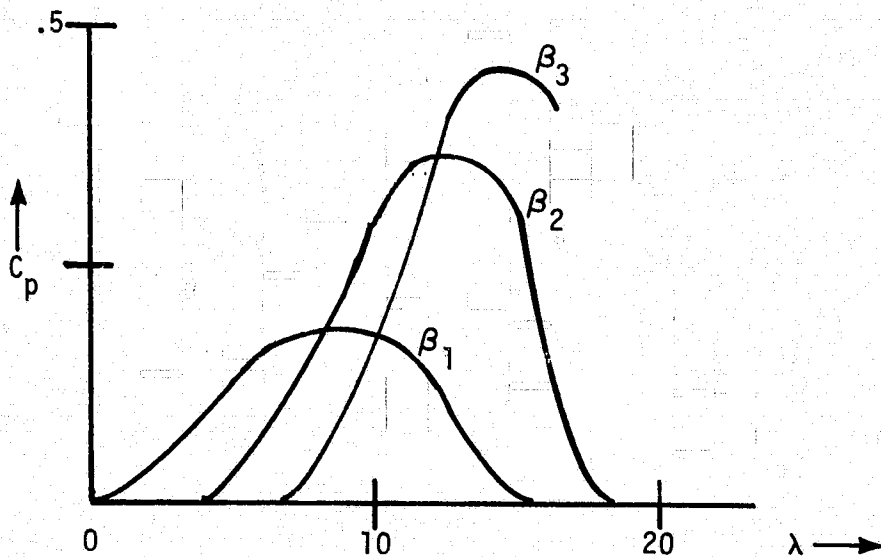


Figure 4.7-2 Coefficient of Power Design Curves

The torque output at the hub is the sum of the torque obtained from (4.35) and a blade angle dependent disturbance:

$$T_{HUB} = (1 + K \cdot \sin(2\theta_H + \frac{\pi}{2})) P_{WIND} / \omega_H \quad (4.36)$$

where

$K$  = disturbance gain (nominal value = 0.1)

$\theta_H$  = rotor hub angle relative to horizontal blades

## ● Shaft Dynamics

The shaft dynamics are represented schematically by Figure 4.7-3. The differential equations for  $\theta_H$ ,  $\omega_H$ ,  $\delta_S$  and  $\omega_S$  are:

$$\dot{\theta}_H = \omega_H \quad (4.37)$$

$$J_H \dot{\omega}_H = T_{HUB} - D_H \omega_H + D_Q (\omega_S - \omega_H) + K_Q \delta_S \quad (4.38)$$

$$\dot{\delta}_S = \omega_S - \omega_H \quad (4.39)$$

$$J_S \dot{\omega}_S = -D_S \omega_S + D_Q (\omega_H - \omega_S) - K_Q \delta_S + D_G (\omega_G^! - \omega_S) \quad (4.40)$$

where

$J_H, J_S$  = rotor hub and drive shaft inertia

$D_H, D_S$  = hub and shaft damping

$D_Q, K_Q$  = quill shaft damping and compliance

$D_G$  = hydraulic damping between shaft and generator

$\omega_G^!$  = generator speed/gear ratio.

The output torque to the gearbox is given by

$$T_S = D_G (\omega_S - \omega_G^!) \quad (4.41)$$

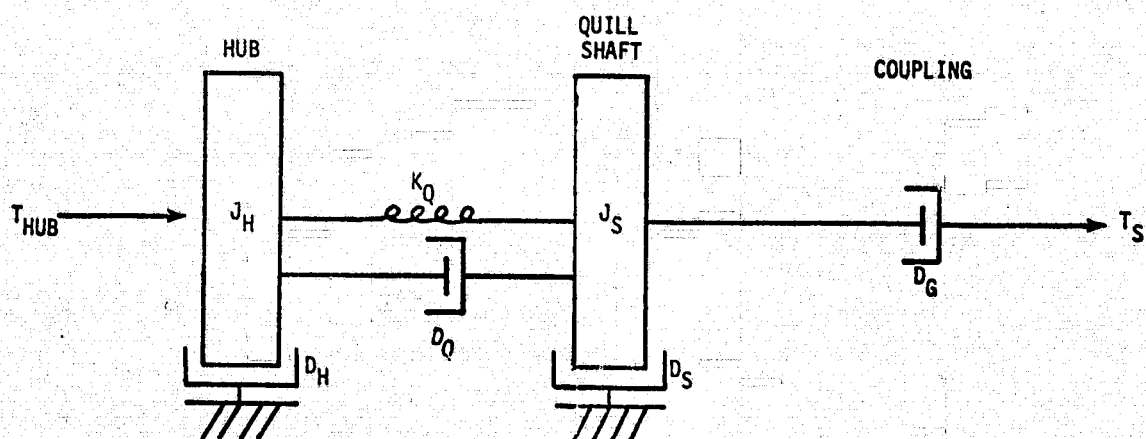


Figure 4.7-3 Turbine Shaft Dynamics

- Gearbox

The power loss in the gearbox is modeled by a lookup table  $L(T)$ :

$$T_M = G \cdot T_S - L(G \cdot T_S) \quad (4.42)$$

where  $G$  denotes the gear ratio.

- Pitch Controls

Representative pitch controls are easily summarized using transfer function equations. A raw pitch command  $\beta_C$  is generated using a fixed value or integral plus proportional feedback:

$$\beta_C = (K_1 + K_2/s) (P_{REF} - P_G) + (K_2 + K_3/s) (\omega_{REF} - \omega_H) \quad (4.43)$$

where  $P_{REF}$  is the rated output power of the turbine/generator and  $\omega_{REF}$  is the reference speed for synchronous operation. The pitch command is notch filtered and input to a pitch actuator. The pitch output  $\beta$  is given by

Actuator	Notch Filter	
$\beta = (1/(T_A s + 1)) \cdot (s^2 + .02s \omega_{REF} + \omega_{REF}^2) / (s^2 + 0.2s \omega_{REF} + \omega_{REF}^2)$		(4.44)

where  $T_A$  = actuator time constant.

The above pitch controls would not be built into the wind turbine component since they are easily constructed from transfer function components, and more generality is obtained this way.

#### 4.8 SUMMARY CONCLUSIONS

A general technical approach for development of a transient power system library using the SIMWEST/EASY computer program has been outlined. Although the

problem formulation is an adaptation of power industry transient stability program models and solution methods, its purpose and capabilities are rather different. The SIMWEST dynamic component library would be an excellent research tool for investigation and design of innovative or unconventional energy systems interconnected to a power grid, whereas transient stability programs are usually production codes used to represent existing or proposed power systems networks. As a consequence of the design objectives SIMWEST has more emphasis on user simplicity, modeling flexibility, and control system analysis than does a transient stability program. It thus would provide a unique capability for solar energy and energy storage power systems research.

One conclusion that became clear in the formulation of the dynamic library is that an expanded version of the EASY program (version 5) should be used as the basis for a power transient program, rather than version 4, which was the basis for SIMWEST. Version 5 has vector and matrix input/output and module connection capabilities not available with the earlier program versions. These capabilities enable a user to model medium size networks rather than being limited to ten active busses, provide more user input and output capability for complex models, and simplify development of library component subroutines.

A major technical problem that arises in creation of transient power system codes is that the system models are in general implicit, and require iteration techniques to obtain convergence of all system variables. The technical approach used has been to formulate the models so that the network solution is explicit, reducing the complexity and expense of the solution process. In the initialization process, however, a load flow component is needed to solve the implicit power flow conditions which balance real and reactive generation to the loads. This approach is easily modified for more complex system models with implicit variables and nonlinearities by use of the iteration method currently used in SIMWEST. Thus, the dynamic library models formulated above would provide an excellent base of power system models for transient analyses which can accommodate growth and expansion for general solar energy research studies.

## 5.0 REFERENCES

- [1] R. W. Edsinger, Y. K. Chan, A. W. Warren, "A Simulation Model for Wind Energy Storage Systems," Volume I: Technical Report, NASA CR-135283, prepared by Boeing Computer Services Company, August 1977.
- [2] A. W. Warren, R. W. Edsinger, J. D. Burroughs, "A Simulation Model for Wind Energy Storage Systems," Volume II: Operation Manual, NASA CR-135284, prepared by Boeing Computer Services Company, August 1977.
- [3] SOLMET User's Manual, TD-9724, National Climatic Center, Ashville, North Carolina, December 1977.
- [4] J. K. Linn, "Photovoltaic System Analysis Program--SOLCEL," Sandia Laboratories Report SAND77-1268, August 1977.
- [5] D. P. Carroll and D. M. Triezenberg, "Security Assessment of Power Systems Including Energy Storage," Progress Report COO-4206-3, prepared for Division of Electric Energy Systems, DOE, January 1978.
- [6] EPRI - Transient Stability Program User Manual, EPRI EL-597, Electric Power Research Institute, Palo Alto, Ca., November 1978.

PAGE 100 INTENTIONALLY BLANK